January-March 2013 Volume 47 Number 1
ISSN 2277-8969
eISSN 2278-0262

Journal of Postgraduate Medicine Education and Research

The Official Journal of Postgraduate Institute of Medical Education and Research, Chandigarh, India

Editor-in-Chief
Mandeep S Dhillon

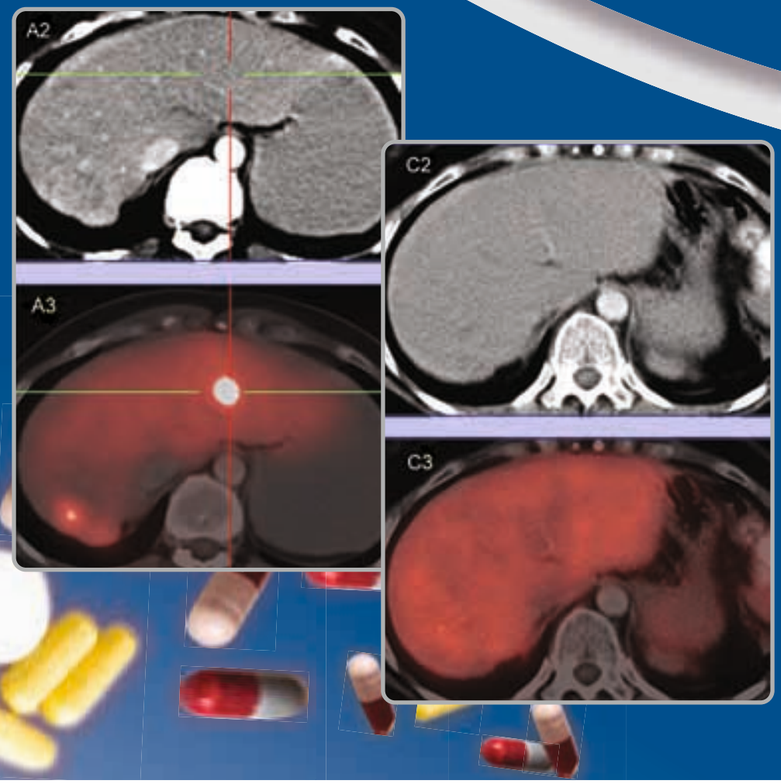

JPMER
Also available online at
www.jaypeejournals.com
www.jpmer.com

Bibliographic Listings:
IndexCopernicus, EBSCO

JAYPEE

January-March 2013 Vol. 47 No. 1 Journal of Postgraduate Medicine, Education and Research ISSN 2277-8969

Journal of Postgraduate Medicine, Education and Research

1. Aims and Scope

The *Journal of Postgraduate Medicine, Education and Research* is a 46-volume-old publication, which is the official publication of the Post Graduate Institute of Medical Education and Research, Chandigarh, India. This is perhaps one of the oldest multispeciality journals published in India, aiming to provide a platform for authors to publish scientific papers relating to various clinical aspects of Medicine and Surgery, including Dentistry and Medical Education, and has been appearing quarterly for 46 years with a rich and diverse academic content. The journal aims to publish quality, peer-reviewed original research and topical reviews on all aspects of medical research and surgical advances, community medicine, basic sciences, advanced techniques, new processes and products as well as a clinico-pathological case conference in each issue. Papers included range from well designed, controlled clinical trials and analytical epidemiology involving medical issues as well as systematic reviews of literature in various fields of medicine. Case reports and Images of interest are included as well as Book reviews and Invited reviews. Thematic dedicated issues focussed on a single speciality are planned each year, and Guest symposia on a burning topic of medical interest would form a part of each issue.

The journal has been renamed from the old name of bulletin PGIMER and the present name becomes effective in 2012. This has been put online with free access to all. The international and national Editorial Board has been revamped and includes luminaries in their respective fields. The editors now encourage papers from all the countries across the globe, as the journal aims to provide clinicians, scientists and medical students with a knowledge transfer platform for rapid publication of reports through an online rapidly evolving international journal.

Being free online, the journal appeals to a substantial international readership seeking to keep up-to-date with research and developments in the field of medical science with an emphasis on new knowledge and innovations pertinent to the contemporary practice of medical sciences and medical education. Its scope, therefore, is broad, inclusive and international.

2. Ethical Considerations

Manuscripts submitted for publication must comply with the following ethical considerations:

Informed Consent

Informed consent of the patients must be taken before they are considered for participation in the study. Patient identifying information, such as names, initials, hospital numbers, or photographs should not be included in the written descriptions. Patient consent should be obtained in written and archived with the authors.

Protection of Human Subjects and Animals in Research

When conducting experiments on human subjects, appropriate approval must have been obtained by the relevant ethics committees. All the procedures must be performed in accordance with the ethical standards of the responsible ethics committee both (institutional and national) on human experimentation and the Helsinki Declaration of 1964 (as revised in 2008). When reporting experiments on animals, authors must follow the institutional and national guidelines for the care and use of laboratory animals.

3. Copyright

Following guidelines must be followed before submission of the manuscript:

The articles must represent original research material, should not have been published before, and should not be under consideration of publication else where. This however does not include previous publication in form of an abstract or as part of published literature (review or thesis). It is the duty of the author to obtain the necessary permissions for extensive quotations, tables, illustrations, or any other copyrighted material they are using in the paper before a paper can be considered for publication. Copyright of the article gets transferred to Jaypee Brothers, once the article has been accepted for publication. The author would be asked to sign the "Copyright Transfer Form" before his/her article is considered for publication. Once the Copyright Transfer statement has been signed by the corresponding author, no change in authorship or in the order of the authors listed on the article would be accepted by Jaypee Brothers. Also by signing the above mentioned form, the author reassigns the rights of copublishing, or translation if considered necessary in future to the publisher. In the advent of occurrence of any dispute, the matter would be resolved within the jurisdiction of New Delhi court.

While all care has been taken to provide accurate and correct information in accordance with the date of publication, neither the authors, editors not the publisher takes any legal responsibility for any unintentional omission or error. The publisher makes no expressed or implied warranty with respect to the information contained herein. The published material cannot be photocopied for the following purposes: general distribution, promotion, new works or resale. If this is required, specific written permission requires to be obtained from the publisher. Exclusive rights to reproduce and distribute the articles in this journal have been protected by copyright. This also covers the rights to reproduce or distribute the article as well as the translation rights. No material published in this journal can be reproduced in digital format or stored in form of electronic databases, video disks, etc.

Both the conflict of interests and financial disclosure needs to be handled well while conducting the research study. Disclosure of such relationships is also important in connection with all articles submitted for publication. Both of these have also been included in the copyright transfer form. Authors should give due acknowledgement to the individuals who provide writing or other assistance while conducting the research study and also disclose the funding source for the research study.

4. Subscription Information

ISSN 2277-8969
eISSN 2278-0262

• Subscription rates

For information on subscription rates and the other journal related enquiries please contact:

journals@jaypeebrothers.com

• Orders

Journals Department
Jaypee Brothers Medical Publishers (P) Ltd.
4838/24, Ansari Road, Daryaganj
New Delhi 110 002, India
Phone: +91-11-4357 4357
Fax: +91-11-4357 4314
e-mail: subscriptions@jaypeejournals.com

Back volume. Prices are available on request.

5. Electronic Media

An electronic edition of this journal is available at **www.jaypeejournals.com**
Manuscripts can be submitted online at **www.jpmer.com**

6. Advertisement

For advertisement queries please contact:
Journals Department
Jaypee Brothers Medical Publishers
e-mail: advertisements@jaypeejournals.com

For any queries regarding online submission, please e-mail us at: help-desk@jaypeejournals.com

For editorial queries, please contact:
chetna.malhotra@jaypeebrothers.com

The Journal is printed on acid free paper.

www.jaypeebrothers.com
www.jaypeejournals.com

UNIVERSITY OF IOWA HOSPITALS & CLINICS
University of Iowa Health Care

2nd World Congress on Ga-68

(Generators and Novel Radiopharmaceuticals) Molecular Imaging (PET/CT), Targeted Radionuclide Therapy, and Dosimetry (SWC-2013): On the Way to Personalized Medicine

28th February - 2nd March, 2013

SWC - 2013

Organized by :

Department of Nuclear Medicine & PET, PGIMER, Chandigarh, India

Tel: +91-172-2756725, Mobile: +91-9914209725, Fax: +91-172-2747725
E-mail: secondworldcongressga68prrnt@yahoo.com
Website: www.2ndworldcongress-ga-68.de

January-March 2013 Volume 47 Number 1 ISSN 2277-8969

Journal of Postgraduate Medicine, Education and Research

The Official Journal of
Postgraduate Institute of Medical
Education and Research, Chandigarh, India

www.jaypeebrothers.com
www.jaypeejournals.com

JPMER

Journal of Postgraduate Medicine, Education and Research

January-March 2013 Vol. 47 No. 1

Editorial Office
Journal/Bulletin Section
Room No. 617, 6th Floor, Research Block A
Postgraduate Institute of Medical
Education and Research, Sector-12
Chandigarh-160012, India

Production Office
Jaypee Brothers Medical Publishers (P) Ltd.
4838/24, Ansari Road, Daryaganj
New Delhi-110 002, India
Phone: +91-11-43574357
Fax: +91-11-43574314
e-mail: journals@jaypeebrothers.com

Advertisements
Rakesh Sheoran
Phone: +91-9971020680
e-mail: advertisements@jaypeejournals.com
rakesh.sheoran@jaypeebrothers.com

Subscriptions/Reprints
Abhinav Kumar
Phone: +91-9810279794
e-mail: subscriptions@jaypeejournals.com
abhinav.kumar@jaypeebrothers.com

Website Manager
Rohit Gorawara
Phone: +91-9871855331
e-mail: contact@jaypeejournals.com
rohit.gorawara@jaypeebrothers.com

Journal of Postgraduate Medicine, Education and Research

January-March 2013 Volume 47 Number 1

Contents

Editorial

Receptor-targeted Molecular Imaging and Radionuclide Therapy: A Path to personalized Medicine

Baljinder Singh

BR Mittal

Richard P Baum

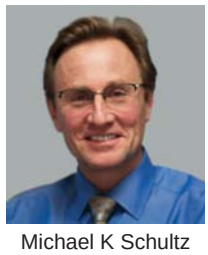

Michael K Schultz

It is our pride privilege and great honor to guest edit this thematic issue of the Journal of Postgraduate Medicine Education and Research (JPMER). All of us decided to take 'Receptor-targeted Molecular Imaging and Radionuclide Therapy: A Path to personalized Medicine' as the theme of this issue of JPMER.

Since, the first World Congress on '^{68}Ga Molecular Imaging and Radionuclide Therapy' organized under the stewardship of Prof Richard P Baum (June, 2011, Bad Berka, Germany), we have continued to witness the proliferation of new ^{68}Ga-labeled compounds for molecular imaging of cancer. Much as early discoveries of differences in cancer cell metabolism led to the development of small molecule imaging agents (e.g. ^{18}F-FDG and ^{18}F-FLT), these new applications for ^{68}Ga are founded on discoveries that identify fundamental differences in tumor cell extracellular antigen expression, relative nonmalignant cells. These discoveries are the foundation for the next generation of molecular targets for selective delivery of radiation dose to tumor cells for diagnosis, monitoring and selecting patients that can benefit most from receptor-targeted radionuclide therapies. Thus, our efforts in this area have the potential to advance molecular imaging science toward personalized medicine.

In the second World Congress (SWC-2013) organized (28th Feb-2nd March, 2013) by the Department of Nuclear Medicine and PET at the Postgraduate Institute for Medical Education and Research (Chandigarh, India), leading scientists and physicians in ^{68}Ga-based molecular imaging and peptide receptor-targeted radionuclide therapy gathered to share their latest discoveries and technical developments that are shaping the future for this field. New applications for ^{68}Ga are highlighted and the latest developments in generator technologies as well as new directions for targeted radionuclide therapy are presented. The scientific deliberations of the SWC-2013 (attended by more than 500 Experts/Delegates from over 30 countries) promised a brighter future for these modalities of imaging and therapy as we discover new molecular targets that are enabling us to selectively target cancer cells. The challenge, as we move forward, is to combine our advances in radionuclide technologies with new discoveries of molecular target expression in cancer cells for more precise delivery of therapies. In this way, we move forward toward a personalized approach to molecular diagnostics and targeted therapies.

The compilation of the presentations and discussions as original and review articles in this Congress dedicated thematic issue of JPMER provides a very comprehensive document for those practicing 'Receptor Targeted Molecular Imaging and Radionuclide therapy' with the common aim of achieving the goal of providing personalized medicine to the patients.

We sincerely thank all the authors for contributing exceptionally high quality scientific original and review articles. The guest editors also thank the JPMER editorial team (PGIMER, Chandigarh, India) for entrusting us with the task of bringing out this thematic issue of the journal.

Sincerely yours

Baljinder Singh
Professor, Department of Nuclear Medicine
Postgraduate Institute of Medical Education and Research
Chandigarh, India

BR Mittal
Professor and Head, Department of Nuclear Medicine
Postgraduate Institute of Medical Education and Research
Chandigarh, India

Richard P Baum
Professor and Chairman, Clinical Director
Department of Theranostics, Center for Molecular Radiotherapy and Molecular Imaging, Zentralklinik Bad Berka, Bad Berka Germany

Michael K Schultz
Professor, Department of Radiology
Division of Nuclear Medicine, Carver College of Medicine
The University of Iowa, 500 Newton Drive
MLB180 FRRB, Iowa City, Iowa-52242, USA

10.5005/jp-journals-10028-1049
ORIGINAL ARTICLE

Ga-68 DOTATATE PET/CT in Neuroendocrine Tumors: Initial Experience

Bhagwant Rai Mittal, Kanhaiyalal Agrawal, Jaya Shukla, Anish Bhattacharya, Baljinder Singh Ashwani Sood, Anil Bhansali

ABSTRACT

Introduction: Neuroendocrine tumors (NET) are a heterogeneous group of neoplasms, majority of which express somatostatin (SST) receptors. Recently, with the widespread use of positron emission tomography/computed tomography (PET/CT) and development of novel PET tracers like Ga-68 DOTA peptide which specifically bind to somatostatin receptors (SSTR), Ga-68 DOTA peptide PET/CT is used in management of NET.

Objective: To study the various indications for which Ga-68 DOTATATE PET/CT scan was performed and the utility of the scans.

Materials and methods: Retrospective evaluation of the patients data was performed who underwent Ga-68 DOTATATE PET/CT as part of their diagnostic workup between June 2011 and July 2012. A total of 145 patients aged 1 to 71 years (mean: 37.4 years) were studied during this period.

Results: Ga-68 DOTATATE PET scan was positive in 23/39 patients referred for characterization or diagnosis, in 6/19 patients for localization, in 13/24 patients for detection of unknown NET primary, in 16/17 patients for staging, in 6/7 patients for recurrence assessment, 12/12 patients for response evaluation, 7/18 patients in restaging and in 5/5 differentiated thyroid cancer patients with thyroglobulin elevated but negative iodine scan.

Conclusion: Ga-68 DOTATATE PET/CT is a useful modality in characterization, localization, detection of unknown NET primary, staging, restaging, recurrence and response evaluation to treatment in patients with NET.

Keywords: Neuroendocrine tumors, Somatostatin, Gallium-68, DOTATATE, Positron emission tomography/computed tomography.

How to cite this article: Mittal BR, Agrawal K, Shukla J, Bhattacharya A, Singh B, Sood A, Bhansali A. Ga-68 DOTATATE PET/CT in Neuroendocrine Tumors: Initial Experience. J Postgrad Med Edu Res 2013;47(1):1-6.

Source of support: Nil

Conflict of interest: None declared

INTRODUCTION

Neuroendocrine tumors (NET) are heterogeneous group of neoplasms that arise from endocrine cells of the glands (adrenal medulla, pituitary, parathyroid) or from endocrine islets in the thyroid, pancreas, or the respiratory and gastrointestinal tract. The majority of NETs express somatostatin (SST) receptors. Thus, they can be effectively imaged with radiolabeled SST analogs. 'Somatostatin receptor scintigraphy (SRS)' with In-111 and Tc-99m-labeled SST analogs has been accepted as favored mode of imaging in the assessment of NET. Recently, with the widespread use of positron emission tomography/computed tomography (PET/CT) and development of novel PET tracers (Ga-68 DOTA-peptides), specifically binding to somatostatin receptors (SSTR) overexpressed on the surface of NET cells, allowed the visualization of NET with Ga-68 DOTA peptide PET/CT scans. PET/CT with Ga-68 DOTA peptides has been reported to present a higher sensitivity for the detection of well-differentiated NET than other imaging procedures (particularly CT and SRS).[1-4]

We share our experience of using Ga-68 DOTATATE imaging started in the year 2011. The data was analyzed with the aims to analyze the various indications for which ^{68}Ga-DOTATATE PET/CT scan was performed and the utility of the scans thereof.

MATERIALS AND METHODS

We retrospectively reviewed all patients who underwent Ga-68 DOTATATE PET/CT in the department of nuclear medicine, PGIMER, Chandigarh, India, as part of their diagnostic workup between June, 2011 and July, 2012. A total 145 patients (male 66, female 79) were enrolled in this study. Age of the patients ranged from 1 to 71 years (mean: 37.4 years). Detailed clinical history was available for all patients.

Ga-68 DOTATATE was synthesized in the inhouse radiopharmacy of the Department of Nuclear Medicine. Ga-68 was eluted from a Ge-68/Ga-68 generator (ITG, Germany), and DOTATATE was labeled with Ga-68 following the recommended procedure. Studies were performed on a dedicated PET/CT scanner (DISCOVERY STE-16, GE Healthcare, Milwaukee, USA). Acquisition was started 45 to 60 minutes after intravenous injection of approximately 1.5 MBq/kg body weight of Ga-68 DOTATATE. Whole-body scans were acquired in overlapped bed positions from base of skull to mid-thigh with the arms extended above the head. After transmission scan, 3D PET acquisition was performed at 2 minutes per bed position. Additional leg view was acquired in some patients, if indicated. CT was performed using tube current of 80 to 150 mA, without injection of contrast media. Data obtained from CT acquisition was used for low noise attenuation correction of PET emission data and for fusion

of attenuation corrected PET images with corresponding CT images. Image reconstruction was done using iterative reconstruction (ordered subset expectation maximum) algorithm. Transaxial, coronal and sagittal images were obtained after reconstruction.

RESULTS

Ga-68 DOTATATE was performed in 145 patients for various indications, including characterization or diagnosis in 39 of 145 patients (26.9%), localization in 19 of 145 (13.1%), detection of unknown NET primary in 24 of 145 patients (16.5%), staging in 17 of 145 patients (11.7%), recurrence assessment in seven of 145 (4.8%), response to treatment in 12 of 145 (8.3%), restaging in 18 of 145 (12.4%), surveillance in four of 145 (2.7%) and in thyroglobulin-elevated negative iodine scan (TENIS) patients in differentiated thyroid cancer (DTC) in five of 145 (3.4%). Thirty-nine patients underwent Ga-68 DOTATATE PET/CT for diagnosis or characterization of a lesion (Table 1), 19 patients for localization of the disease (Table 2). All the patients referred with suspicion of insulinoma (n = 5) or having suspicion for pheochromocytoma (n = 5) were PET negative for SSTR expression. Out of eight patients, who were referred to look for the site of primary with suspicious tumor induced osteomalacia, six showed positive results in detecting the site of tumor. One patient with suspicion of primary aldosteronism, PET was negative.

Ga-68 DOTATATE PET/CT was performed in 24 patients with histologically or cytologically proven NET for detection of unknown primary (Table 3). PET/CT localized primary tumor sites in 13/24 patients (54%) accurately and excluded any other site/s of involvement.

Table 2: Ga-68 DOTATATE PET scan results in patients for localization of the disease

Clinical condition	*Total no. of patients*	*Positive*	*Negative*
Insulinoma?	5	0	5
Pheochromocytoma?	5	0	5
Tumor-induced osteomalacia (TIO)	8	6	2
Primary hyperaldosteronism?	1	0	1
Total	19	6	13

Two representative ^{68}Ga-PET/CT scans in patients in whom metastatic NET disease was confirmed on cytology but the site of primary disease was not known, are presented in Figures 1A to 2E. Liver was the site of presentation (metastases in 17 patients of which PET indentified the site of primary in 6 patients.

Ga-68 DOTATATE PET/CT was performed in 17 patients, who were referred for staging of histologically or cytologically confirmed NET (Table 4). Ga-68 DOTATATE PET/CT was performed in seven patients with NET, for recurrence assessment (Table 5). PET was positive in 5/7 of patients (71%), while two patients were negative for recurrence. Ga-68 DOTATATE PET/CT study was done in 12 patients for response evaluation (Table 6). All the patients showed residual disease. Ga-68 DOTATATE PET/CT was performed in 18 patients with histologically or cytologically proven NET tumor for restaging after surgery (Table 7). PET/CT was positive in seven patients for SSTR expressing residual tumors. Ga-68 DOTATATE PET/CT was performed in five patients with TENIS syndrome in follow-up patients with DTC, for detection of dedifferentiated tumor (Table 8). PET/CT in all five patients

Table 1: Details of patients who underwent Ga-68 DOTATATE PET scan for lesion characterization

Clinical diagnosis	*Total no. of patients*	*Positive*	*Negative*	*Comments*
Neuroblastoma?	10	6	4 (2 positive at site other than primary)	Uptake also in bone in 6 and liver in one patient
Pheochromocytoma/ paraganglioma?	15	10	5	Multiple retroperitoneal nodes in one patient
Carcinoid?	3	2	1	Mesenteric carcinoid = 1, bronchial carcinoid = 1
Atypical hemangioma?	1	0	1	
Carotid body tumor?	1	1	-	
Nesidioblastosis?	1	1	-	Diffuse uptake in pancreas
Parathyroid adenoma?	1	0	1	
Pituitary microadenoma?	1	0	1	
MEN 1?	1	1	-	Uptake in head of pancreas and peripancreatic node
NET?	5	2	3	-
Total	39	23	16	

NET: Neuroendocrine tumor

Table 3: Ga-68 DOTATATE PET scan results in patients with histologically proven NET for localizing unknown primary site

Secondary	*Positive*	*Primary identified*
Liver (n = 17)	13	6 (pancreas = 2, multiple sites = 4)
Scalp (n = 1)	1	1 (meningioma)
Stomach (n = 3)	3	3 (stomach)
Cecum (n = 1)	1	1 (cecal carcinoid)
Neck node (n = 1)	1	1 (nasopharyngeal NET)
Postmediastinal mass (n = 1)	1	1 (postmediastinal mass)

Table 4: Ga-68 DOTATATE PET scan results in patients with histologically proven NET for initial staging of the disease

Primary	*No. of patients*	*Positive*	*Negative*	*Comments*
Carcinoid	4	4	–	Distant metastases = 3
Ganglioneuroma	1	1	–	Localized disease
NET breast	1	–	1	Primary was excised
NET pancreas	3	3	–	Distant metastases = 1
Neuroblastoma	6	6	–	Distant metastases = 5
Pituitary macroadenoma	1	1	–	Distant metastases = 1
Small-cell carcinoma pleural cavity	1	1	–	Locoregional metastases

Table 5: Ga-68 DOTATATE PET scan results in patients for evaluation of disease recurrence

Primary	*No. of patients*	*Positive*	*Negative*
Neuroblastoma	1	1	–
Carcinoid	3	2	1
Medullary thyroid cancer	1	1 (neck and mediastinum)	–
Pheochromocytoma	1	–	1
Pancreatic NET	1	1 (pancreas and greater omentum)	–

Table 6: Ga-68 DOTATATE PET scan results in patients studied for response evaluation

Primary	*No. of patients*	*Positive for residual disease*
Ileal carcinoid	5	5
Neuroblastoma	1	1
Medullary thyroid cancer	1	1
NET pancreas	3	3
NET ovary	1	1
NET lung	1	1

showed SRS-positive tissue. Ga-68 DOTATATE PET/CT surveillance scan was performed in four patients with NET (Table 9). All the four patients were negative for recurrence of disease.

DISCUSSION

NET, which constitutes a heterogeneous group of neoplasms, are generally considered as rare tumor.[5,6] However, the surveillance, epidemiology, and end Results (SEER) database analysis shows an increase in the reported annual age-adjusted incidence of NETs from (1.09/100,000) in 1973 to (5.25/100,000) in 2004.[7] Conventional imaging modalities (USG, CT, etc.) have limitation in detection of NET due to the small size, their variable anatomical location and the slow metabolic rate of well-differentiated forms. Scintigraphy with In-111 and Tc-99m-labeled SST analogs, has proven useful in diagnosing SSTR-positive tumors.[8,9]

Table 7: Ga-68 DOTATATE PET scan results in patients studied for restaging

Primary	*No. of patients*	*Positive*	*Negative*
Carcinoid	6	1	5
Pheochromocytoma	1	–	1
Paraganglioma	3	1	2
NET pancreas	3	2	1
NET thymus	1	–	1
NET liver	1	–	1
NET arytenoid	1	1	–
Gastrinoma	1	1	–
Pituitary carcinoma	1	1	–

Table 8: Ga-68 DOTATATE PET scan results in patients studied for TENIS syndrome

Thyroglobulin level (ng/ml)	*Positive SST receptor scan*
115.5	Cervical nodes
17	Cervical nodes
17.90	Remnant and cervical nodes
30	Cervical nodes
82	Thyroid bed soft tissue nodule

TENIS: Thyroglobulin-elevated negative iodine scintigraphy

Table 9: Ga-68 DOTATATE PET scan results in patients studied for surveillance

Primary	*Ga-68 DOTATATE PET/CT findings*
Ileal carcinoid	Negative
NET	Negative
MEN 1	Negative
Thymic carcinoid	Negative

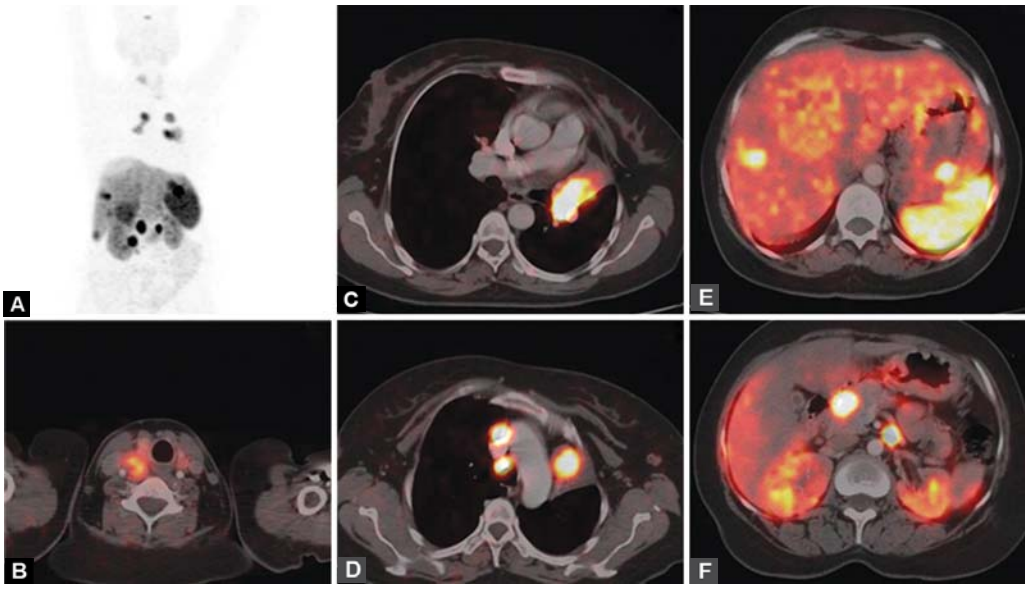

Figs 1A to F: A 42 years old female patient presented with abdominal pain and swelling of face, feet and hand. Ultrasonography of abdomen revealed multiple heterogeneously echoic lesions of varying sizes in both lobes of liver which revealed NET on FNAC. Ga-68 DOTATATE PET/CT scan: (A) MIP showed SSTR-expressing lesions at multiple sites which were further localized in the, (B) left lobe of thyroid gland (likely medullary thyroid cancer), (C) left lung (likely bronchial carcinoid), (D) mediastinal lymph nodes, (E) liver and stomach, (F) head of pancreas and abdominal lymph nodes. The PET scan findings are indicative of multiple endocrine neoplasia

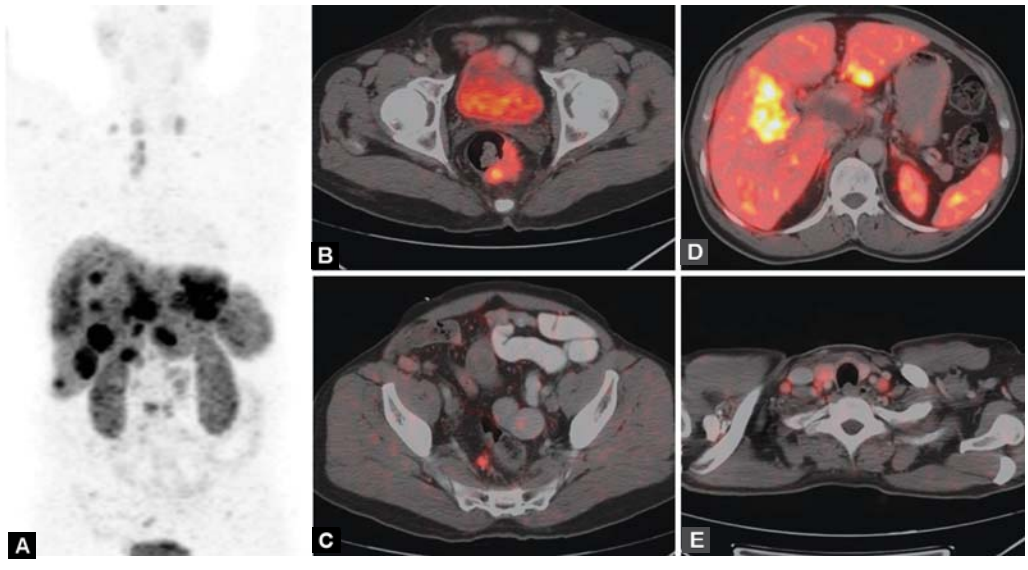

Figs 2A to E: Ga-68 DOTATATE PET/CT images of a 55 years old male patient with metastatic NET in liver and unknown primary showing multiple sites of SSTR-expressing lesions on MIP image: (A) In the rectum, (B) pararectal lymph nodes, (C) liver (D) and cervical and mediastinal lymph nodes (E), indicative of likely primary site in rectum with widespread metastases

The detection rate was reported to be between 80 and 100% in different studies. Moreover, SSTR expression has been correlated well with the prognosis, as SSR expressing NET shows good response to treatment with SST analogs.[10]

Recent introduction of PET/CT and its wide availability has lead to search for several new positron emitting radiotracers. One among this is SST analogs labeled with Ga-68 (Ga-68-DOTA peptides), which has several advantages over conventional SRS. Firstly, gallium-68 is generator produced and labeling of Ga-68 with DOTA peptides is relatively easy. Secondly, resolution of PET/CT imaging is far better than gamma camera, thus better visualization of lesion is a benefit. Also, this is less time-consuming than SRS (roughly 1.5 hours, instead of up to 24 hours acquisition in SRS). Finally, PET/CT provides advantage of semiquantification of the lesions.

Ga-68 DOTA-peptides have high affinity for SSTR.[11,12] SST is a small, cyclic neuropeptide that is present in neurons and endocrine cells; it has a high density in the brain, peripheral neurons, endocrine pancreas and gastrointestinal tract. The majority of NETs express SSTR, so they can be effectively targeted and visualized with radiolabeled SST analogs *in vivo*.[12] Gastroenteropancreatic tumors (both functioning and nonfunctioning), pheochromocytoma,

paraganglioma, neuroblastoma and ganglioneuroma, medullary thyroid carcinoma, pituitary adenoma, Merkel cell carcinoma, small-cell lung cancer usually show high SSTR expression.[4,13-19] Low receptor expression is seen in the breast cancer, melanoma, lymphomas, prostate cancer, non-small cell lung cancer, sarcomas, renal cell carcinoma, DTC, astrocytoma, meningioma.[20,21]

Structurally Ga-68 DOTA peptides are made of three parts, the radioisotope (Ga-68), chelate (DOTA) and a peptide (TOC, NOC, TATE). This later component binds directly to SSTR. Six different types (1, 2A, 2B, 3, 4 and 5) of SSTR have been identified in humans. The three available tracers (DOTA-TOC, DOTA-NOC, DOTA-TATE) differs in their ability to bind with different SST subtypes.[22] All three can bind to SSTR 2, whereas DOTA-NOC also shows good affinity for SSTR 3 and 5 and DOTA-TOC also binds to SSTR 5 (although with lower affinity than DOTA-NOC). ^{68}Ga-DOTATATE presents a predominant affinity for SSTR 2.

The main clinical indication of Ga-68 DOTA-peptides PET/CT is the imaging of NETs. It can be used in some cases of non-NET, if treatment with radiolabeled therapeutic SST analogs is considered. Ga-68 DOTA peptides imaging can be used in NET to localize primary tumors, staging, restaging, recurrence detection[4,13-19,23-25] monitor the response to therapy,[26] to determine SSTR status to select the patients for SSTR radionuclide therapy.[26,27] In the present study, Ga-68 DOTATATE PET scan was positive in 23/39 (59%) patients referred for characterization or diagnosis, in 6/19 (31.5%) patients for localization, in 13/24 (54%) patients for detection of unknown NET primary, in 16/17 (94%) patients for staging, in 6/7 (85%) patients for recurrence assessment, 12/12 (100%) patients for response evaluation and 7/18 (38.8%) patients in restaging. All the five DTC patients, who underwent ^{68}Ga-DOTATATE PET scan for TENIS syndrome showed tracer uptake, thus guiding the further management in these patients.

Usually no patient preparation is needed before the test and there is no need for fasting before the test, unlike FDG PET/CT study. Some experts recommend temporary withdrawal of SST analog therapy, if possible, to avoid SSTR blockade. The time interval between withdrawal of therapy and Ga-68 DOTA peptides scan depends on the type of drugs used: One day is suggested for short-lived molecules and 3 to 4 weeks for long-acting analogs. However, this issue is still controversial. The minimum recommended administered activity for adult patient is 100 MBq. Maximal tumor activity accumulation is reached 50 to 90 minutes postinjection.[2]

Physiological tracer uptake is seen in the liver, spleen, kidneys and pituitary. The thyroid and salivary glands are faintly visible. The prostate gland and breast glandular tissue may show diffuse low-grade Ga-68 DOTA-conjugate peptides uptake. The pancreas shows variable uptake of Ga-68 DOTA peptides, due to physiological presence of SSTR 2. A potential pitfall in image interpretation may be the uptake of tracer in the pancreatic head due to accumulation of islets in one pancreatic region, which may mimic focal tumor disease.[4] Inflammation may be the another potential cause of pitfalls in image interpretation, since SST are expressed on activated lymphocytes, and therefore Ga-68 DOTA peptides may be falsely positive in inflamed areas. Moreover, an accessory spleen or physiological activity at the adrenal level should be borne in mind while interpreting the images.

One point the referring physician should be aware of, is the positive findings on ^{68}Ga-DOTA peptides PET/CT reflects increased density of SSTR rather than malignant disease. Thus, a poorly differentiated NET, i.e. poorly SSTR expressing tumor, may not show tracer uptake. Also heterogeneous expression of SSTR subtypes may influence the affinity for ^{68}Ga-DOTA peptides.

CONCLUSION

Ga-68 DOTATATE PET/CT is useful in characterization, localization, unknown NET primary, staging, restaging, recurrence and response evaluation to treatment in NET.

REFERENCES

1. Kaltsas G, Rockall A, Papadogias D, et al. Recent advances in radiological and radionuclide imaging and therapy of neuroendocrine tumours. Eur J Endocrinol 2004;151:15-27.
2. Hofmann M, Maecke H, Borner R, et al. Biokinetics and imaging with the somatostatin receptor PET radioligand ^{68}Ga-DOTATOC: Preliminary data. Eur J Nucl Med 2001;28:1751-57.
3. Kowalski J, Henze M, Schuhmacher J, Macke HR, Hofmann M, Haberkorn U. Evaluation of positron emission tomography imaging using ^{68}Ga-DOTA-D-Phe 1-Tyr3-octreotide in comparison to [111 In]-DTPAOC SPECT: First results in patients with neuroendocrine tumors. Mol Imag Biol 2003;5:42-48.
4. Gabriel M, Decristoforo C, Kendler D, et al. ^{68}Ga-DOTA-Tyr3-octreotide PET in neuroendocrine tumors: Comparison with somatostatin receptor scintigraphy and CT. J Nucl Med 2007;48:508-18.
5. Modlin IM, Kidd M, Latich I, Zikusoka MN, Shapiro MD. Current status of gastrointestinal carcinoids. Gastroenterology 2005;128:1717-51.
6. Taal BG, Visser O. Epidemiology of neuroendocrine tumours. Neuroendocrinology 2004;80(Suppl 1):3-7.
7. Yao JC, Hassan M, Phan A, et al. One hundred years after 'carcinoid': Epidemiology of and prognostic factors for neuroendocrine tumors in 35,825 cases in the United States. J Clin Oncol 2008;26:3063-72.
8. Olsen JO, Pozderac RV, Hinkle G, et al. Somatostatin receptor imaging of neuroendocrine tumors with indium-111 pentetreotide (Octreoscan). Semin Nucl Med 1995 Jul;25(3):251-61.

9. Bombardieri E, Maccauro M, De Deckere E, Savelli G, Chiti A. Nuclear medicine imaging of neuroendocrine tumours. Ann Oncol 2001;12 (Suppl 2):S51-61.
10. Lebtahi R, Cadiot G, Sarda L, et al. Clinical impact of somatostatin receptor scintigraphy in the management of patients with neuroendocrine gastroenteropancreatic tumors. J Nucl Med 1997;38:853-58.
11. Reubi JC. Peptide receptors as molecular targets for cancer diagnosis and therapy. Endocr Rev 2003;24:389-427.
12. Reubi JC, Waser B. Concomitant expression of several peptide receptors in neuroendocrine tumors: Molecular basis for in vivo multireceptor tumour targeting. Eur J Nucl Med Mol Imag 2003;30:781-93.
13. Ambrosini V, Marzola MC, Rubello D, Fanti S. (68)Ga-somatostatin analogues PET and (18)F-DOPA PET in medullary thyroid carcinoma. Eur J Nucl Med Mol Imag 2010;37:46-48.
14. Conry BG, Papathanasiou ND, Prakash V, et al. Comparison of (68)Ga-DOTATATE and (18)F-fluorodeoxyglucose PET/CT in the detection of recurrent medullary thyroid carcinoma. Eur J Nucl Med Mol Imag 2010;37:49-57.
15. Kayani I, Bomanji JB, Groves A, et al. Functional imaging of neuroendocrine tumors with combined PET/CT using ^{68}Ga-DOTATATE (DOTA-DPhe1,Tyr3-octreotate) and 18F-FDG. Cancer 2008;112:2447-55.
16. Ambrosini V, Tomassetti P, Castellucci P, et al. Comparison between ^{68}Ga-DOTA-NOC and ^{18}F-DOPA PET for the detection of gastro-entero-pancreatic and lung neuroendocrine tumours. Eur J Nucl Med Mol Imag 2008;35:1431-38.
17. Fanti S, Ambrosini V, Tomassetti P, et al. Evaluation of unusual neuroendocrine tumours by means of ^{68}Ga-DOTA-NOC PET. Biomed Pharmacother 2008;62:667-71.
18. Kayani I, Conry BG, Groves AM, et al. A comparison of ^{68}Ga-DOTATATE and ^{18}F-FDG PET/CT in pulmonary neuroendocrine tumors. J Nucl Med 2009;50:1927-32.
19. Ambrosini V, Castellucci P, Rubello D, et al. ^{68}Ga-DOTA-NOC: A new PET tracer for evaluating patients with bronchial carcinoid. Nucl Med Commun 2009;30:281-86.
20. Klutmann S, Bohuslavizki KH, Brenner W, et al. Somatostatin receptor scintigraphy in postsurgical follow-up examinations of meningioma. J Nucl Med 1998;39:1913-17.
21. Henze M, Dimitrakopoulou-Strauss A, Milker-Zabel S, et al. Characterization of ^{68}Ga-DOTA-D-Phe1-Tyr3-octreotide kinetics in patients with meningiomas. J Nucl Med 2005;46: 763-69.
22. Antunes P, Ginj M, Zhang H, et al. Are radiogallium-labelled DOTA-conjugated somatostatin analogues superior to those labelled with other radiometals? Eur J Nucl Med Mol Imag 2007;34:982-93.
23. Prasad V, Ambrosini V, Hommann M, Hoersch D, Fanti S, Baum RP. Detection of unknown primary neuroendocrine tumours (CUP-NET) using (68)Ga-DOTA-NOC receptor PET/CT. Eur J Nucl Med Mol Imag 2010;37:67-77.
24. Putzer D, Gabriel M, Henninger B, et al. Bone metastases in patients with neuroendocrine tumor: ^{68}Ga-DOTA-Tyr3-octreotide PET in comparison to CT and bone scintigraphy. J Nucl Med 2009;50:1214-21.
25. Ambrosini V, Nanni C, Zompatori M, et al. (68)Ga-DOTA-NOC PET/CT in comparison with CT for the detection of bone metastasis in patients with neuroendocrine tumours. Eur J Nucl Med Mol Imag 2010;37:722-27.
26. Gabriel M, Oberauer A, Dobrozemsky G, et al. ^{68}Ga-DOTA-Tyr3-octreotide PET for assessing response to somatostatin-receptor-mediated radionuclide therapy. J Nucl Med 2009;50: 1427-34.
27. Ugur O, Kothari PJ, Finn RD, et al. Ga-66 labeled somatostatin analogue DOTA-DPhe1-Tyr3-octreotide as a potential agent for positron emission tomography imaging and receptor mediated internal radiotherapy of somatostatin receptor positive tumors. Nucl Med Biol 2002;29:147-57.

ABOUT THE AUTHORS

Bhagwant Rai Mittal (Corresponding Author)

Professor and Head, Department of Nuclear Medicine and PET Postgraduate Institute of Medical Education and Research Chandigarh India, Phone: 91-172-2756722, Fax: 91-172-2742858 e-mail: brmittal@yahoo.com

Kanhaiyalal Agrawal

Senior Resident, Department of Nuclear Medicine and PET Postgraduate Institute of Medical Education and Research, Chandigarh India

Jaya Shukla

Assistant Professor, Department of Nuclear Medicine and PET Postgraduate Institute of Medical Education and Research, Chandigarh India

Anish Bhattacharya

Additional Professor, Department of Nuclear Medicine and PET Postgraduate Institute of Medical Education and Research, Chandigarh India

Baljinder Singh

Professor, Department of Nuclear Medicine and PET, Postgraduate Institute of Medical Education and Research, Chandigarh, India

Ashwani Sood

Assistant Professor, Department of Nuclear Medicine and PET Postgraduate Institute of Medical Education and Research, Chandigarh India

Anil Bhansali

Professor and Head, Department of Endocrinology, Postgraduate Institute of Medical Education and Research, Chandigarh, India

10.5005/jp-journals-10028-1050
ORIGINAL ARTICLE

Can the Standardized Uptake Values derived from Diagnostic ^{68}Ga-DOTATATE PET/CT Imaging Predict the Radiation Dose delivered to the Metastatic Liver NET Lesions on ^{177}Lu-DOTATATE Peptide Receptor Radionuclide Therapy?

Baljinder Singh, Vikas Prasad, Christiane Schuchardt, Harshad Kulkarni, Richard P Baum

ABSTRACT

Introduction: Neuroendocrine neoplasms express somatostatin receptors, enabling the use of somatostatin analogs for molecular imaging, when labeled with the positron-emitter ^{68}Ga for receptor positron emission tomography/computed tomography (PET/CT), and targeted radionuclide therapy, when labeled with beta-emitters, e.g. ^{90}Y and ^{177}Lu.

Aim: To investigate if ^{68}Ga-DOTATATE PET-derived standardized uptake values (SUV) correlate with the dose delivered to the liver lesions following ^{177}Lu-DOTATATE radionuclide therapy in patients with neuroendocrine neoplasms.

Materials and methods: Twelve adult (8M: 4F; mean age: 55.9 ± 14.5 years; range: 23-78 years) patients with documented neuroendocrine tumor (NET) disease and liver metastases were enrolled in the study. Ten patients were subjected to ^{68}Ga DOTATATE and one patient each underwent ^{68}Ga-DOTA-TOC and ^{68}Ga-DOTANOC diagnostic PET/CT imaging. Subsequently, on the basis of positive PET/CT scan findings for the metastatic NET disease, all these patients were subjected to peptide receptor radionuclide therapy (PRRNT) with ^{177}Lu-DOTATATE. The reconstructed PET/CT data was used to calculate the SUVs on the identifiable liver lesions. The scintigraphic data acquired (anterior and posterior whole body images) following therapeutic doses of ^{177}Lu-DOTATATE were subjected to the quantitative analysis (HERMES workstation and OLINDA/EXM software) to calculate the dose delivered to the hepatic lesions.

Results: The initial results of this preliminary study indicate poor correlation between SUV and the tumor dose and the linear regression analysis provided R2 values which explained only a small fraction of the total variance.

Conclusion: The SUVs derived from ^{68}Ga-DOTA-peptide PET/CT images should be used with caution for the prediction of tumor dose on ^{177}Lu-DOTA-peptide therapy as there are large intra- and interpatient variability. Further studies with large numbers of patients are warranted to establish such a correlation between SUV, tumor dose and the response assessment.

Keywords: ^{68}Ga-DOTATATE, Positron emission tomography/computed tomography, Neuroendocrine tumors, ^{177}Lu-DOTATATE, Peptide receptor radionuclide therapy, Standardized uptake values, Dosimetry.

How to cite this article: Singh B, Prasad V, Schuchardt C, Kulkarni H, Baum RP. Can the Standardized Uptake Values derived from Diagnostic ^{68}Ga-DOTATATE PET/CT Imaging Predict the Radiation Dose delivered to the Metastatic Liver NET Lesions on ^{177}Lu-DOTATATE Peptide Receptor Radionuclide Therapy? J Postgrad Med Edu Res 2013;47(1): 7-13.

Source of support: Nil

Conflict of interest: None declared

INTRODUCTION

A major factor in the evaluation of newer radiopharmaceuticals used for diagnosis and treatment is the absorbed dose from internally deposited radionuclides. Metastasized neuroendocrine tumors (NETs) have only a few treatment options. As majority of the NETs or gastroenteropancreatic (GEP) tumors possess somatostatin receptors (SSTRs) and therefore, can be diagnosed and treated with radiolabeled octreotide analogs.[1] ^{68}Ga-DOTA-[Tyr^3]octreotide (DOTA-TOC), ^{68}Ga-DOTA-[Tyr^3] octreotate (DOTATATE) or ^{68}Ga-DOTA-[1-NaI^3]octreotide (DOTANOC) have been used effectively for the accurate diagnosis of NETs due to the high affinity of these radioligands to the SSTR expression on these tumors.[2-5]

Radiopeptide therapy in patients with metastasized NETs is most commonly performed by using yttrium-90 (^{90}Y) and lutetium-177 (^{177}Lu).[6,7] ^{90}Y, being a pure β-emitter, does not allow the direct measurements of the dosimetric data, only the indirect estimates are possible with the use of ^{111}In-peptide that mimic the biodistribution and dose delivery response of ^{90}Y. On the contrary, ^{177}Lu despite having β-emission and good labeling efficiency with the octreotide analogs also have gamma emission suitable for scintigraphy and appropriate dosimetry. Therefore, ^{177}Lu-labeled DOTATOC/TATE are the most suitable radiopeptides for treating NETs.^{177}Lu-DOTATATE has been reported to be very effective in the treatment of NETs in experimental animals and subsequently since its first clinical use in humans.[8,9] Among all the commercially available SSTR analogs, DOTANOC is reported to have the highest affinity to SSTR-3 and 5 followed by SSTR-2.[4,5] However, a recent study has shown that the higher affinity of DOTANOC to SSTR-3, 4, 5 leads to a higher uptake in normal tissue and therefore results in an increase in the whole body dose as compared to ^{177}Lu-DOTATATE.[10]

It is generally considered that the patients with NET metastatic lesions having high standardized uptake values (SUV) on ^{68}Ga-DOTA-peptide positron emission tomography (PET) have good prognosis following peptide receptor radionuclide therapy (PRRNT). But, no information exits in the literature on the correlation between the SUV values, and the dose delivered to the target lesions on PRRT. Therefore, in the present study, we report our first preliminary results on the correlation between SUV (derived from ^{68}Ga-PET data) and the tumor dose delivered to the liver target lesions after the PRRT with ^{177}Lu-DOTATATE in patients with metastatic NET disease.

MATERIALS AND METHODS

Radiochemistry

^{68}Ga was eluted from ^{68}Ge/^{68}Ga generator (Eckert and Ziegler, Berlin, Germany) and radiolabeled with peptides as ready to use (intravenous) patients' preparations were prepared in house by the Radiopharmacy Division of the Zentralklinik, Bad Berka, Germany and the detailed methodology is described elsewhere.[2]

Pure salts of DOTATOC, DOTATATE and DOTANOC were procured from JPT (JPT Peptide Technologies GmbH, Volmerstrasse 5 (UTZ) 012489, Berlin, Germany) and a standard laboratory procedure for radiolabeling peptides with ^{177}Lu was followed.[11] Briefly, a solution of 500.0 µg of 2, 5 dihydroxybenzoic acid and 50.0 µg of the corresponding DOTA-peptide in 50.0 µl of 0.4 M sodium acetate buffer (pH adjusted to 5.5) was added to 1.0 GBq of ^{177}Lu (high specific activity of ≥80.0 Ci/mg, RNP > 99%, supplied by ITG Isotope technologies, Garching GmbH, Germany) contained in 30 µl of 0.05 M HCl. The contents were heated at 90°C for 30 minutes and then diluted with 0.9% saline solution followed by appropriate sterile filtration. The radiochemical purity of the labeled DOTA-peptides was always greater than 99%.

Patients

Twelve adult patients (8M:4F; mean age: 55.9 ± 14.5 years; range: 23-78 years) having documented NET with liver metastases were enrolled in the study. Intense SSTR expression on the primary tumors and metastases rendering the patients inoperable was the inclusion criteria for considering the patients for PRRNT. Ten patients were subjected to ^{68}Ga-DOTATATE and one patient each underwent ^{68}Ga-DOTATOC and ^{68}Ga-DOTANOC diagnostic positron emission tomography/computed tomography (PET/CT) imaging. Subsequently, based on positive ^{68}Ga-PET/CT scan findings for the metastatic NET disease, all these patients were subjected to PRRNT with ^{177}Lu-DOTATATE. An informed written consent was taken from all the patients who participated in the study and the study protocol was approved by the ethics committee of the institute.

Prior to PET/CT imaging and PRRNT, the patients were instructed to intake of long-acting release preparation of sandostatin for 4 to 6 weeks and subcutaneous treatment with octreotide for at least 2 days. Patients were adequately hydrated and just before the PET/CT acquisition were administered with 1.5 L of oral contrast (Gastrografin dispersion).

The scanning was performed on a dual modality PET/CT (Biograph duo, Siemens Medical Solutions, Germany) at a mean postinjection (PI) time of 72.9 ± 12.0 minutes (range: 60-95 minutes) following an intravenous injection of a mean activity of 130.0 ± 18.5 MBq (106-182 MBq) of ^{68}Ga-labeled peptide. The patients were instructed to void the bladder and lie supine on the table with the arms extending over the head. First a topogram from the skull to the upper thighs was acquired over 1,024 mm axially in 7-8 bed positions. After administration of 100 ml of contrast (given as IV infusion), contrast enhanced CT was acquired in the craniocaudal direction with a 30-second delay. CT was performed in the spiral mode using a continuous acquisition at 130 kVp, 115 mAs, 4 mm collimation, 5 mm slice width, a table feed of 8 mm per rotation at 0.8-second rotation time and 2.4 mm slice spacing. During the CT acquisition, a limited breath hold protocol was followed and after completion of the CT acquisition, the patients were automatically moved to the PET start position (rear of the gantry) and 3D PET emission scanning started in the caudocranial direction. An emission scan time of 1 to 2 minutes (normalized to the height and weight of the patient) per bed position was used with a total emission scan time of no more than 24 minutes and a total PET/CT acquisition of about 30 minutes.

The reconstructed PET/CT images were displayed in three (cross-sectional, coronal and sagittal) different planes and all the metastatic target lesions on the liver and elsewhere were identified by two experienced nuclear medicine physicians and a radiologist. All the target lesions were subjected to a quantitative analysis to calculate the SUV_{max}, SUV_{mean} and molecular tumor volume (MTV; cm^3). In addition, the diagnostic CT data were used to calculate the thickness of liver, spleen, kidney and body thickness in the abdominal region harboring the metastatic liver disease and volumetric measurements of the target lesions.

Post PRRNT Scan

Anterior and posterior whole body images were acquired, at different time intervals following an IV infusion of ^{177}Lu-DOTATATE (mean activity: 6,711 ± 659 MBq; range: 5,500-8,500 MBq), under the dual head gamma camera (MEDISO, Medical Imaging Systems, Badapast, Hungary) peaked at 208 keV; 15% energy window, scan speed 15 cm/min) by using medium energy general purpose (MEGP) collimator. The first whole body scan acquired immediately without allowing the patients to void represented 100% of the administered radioactivity. The subsequent scans acquired at 3, 20, 44 and 68 hours following radioactivity infusion reflected only the percent fraction of the total injected activity. The quantitative analysis was carried out first on the 20 hours whole body images by drawing regions of interest (ROIs) manually over the source organ by using a dedicated HERMES computer system (Gold software version 3.0.92, HERMES, Medical Solutions, Stockholm, Sweden). The whole body anterior and posterior scans were displayed (by using the HERMES, computer algorithm, Whole Body Display whole Version 3.3) and the ROIs drawn on the 20-hour scans were applied to the scans acquired at the other four intervals. The quantification was always done by the same physicist under the guidance of a nuclear medicine physician who decided the quantifiable lesions as 'target lesions' for dosimetric evaluation. For these calculations, always the geometric mean data normalized for the background were calculated which accounted for the physical characteristics of the organ/patient and also for the counts due to the adjacent background or the underlying organs. The time-activity curves were drawn which were fitted depending upon the nature of the curve whether mono and/or biexponential function. The integration of this curve gave the total number of disintegrations or the residence times (equivalent to the cumulated activity) of the region. The effective half-lives of the radiopharmaceutical (^{177}Lu-DOTATATE) was determined by using the exponential fit-function by using a computer program (Origin Pro 7.0G). Finally, the absorbed organ and tumor doses were estimated using the residence times and the computer software OLINDA/EXM which used the S-values for the radionuclide and different phantoms. Specifically, the mean absorbed tumor doses were estimated by using the unit density sphere module of OLINDA/EXM. Dosimetry results were obtained for the whole body, normal tissue, spleen, kidneys and for liver metastatic lesions. An appropriate statistical analysis of the data was conducted to find a significant correlation, if any, between the SUV values, volumetric data of the tumors/target lesions and the dose delivered to these target lesions.

RESULTS

The patients' demographic details and the various quantitative parameters on the lesions' characterization and the dose delivered (sV) to the target lesions are presented in Table 1. A total of 27 liver metastatic lesions (range 1-6 lesions with at least 1 lesion/patient) were visualized

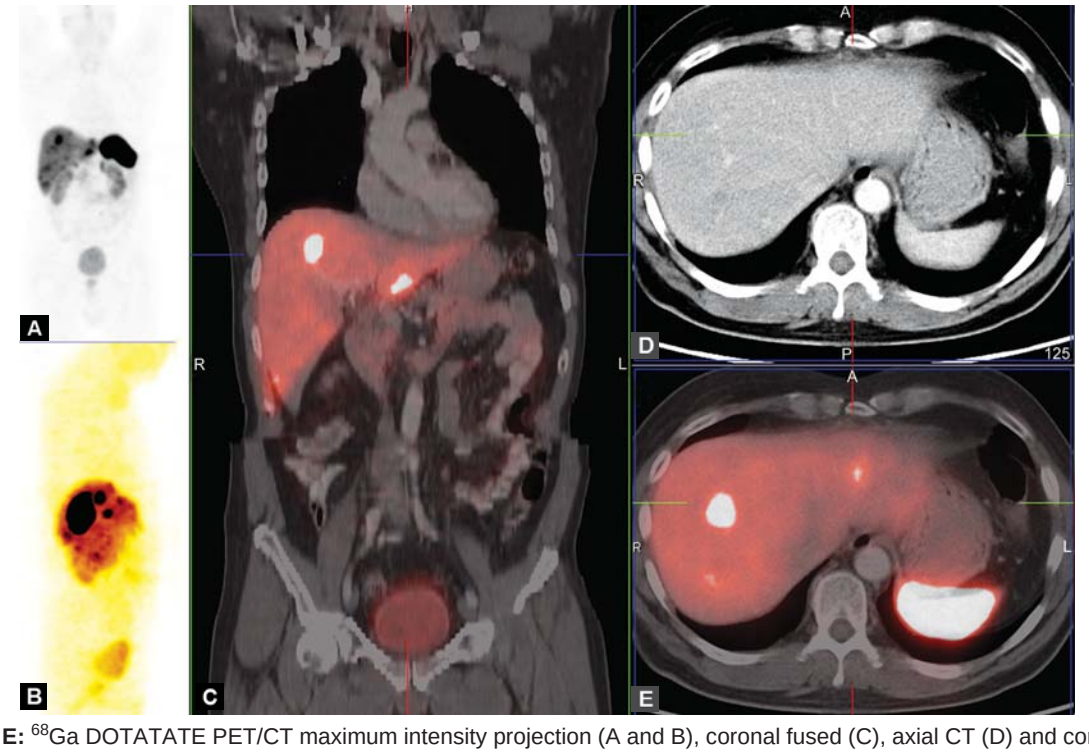

Figs 1A to E: ^{68}Ga DOTATATE PET/CT maximum intensity projection (A and B), coronal fused (C), axial CT (D) and corresponding axial fused (E) images demonstrating multiple areas of focal tracer uptake in the liver

Table 1: Patients' demographic details, radionuclide doses, location of liver metastatic lesions and their characterization on the PET/CT imaging and the dose delivered to the target lesions on ^{177}Lu-PRRT

Sr. no.	*Age (year)*	*Sex*	*^{68}Ga-scanning PET scanning*		*Postinjection scan time (min)*	*^{177}Lu-DOTATATE-PRRT therapy dose (MBq)*	*Lesion no.*	*Location*	*Standard uptake value (SUV)*		*Mean tumor volume (cm^3)*	*Dose delivered to the tumor after ^{177}Lu-PRRT*
			Radiopharma-ceutical	Dose (MBq)					SUV_{max}	SUV_{mean}	MTV (cm^3)	sV
1.	23	M	DOTATATE	126.0	65	7000	1.	S7 (apicocentral)	7.2	5.8	5.5	8
							2.	S6 (caudal)	7.6	5.4	6.9	16
							3.	S4b (caudal)	8.5	5.3	8.0	47
2.	65	M	DOTATATE	129.0	60	7400	4.	S2-apical	10.8	6.9	12.2	111
3.	72	F	DOTATATE	122.0	65	6000	5.	S7/S8 (apicodorsal)	9.6	6.1	5.2	54
4.	54	M	DOTATATE	135.0	80	7000	6.	S2/S8	14.8	7.5	159.4	36
							7.	S4b (caudal)	11.5	7.3	63.4	81
5.	59	M	DOTATATE	182	65	7000	8.	S2 (apical)	10.1	6.6	15.3	143
6.	50	F	DOTATATE	106	65	8500	9.	S5	8.6	6.6	5.8	253
7.	45	M	DOTATATE	117.0	95	6000	10.	S6 (caudal)	17.3	8.3	5.9	80
							11.	S6 (caudal)	10.3	6.3	4.3	80
8.	66	F	DOTATOC	133.0	70	7500	12.	S8	39.4	22.6	14.4	92
							13.	S4b	37.8	22	6.6	100
							14.	S6	53.4	29.4	11.2	65
9.	62	M	DOTANOC	129.0	80	7000	15.	S3 (caudal)	16.1	8.9	22.3	83
10.	49	M	DOTATATE	117.0	70	7000	16.	S3 (caudal)	11.7	6.4	9.2	82
							17.	S4a	14.2	7.9	23.8	38
							18.	S5 (caudal central)	15.1	8.5	29.9	54
							19.	S5	13	8.1	62.2	26
11.	78	M	DOTATATE	135	65	7000	20.	S2/S3	40.6	23.8	17.2	72
							21.	S3 (caudal)	28.9	17.2	10.7	27
12.	48	F	DOTATATE	129.0	95	5500	22.	S2/S3	37.3	23	56.8	38
							23.	S5	25.1	15.2	20.9	52
							24.	S3	29.5	16	11.8	20
							25.	S6 (caudal)	37	21.7	14.5	30
							26.	S3	29.6	16.9	25.3	11
							27.	S4a	32.2	20.2	69.8	56
Mean ± SD	55.9 ± 14.5 (23-78)	8M:4F		130.0 ± 18.5 (106-182)	72.9 ± 12.0 (60-95)	6908 ± 787 (5500-8500)			21.4 ± 13.1 (7.2-53.4)	12.6 ± 7.4 (5.3-29.4)	25.9 ± 32.9 (5.2-159.4)	65 ± 49 (8-253)

Table 2: Linear regression analysis of the dose delivered to the target lesions with the SUV_{max} or SUV_{mean}

Variable	*β (SE)*	*Significance*	*Constant*	*R2*
SUV_{max}	–0.629 (0.751)	0.41	78.44	0.027
SUV_{mean}	–0.996 (1.33)	0.46	77.55	0.022

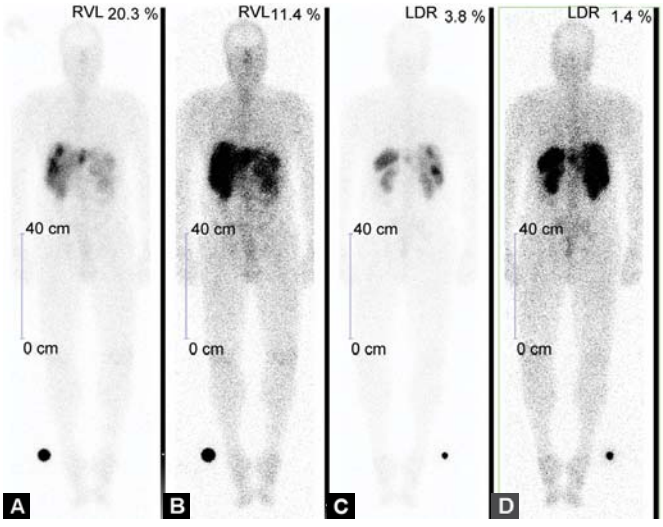

Figs 2A to D: ^{177}Lu-DOTATATE whole body dual intensity anterior (A and B) and posterior (C and D) images at 24 hours post injection

on PET/CT metabolic imaging and were quantifiable both on ^{68}Ga-DOTA-peptide PET/CT images as well on ^{177}Lu-DOTATATE therapeutic whole body scintigraphic scans. A representative ^{68}Ga-DOTATATE PET/CT scan (Figs 1A to E) showing three lesions in the right liver lobe very distinctly delineated on the transversal PET/CT fusion image. The corresponding liver lesions are also demonstrated on anterior and posterior whole body ^{177}Lu-DOTATATE images in the same patient acquired at 24 hours postinjection (Figs 2A to D).

The average SUV_{max} and SUV_{mean} for the liver metastatic lesions (n = 27) were 21.4 ± 13.1 (range: 7.2-53.4) and 12.6 ± 7.4 (range: 5.3-29.4) respectively. The mean tumor volume (MTV-cm^3 by PET/CT) was 25.9 ± 32.9 cm^3 (range: 5.2-159.4). The mean tumor dose delivered to the target liver lesions was 65.0 ± 49.0 sV (range: 8-253).

The SUV_{max} values were observed to be highly variable (7.2-53.4). For the lesion (lesion-9, patient-6, Table 1) with SUV_{max} of 8.6, the dose delivered was 253 sV. On the other hand, in the lesion (lesion-14, patient-8) with SUV_{max} of 53.4, the dose delivered was 65.0 sV.

STATISTICAL ANALYSIS

Nonparametric Spearman's test (SPPS-16 for Windows) was used to study the correlations between the various parameters. No significant correlation was observed between the SUV_{max} or SUV_{mean} with the dose delivered to the target lesions (r = 0.039 and 0.007). Linear regression analysis of dose delivered with the SUV_{max} or mean values did not reveal any significant associations (Table 2). The R2 values were very low suggesting that the equations explained only a very small fraction of the total variance.

DISCUSSION

PPRNT using the somatostatin analog [^{177}Lu-DOTA^0, Try^3] octreotide is a convincing treatment modality for metastasized NETs. The radionuclide in turn is retained in the lysosomes of the tumor cells, close to the nuclei and the irradiation to these nuclei will damage DNA leading to apoptosis and necrosis of the cell.[11] The maximal tissue range of 2 mm with ^{177}Lu appears to be more favorable for the treatment of small metastases, while ^{90}Y with a maximal range of 11.3 mm has a stronger cross fire effect and seems to have better efficiency in bigger tumors.[12,13] ^{177}Lu-labeled analogs have been reported to show less nephrotoxicity than the ^{90}Y-labeled counterparts.[14] In a recent study, Wehrmann et al[10] have reported that ^{177}Lu-DOTANOC due to its higher affinity lead to a higher uptake in normal tissue and therefore resulted in a higher whole body dose, however the uptake in tumor lesions and the mean absorbed tumor dose was higher for ^{177}Lu-DOTATATE.[10] It was thus, decided to treat our patients subsequently with ^{177}Lu-DOTATATE and to perform dosimetry to see correlation, if any, between the SUV and the dose delivered to the metastatic liver-target lesions. The currently used, regimens of cumulative dose of about 800 mCi of ^{177}Lu-DOTATATE therapy in four cycles (after 6-10 d) of 200 mCi (7,400 MBq) has been reported to be effective in treating the metastatic NET disease without any renal toxicity.[7] With this approach, approximately, 80% of the patients having progressive disease at the start of therapy are reported to attain stable disease, partial or complete remission.[12,15,16]

The uptake of the radionuclide and thus the dose delivered to the target metastatic NET lesions on PRRT with DOTATATE will largely depend upon the tissue density of SSTR-2 as the ^{177}Lu-DOTATATE used in this study exhibit high affinity to this subtype of SSTR.[4,5] Our preliminary findings indicated no significant correlation between SUV (both max and mean) and the dose delivered to the target lesion on PRRT using ^{177}Lu-DOTATATE. These findings thus, indicate that the absolute SUVs derived

on the ^{68}Ga-DOTA-peptide PET images localizing metastatic NET lesions cannot predict the dose delivered to these lesions. In other words, the PRRT response is individualized and may vary as a function of histochemical variations or SSTR expression on the different lesions. Even the two lesions in the same patient are noted to exhibit different response to PRRNT, which is observed to be independent of the SUVs derived on the ^{68}Ga-somatostatin receptor imaging. Wehrmann et al[10] have reported that although the mean absorbed tumor dose was higher for DOTATATE, but the high intra- and interpatient variability of the dosimetry results with ^{177}Lu DOTATATE and ^{177}Lu DOTANOC makes it obligatory to perform the individual patient dosimetry.

The mechanism of localization of the NETs either by ^{68}Ga-DOTATATE or ^{177}Lu-DOTATATE remains the same as the same peptide-ligand has been used both for diagnosis and PRRT in these patients. However, the variations in the affinity profiles (IC50) of somatostatin receptor subtypes for different somatostatin analogs used in different diagnostic imaging with PET/CT or SPECT/CT have been reported.[1,4,5,17,18] These results for affinity profiles for different somatostatin analogs have been summarized by Prasad et al,[3] e.g. the IC50 of ^{90}Y-DOTA-TOC and ^{68}Ga-DOTATOC for SSTR-2 are 11.0 and 2.5 respectively. The lower value represents higher receptor affinity and thus the affinity of the therapeutic ^{90}Y-DOTATOC is about four times lesser as compared to the diagnostic Ga-DOTATOC. Similarly, the affinities of ^{68}Ga-DOTATATE and ^{177}Lu-DOTATATE may also differ which can contribute toward the observed noncorrelation between the SUVs and the amount of the dose delivered to the target lesions. Also, the variations in the SSTR expression at the time of ^{68}Ga-PET imaging and ^{177}Lu therapy could be another factor which explains the absence of any correlation between the SUVs and the dose delivered to the metastatic liver lesions on PRRT.

In a recent experimental study, Meils et al[19] reported that a high SSTR-2 density on the tumor cells at every PRRNT cycle is a crucial prerequisite to enable targeting of the tumor and subsequently for the internalization of the radiolabeled somatostatin analogs. These authors reported a very strong correlation between the increased SSTR expression following low dose ^{177}Lu-DOTATATE therapy and the effectiveness of the subsequent high dose PRRNT in CA-20948 tumor-bearing rats.[19] As indicated in this experimental study, thus there is a possibility of induction of near uniform receptor expression/density by upregulation of SSTR-2 on the NET lesions/tumors by subjecting these patients to first low dose ^{177}Lu-DOTATATE radionuclide therapy. However, more detailed experimental validation of this concept is needed to establish a correlation between the SSTR expression, SUVs, dose delivered to the tumors to predict the overall response of PRRNT in metastatic NETs. The future possibility of upregulation or induction of SSTR expression to achieve significant density of these receptors on the tumor surface and subsequent treatment with high dose ^{177}Lu-DOTATATE may present a positive correlation between SUVs and the dose delivered to the tumor to predict an overall response to PRRT.

In a recent study, Ezziddin et al[20] have shown that somatostatin receptor PET imaging may predict tumor absorbed doses on PRRNT. However, our initial results indicate poor correlation between SUV and the tumor dose and the linear regression analysis provided R2 values which explained only a small fraction of the total variance. Therefore, with the currently used fractionation and cumulative PRRNT treatment protocol, the SUV derived from ^{68}Ga-DOTA-peptide PET images should be used with caution for the prediction of tumor dose on ^{177}Lu-DOTA-peptide therapy as there are large intra- and interpatient variability. However, further studies with large numbers of patients are warranted to validate the results.

ACKNOWLEDGMENTS

One of the authors (Baljinder Singh) is thankful to the International Union against cancer (UICC, Switzerland, Geneva) for providing him the ICRETT fellowship for analyzing the data of the present study at the Department of Nuclear Medicine/Center for PET, Zentralklinik Bad Berka, Robert-Koch-Allee-9, 99437, Bad Berka, Germany. He is also thankful to Prof RP Baum, Director of the Department, at this center to accept him as a UICC fellow.

REFERENCES

1. Rufini V, Calcagni ML, Baum RP. Imaging of neuroendocrine tumors. Semin Nucl Med 2006;36:228.
2. Meyer GJ, Macke H, Schuhmacher J, Knapp WH, Hofmann M. ^{68}Ga-labelled DOTA-derivatised peptide ligands. Eur J Nucl Med Mol Imaging 2004;31:1097-104.
3. Prasad V, Ambrosini V, Alavi A, Fanti S, Baum RP. PET/CT in neuroendocrine tumors: Evaluation of receptor status and metabolism. PET Clinics 2008;2:351-75.
4. Wild D, Macke HR, Waser B, Reubi JC, Ginj M, Rasch H, Müller-Brand J, Hofmann M. ^{68}Ga-DOTA-NOC a first compound for PET imaging with high affinity for somatostatin receptor subtypes 2 and 5. Eur J Nucl Med Mol Imaging 2005;32:724.
5. Wild D, Schmit JS, Ginj M, et al. DOTA-NOC: A high affinity ligand for somatostatin receptors subtypes 2 and 5 for labeling with various radiometals. Eur J Nucl Med Mol Imaging 2003;30:1338-47.

6. Siegel JA, Thomas SR, Stubbs JB. MIRD Pamphlet 16: Techniques for quantitative radiopharmaceuticals biodistribution data acquisition and analysis for use in human radiation dose estimates. J Nucl Med 1999;40:37S.
7. Pauwels SA, Barone R, Walrand S. Practical dosimetry of peptide receptor radionuclide therapy with ^{90}Y-labeled analogs. J Nucl Med 2005;46:92S.
8. Erion JL, Bugaj JE, Schmidt MA, Wilhelm RR, Srinivasan A. High radiotherapeutic efficacy of ^{177}Lu-DOTA-Y^{3}-octreotate in rat tumor model. J Nucl Med 1999;40(S):223.
9. Kwekkeboom DJ, Bakker WH, Kam BL, et al. Treatment of patients with gastroentero-pancreatic (GEP) tumors with the novel radiolabelled somtaostatin analogue [^{177}Lu-DOATA^{0}, Tyr^{3}] octreotate. Eur J Nucl Med 2003;30:417.
10. Wehrmann C, Senftleben S, Zachert C, Muller D, Baum RP. Results of individual patient dosimetry in peptide receptor radionuclide therapy with ^{177}Lu-DOTA-TATE and ^{177}Lu-DOTA-NOC. Cancer Biotherapy and Radiopharmaceuticals 2007;22:406-16.
11. Duncan JR, Stephenson MT, Wu HP, Anderson CJ. Indium-111-diethylenetriaminepentaacetic acid-octreotide is delivered in vivo to pancreatic, tumor cell, renal and hepatocyte lysosomes. Cancer Res 1997;57:659-71.
12. Kwekkeboom DJ, Bakker WH, Kooij PP, Konijnenberg MW, Srinivasana, Erion JL, et al. ^{177}Lu-DOTA^{0},Try^{3}: Comparison with [^{111}In DTPTA^{0} octreotide in patients. Eur J Nucl Med 2001; 28:319-25.
13. Cremonesi M, Ferrari M, Bodei L, Tosi G, Paganelli G. Dosimetry in peptide radionuclide receptor therapy: A review. J Nucl Med 2006;47:1467-75.
14. Valkema R, Pauwels SA, Kvols LK, Kwekkeboom DJ, Jamar F, de Jong M, et al. Long-term follow-up of renal function after peptide receptor radiation therapy with (90)Y-DOTA (0), Try (3)-octreotide and ^{177}Lu-DOTA0, Try3-octreotate. J Nucl Med 2005;46(S)1:83S-91S.
15. Kwekkeboom DJ, Teunissen JJ, Bakker WH, Kooij PP, de Herder WW, Feelders RA, et al. Radiolabeled somatostatin analog [^{177}Lu-DOTA^{0}, Tyr^{3}] octreotate in patients with endocrine gastroenteropancreatic tumors. J Clin Oncol 2005;23: 2754-62.
16. Teunissen JJ, Kwekkeboom DJ, Krenning EP, Quality of life in patients with gastroenteropancreatic tumors treated with [^{177}Lu-DOTA^{0}, Tyr^{3}] octreotate. J Clin Oncol 2004;22:2724-29.
17. Reubi JC, Schar JC, Waser B, et al. Affinity profiles for human somatostatin receptor subtypes SST1-SST5 of somatostatin radiotracers selected for scintigraphic and therapeutic use. Eur J Nucl Med 2000;27:273-82.
18. Ginj M, Zhang H, Waser B, Cescato R, Wild D, Erchegyi J, et al. Radiolabeled somatostatin receptor antagonists are preferable to agonists for in vivo peptide receptor targeting of tumors. Proc Natl Acad Sci USA 2006;103: 16436-41.
19. Meils M, Forrer F, Capello A, Bijster M, Bernard BF, Reubi JC, et al. Up-regulation of somatostatic receptor density on rat CA20948 tumors escaped from low dose [^{177}Lu-DOTA^{0}, Try^{3}]octreotide therapy. Q J Nucl Med Mol Imaging 2007;51:324-33.
20. Ezziddin S, Lohmar J, Yong-Hing CJ, Sabet A, Ahmadzadehfar H, Kukuk G, et al. Does the pretherapeutic tumor SUV in ^{68}Ga DOTATOC PET predict the absorbed dose of ^{177}Lu octreotate? Clin Nucl Med 2012;37(6):e141-e47.

ABOUT THE AUTHORS

Baljinder Singh

Professor, Department of Nuclear Medicine and PET, Postgraduate Institute of Medical Education and Research, Chandigarh, India

Vikas Prasad

Associate Clinical Director, Department of Nuclear Medicine/Centre for PET, Zentralklinik Bad Berka, Robert-Koch-Allee 9, 99437, Bad Berka, Germany

Christiane Schuchardt

Scientist, Department of Nuclear Medicine/Centre for PET Zentralklinik Bad Berka, Robert-Koch-Allee 9, 99437, Bad Berka Germany

Harshad Kulkarni

Resident Physician, Department of Nuclear Medicine/Centre for PET Zentralklinik Bad Berka, Robert-Koch-Allee 9, 99437, Bad Berka Germany

Richard P Baum (Corresponding Author)

Professor, Chairman and Clinical Director, Department of Nuclear Medicine/Centre for PET, THERANOSTICS Center for Molecular Radiotherapy and Molecular Imaging, ENETS Center of Excellence Zentralklinik Bad Berka, Robert-koch-Allee 9, 99437 Bad Berka Germany, Phone: +49 364 585 2200, Fax: +49 364 585 3515 e-mail: richard.baum@zentralklinik.de

10.5005/jp-journals-10028-1051
ORIGINAL ARTICLE

Targeted Alpha-Particle Immunotherapy with Bismuth-213 and Actinium-225 for Acute Myeloid Leukemia

Joseph G Jurcic

ABSTRACT

Lintuzumab, a humanized anti-CD33 antibody, targets myeloid leukemia cells and has modest activity against acute myeloid leukemia (AML). To increase the antibody's potency yet avoid nonspecific cytotoxicity seen with β-emitting isotopes, lintuzumab was conjugated to the α-emitters bismuth-213 (^{213}Bi) and actinium-225 (^{225}Ac). The 46-minute half-life of ^{213}Bi limits its widespread use. Therefore, ^{225}Ac was also conjugated to various antibodies using DOTA-SCN. We conducted a phase I trial of ^{213}Bi-lintuzumab and subsequently administered cytarabine with ^{213}Bi-lintuzumab in a phase I/II study. The toxicity and biological activity of ^{225}Ac-linutuzumab in patients with relapsed/refractory AML in a phase I dose-escalation trial was determined. An initial phase I trial demonstrated the feasibility, safety and antileukemic activity of ^{213}Bi-lintuzumab. ^{213}Bi-lintuzumab produced responses in 24% of AML patients receiving doses ≥ 37 MBq/kg after partial cytoreduction with cytarabine. ^{225}Ac-labeled immunoconjugates killed *in vitro* at doses at least 1,000 times lower than ^{213}Bi analogs. Eighteen patients with relapsed/refractory AML received 18.5 to 148 kBq/kg of ^{225}Ac-lintuzumab in a phase I study. Dose-limiting toxicities were myelosuppression lasting >35 days in one patient and death due to sepsis in two patients. The maximum tolerated dose (MTD) was 111 KBg/kg. Bone marrow blast reductions were seen across all dose levels. Targeted α-particle immunotherapy with ^{213}Bi- and ^{225}Ac-lintuzumab is safe, has significant antileukemic effects, and can produce remissions after partial cytoreduction.

Keywords: Alpha particle, Immunotherapy, Acute myeloid leukemia.

How to cite this article: Jurcic JG. Targeted Alpha-Particle Immunotherapy with Bismuth-213 and Actinium-225 for Acute Myeloid Leukemia. J Postgrad Med Edu Res 2013;47(1): 14-17.

Source of support: Nil

Conflict of interest: None declared

INTRODUCTION

Although standard induction therapy with cytarabine and an anthracycline produces complete remissions (CR) in 50 to 70% of patients with acute myeloid leukemia (AML), but long-term survival is seen in only 20 to 40% of patients.[1] Following relapse, salvage chemotherapy produces remissions in only 20 to 25% of patients. While allogeneic hematopoietic cell transplantation (HCT) can result in long-term survival in approximately 30% of patients with relapsed AML, most patients are not appropriate candidates due to age, comorbidities or lack of a suitable donor.[2] The prognosis for elderly patients is even worse with a 5-year survival rate of 5% for patients more than 65 years of age.[3] Therefore, new therapies are needed to improve survival and reduce therapy-related toxicity.

Early studies showed that anti-CD33 constructs containing β particle-emitting iodine-131 or yttrium-90 could eliminate large leukemic burdens but resulted in prolonged myelosuppression requiring HCT.[4,5] The unique physical and radiobiological properties of α-particles may provide more efficient tumor cell killing and reduce the nonspecific cytotoxic effects seen with β-emitters. The α-particles have a shorter range (50-80 μm compared to 800-10,000 μm of β-particles) and a higher linear energy transfer (LET) (100 keV/μm compared to 0.2 keV/μm of β-particles).[6] As few as one or two α-particles can kill a target cell. Therefore, the potential for more efficient and specific antitumor effects with less damage to surrounding normal tissues makes α-particle immunotherapy an attractive approach for the treatment of cytoreduced or minimal disease.

Lintuzumab (HuM195) is a humanized monoclonal antibody that targets CD33, a 67-kDa cell surface glycoprotein expressed on most myeloid leukemia cells. It is also found on committed myelomonocytic and erythroid progenitors but not on pluripotent stem cells, granulocytes or nonhematopoietic tissues.[7,8] Lintuzumab induces antibody-dependent cell-mediated cytotoxicity and can fix human complement *in vitro*.[9] Previous studies demonstrated that lintuzumab can target leukemia cells in patients without immunogenicity,[10] eliminate minimal residual disease in acute promyelocytic leukemia,[11] and produce occasional remissions in AML.[12-14] To increase the potency of the antibody but avoid the nonspecific cytotoxicity seen with the β-emitters like iodine-131 (^{131}I) and yttrium-90 (^{90}Y), we conjugated lintuzumab to bismuth-213 (^{213}Bi) and actinium-225 (^{225}Ac), the α-emitters.

Alpha-Particle Immunotherapy with ^{213}Bi-Lintuzumab Preclinical Studies

^{213}Bi (t½ = 45.6 minutes) is a radiometal that emits α-particle with 8 MeV energy. Additionally, a 440 keV photon emission accompanies 26.5% of ^{213}Bi decays, allowing detailed biodistribution and dosimetry studies to be performed. Bismuth-labeled lintuzumab *in vitro* resulted in dose- and specific activity-dependent killing of CD33^{+} HL60 cells. Approximately 50% of target cells were killed

when only two bismuth atoms were bound to the cell surface.[16]

Single-Agent Phase I Trial

In our previous work, based on these preclinical data, 18 patients with relapsed and refractory AML (17 patients) or chronic myelomonocytic leukemia (one patient) were treated with ^{213}Bi-lintuzumab.[17] The drug was given as a 5-minute infusion, two to four times daily in 148 to 925 MBq fractions over 2 to 4 days. Because ^{213}Bi yields were limited by the activity of each ^{225}Ac/^{213}Bi generator and because of constraints on the specific activity that could be achieved for any one injection, we escalated radioactivity doses by increasing the number of injections. Patients received a total of 3 to 7 injections. Five dose levels were studied: 10.36, 15.54, 20.72, 25.9 and 37 MBq/kg. Biodistribution and dosimetry studies were performed by obtaining γ camera images after the first and last dose of ^{213}Bi-lintuzumab. Using a 20% photopeak window centered at 440 keV, thirty, 1-minute images beginning at the start of each injection followed by ten, 3-minute images were collected.[18]

No significant extramedullary toxicities were seen. Grade I and II liver function abnormalities were seen in four patients (22%). The onset was typically 5 to 14 days following treatment, and these abnormalities resolved within 3 to 14 days. All 17 evaluable patients developed myelosuppression with a median time to recovery of 22 days (range: 12-41 days). Nearly all the ^{213}Bi-lintuzumab rapidly localized to and was retained in areas of leukemic involvement, including the bone marrow, liver and spleen. Despite avidity for free bismuth, the kidneys were not visualized. There was no significant catabolism or clearance of the drug, confirming the stability of the construct. The mean absorbed dose per amount of injected activity to the marrow, and therefore to CD33$^+$ target cells, was 9.8 mSv/MBq (range: 2.6-29.4 mSv/MBq). Absorbed dose ratios between these sites and the whole body were 1,000-fold greater than those seen with β-emitting constructs in this antigen system and patient population. Blood and plasma antibody concentrations displayed typical α distributions over the first 20 to 40 minutes, followed by slower β clearance over the remaining 3 hours of sample collection.[17]

Fourteen (93%) of 15 evaluable patients had reductions in circulating blasts, and 14 (78%) of 18 patients had reductions in the percentage of bone marrow blasts (Fig. 1). No patients achieved CR, likely due to large tumor burdens in heavily pretreated patients and to the relatively low specific activities (329-766 MBq/mg) of ^{213}Bi-lintuzumab. Nevertheless, this study demonstrated the safety, feasibility and antileukemic effects of ^{213}Bi-lintuzumab and was the first proof-of-concept for systemic targeted α-particle immunotherapy in humans.[17]

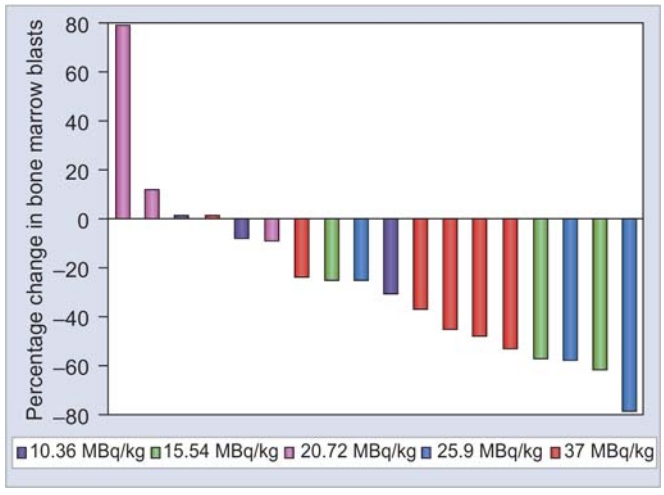

Fig. 1: Percentage change in bone marrow blasts after treatment with ^{213}Bi-lintuzumab in 18 patients in a phase I trial

Sequential Cytarabine and ^{213}Bi-Lintuzumab

It may be hypothesized that a 1-2 log reduction in tumor burden could increase the number of ^{213}Bi atoms delivered to leukemia cells and produce remissions. To determine the effects of ^{213}Bi-lintuzumab against cytoreduced disease, the authors conducted a phase I/II trial in which patients first received a nonremittive dose of cytarabine to decrease the leukemic burden.[19] Thirty-one patients with newly diagnosed (n = 13) or relapsed/refractory (n = 18) AML were treated. Patients received cytarabine at a dose of 200 mg/m^2 daily by intravenous continuous infusion for 5 days. Within 8 days after completion of cytarabine, 2 to 4 injections of ^{213}Bi-lintuzumab (518–1, 262 MBq each) were given over 1 to 2 days. Four dose levels of ^{213}Bi-lintuzumab were administered in the phase I portion of the trial: 18.5, 27.75, 37 and 46.25 MBq/kg. An additional 16 patients were treated at the maximum tolerated dose (MTD) in the phase II portion of the trial.

During the phase I portion, dose-limiting myelosuppression (defined as grade IV leukopenia lasting ≥ 35 days) was seen in two of four patients treated with 46.25 MBq/kg. The MTD of ^{213}Bi-lintuzumab following cytarabine was found to be 37 MBq/kg. Extramedullary toxicities were mainly limited to grade I and II events, including infusion-related reactions in nine patients (29%). Transient grade III/IV liver function abnormalities were seen in five patients (16%). No patient had evidence of sinusoidal obstructive syndrome. Treatment-related deaths occurred in two of 21 patients (10%) who received the MTD.[19]

Table 1: Results by disease status for sequential cytarabine/^{213}Bi-lintuzumab

Disease status	*No. of patients*	*CR*	*CRp*	*PR*	*Overall response*
Untreated AML, untreated relapse	18	2	2	2	6 (33%)
Primary refractory, refractory relapse	7	0	0	0	0

Significant reductions in marrow blasts were seen across all dose levels. Clinical responses were observed in six of the 25 patients (24%; 95% CI: 11-44) who received doses of ≥37 MBq/kg [2 CR, 2 CR with incomplete platelet recovery (CRp), and 2 PR] (Table 1). All responders had poor-risk features, including age ≥70 years or secondary AML; however, none of the six patients receiving less than 37 MBq had a clinical response. None of the seven patients either with primary refractory AML or multiple treated relapsed disease responded, indicating that effective cytoreduction was necessary to achieve remission after administration of ^{213}Bi-lintuzumab. The median response duration was 6 months (range: 2-12) with the median survival of 13.7 months (range: 5-30 months) among responders.[19]

Four patients (one at each dose level) underwent detailed biodistribution and pharmacokinetic studies. In contrast to the results seen in the initial phase I trial where ^{213}Bi-lintuzumab was given as a single agent,[15] cardiac blood pooling was seen after the last injection in one patient treated with 27.5 MBq/kg, indicating saturation of CD33 antigen sites within the bone marrow, liver and spleen. Moreover, reduced bone marrow uptake of ^{213}Bi-lintuzumab was seen after multiple injections in all four patients, indicating saturation of antigen sites after partial cytoreduction with cytarabine. Although a relatively small group of heterogeneous patients were included in this trial, it showed that targeted α-particle immunotherapy can be effective at reducing low-volume disease.

Actinium-225-Lintuzumab: A Targeted Alpha-Particle Nanogenerator

Preclinical Studies

The major obstacles to the widespread use of ^{213}Bi are its short half-life and the requirement of an on-site ^{225}Ac/^{213}Bi-generator. Therefore, the author developed a second generation construct in which the isotope generator is directly conjugated to a tumor-specific antibody. In this strategy, ^{225}Ac (t½ = 10 days) can serve as an *in vivo* generator of four α-particles at or within a cancer cell. The macrocyclic ligand 1,4,7,10-tetraazacyclododecane tetraacetic acid (DOTA) and its derivatives have been used for labeling of antibodies with ^{225}Ac. A two-step procedure was developed in which ^{225}Ac is first conjugated to DOTA-SCN followed by labeling of this construct to antibody.[20] ^{225}Ac-labeled tumor-specific antibodies can kill multiple cell lines *in vitro* with LD_{50} values 1,000 to 10,000 times less than those of analogous ^{213}Bi constructs. These findings led to *in vivo* studies in nude mice bearing human prostate carcinoma and lymphoma xenografts. Single nanocurie doses of ^{225}Ac-labeled tumor-specific antibodies significantly improved survival over controls and cured a substantial fraction of animals.[21]

Phase I Study of ^{225}Ac-Lintuzumab

Based on the activity of ^{225}Ac-containing radioimmunoconjugates in the animal models, we conducted a phase I trial of ^{225}Ac-lintuzumab in advanced AML.[22] Eighteen patients with relapsed (n = 11) or refractory (n = 7) AML were treated with a single infusion of ^{225}Ac-lintuzumab at doses of 18.5 (n = 3), 37 (n = 4), 74 (n = 3), 111 (n = 6) or 148 (n = 2) kBq/kg. Dose-limiting toxicities including myelosuppression lasting more than 35 days in one patient receiving 148 kBq/kg and death from sepsis in two patients receiving 111and 148 kBq/kg occurred. The MTD was determined to be 111 kBq/kg. As expected myelosuppression was the most common toxicity. Median time to resolution of grade IV leukopenia was 27 days (range: 0-71 days). Significant extramedullary toxicities were limited to transient grade III liver function abnormalities in three patients. We analyzed plasma pharmacokinetics by gamma counting at energy windows for two daughters of ^{225}Ac, francium-221 (^{221}Fr) and ^{213}Bi. Two-phase elimination kinetics was seen with mean plasma t½-α and t½-β of 1.9 and 38 hours, respectively, similar to other lintuzumab constructs containing long-lived radionuclides. This is in contrast to ^{213}Bi-lintuzumab, where the half-life is determined primarily by the short-lived radionuclide. Peripheral blasts were eliminated in 10 of 16 evaluable patients (63%), but only at doses of ≥37 kBq/kg. Bone marrow blast reductions were seen in 10 of 15 evaluable patients (67%) at 4 weeks, including eight patients (53%) who had blast reductions of more than 50%. Three patients receiving 37, 111 and 148 kBq/kg respectively achieved marrow blasts of 5% or less.

SUMMARY

Systemically administered targeted α-particle immunotherapy is feasible and has significant antitumor activity.

The shorter range and higher linear energy transfer of α-particles compared with β-particles may allow for more efficient and selective killing of individual tumor cells. These physical properties suggest that radioimmunotherapy with α-emitters may be best suited for the treatment of small-volume disease, as borne out in these clinical trials. Although reductions in leukemic blasts were seen when both ^{213}Bi- and ^{225}Ac-lintuzmab were given as single agents in phase I trials, remissions were only seen after effective cyto-reduction. The use of ^{225}Ac can overcome the logistical difficulties associated with short-lived radionuclides such as ^{213}Bi. Building on the encouraging results seen with ^{213}Bi-lintuzumab for cytoreduced leukemia, we are now conducting a multicenter phase I/II trial of ^{225}Ac-lintuzumab in combination with low-dose cytarabine for elderly patients with untreated AML. These studies provide the rationale for further investigation of targeted α-particle immunotherapy for minimal residual disease or small-volume disease in a variety of malignancies.

REFERENCES

1. Cassileth PA, Harrington DP, Appelbaum FR, Lazarus HM, Rowe JM, Paietta E, et al. Chemotherapy compared with autologous or allogeneic bone marrow transplantation in the management of acute myeloid leukemia in first remission. N Engl J Med 1998;339:1649-56.
2. Stockerl-Goldstein KE, Blume KG. Allogeneic hematopoietic cell transplantation for adult patients with acute myeloid leukemia. In: Thomas ED, Blume KG, Forman SJ (Eds). Hematopoietic cell transplantation. Oxford: Blackwell Science, Inc 1999;823-34.
3. Howlader N, Noone AM, Krapcho M, Neyman N, Aminou R, Altekruse SF, et al. SEER Cancer Statistics Review, 1975-2009 (Vintage 2009 Populations), National Cancer Institute. Bethesda, MD, http://seer.cancer.gov/csr/1975_2009_pops09/, based on November 2011 SEER data submission, posted to the SEER web site, April 2012.
4. Burke JM, Caron PC, Papadopoulos EB, Divgi CR, Sgouros G, Panageas KS, et al. Cytoreduction with iodine-131-anti-CD33 antibodies before bone marrow transplantation for advanced myeloid leukemias. Bone Marrow Transplant 2003;32:549-56.
5. Jurcic JG, Divgi CR, McDevitt MR, Ma D, Sgouros G, Finn RD, et al. Potential for myeloablation with yttrium-90-HuM195 (anti-CD33) in myeloid leukemia. Proc Am Soc Clin Oncol 2000;19:8a (abstr 24).
6. McDevitt MR, Sgouros G, Finn RD, Humm JL, Jurcic JG, Larson SM, et al. Radioimmunotherapy with alpha-emitting nuclides. Eur J Nucl Med 1998;25:1237-47.
7. Andrews RG, Torok-Storb B, Bernstein ID. Myeloid-associated differentiation antigens on stem cells and their progeny identified by monoclonal antibodies. Blood 1983;62:124-32.
8. Griffin JD, Linch D, Sabbath K, Larcom P, Schlossman SF. A monoclonal antibody reactive with normal and leukemic human myeloid progenitor cells. Leuk Res 1984;8:521-34.
9. Caron PC, Co MS, Bull MK, Avdalovic NM, Queen C, Scheinberg DA. Biological and immunological features of humanized M195 (anti-CD33) monoclonal antibodies. Cancer Res 1992;52:6761-67.
10. Caron PC, Jurcic JG, Scott AM, Finn RD, Divgi CR, Graham MC, et al. A phase 1B trial of humanized monoclonal antibody M195 (anti-CD33) in myeloid leukemia: Specific targeting without immunogenicity. Blood 1994;83:1760-68.
11. Jurcic JG, DeBlasio T, Dumont L, Yao TJ, Scheinberg DA. Molecular remission induction with retinoic acid and anti-CD33 monoclonal antibody HuM195 in acute promyelocytic leukemia. Clin Cancer Res 2000;6:372-80.
12. Caron PC, Dumont L, Scheinberg DA. Supersaturating infusional humanized anti-CD33 monoclonal antibody HuM195 in myelogenous leukemia. Clin Cancer Res 1998;4:1421-28.
13. Feldman E, Kalaycio M, Weiner G, Frankel S, Schulman P, Schwartzberg L, et al. Treatment of relapsed or refractory acute myeloid leukemia with humanized anti-CD33 monoclonal antibody HuM195. Leukemia 2003;17:314-18.
14. Raza A, Jurcic JG, Roboz GJ, Maris M, Stephenson JJ, Wood BL, et al. Complete remissions observed in acute myeloid leukemia following prolonged exposure to lintuzumab: A phase 1 trial. Leuk Lymph 2009;50:1336-44.
15. McDevitt MR, Finn RD, Ma D, Larson SM, Scheinberg DA. Preparation of α-emitting ^{213}Bi-labeled antibody constructs for clinical use. J Nucl Med 1999;40:1722-27.
16. Nikula TK, McDevitt MR, Finn RD, Wu C, Kozak RW, Garmestani K, et al. Alpha-emitting bismuth cyclohexylbenzyl DTPA constructs of recombinant humanized anti-CD33 antibodies: Pharmacokinetics, bioactivity, toxicity and chemistry. J Nucl Med 1999;40:166-76.
17. Jurcic JG, Larson SM, Sgouros G, McDevitt MR, Finn RD, Divgi CR, et al. Targeted alpha particle immunotherapy for myeloid leukemia. Blood 2002;100:1233-39.
18. Sgouros G, Ballangrud ÅM, Jurcic JG, McDevitt MR, Humm JL, Erdi YE, et al. Pharmacokinetics and dosimetry of an α-particle emitter labeled antibody: ^{213}Bi-HuM195 (anti-CD33) in patients with leukemia. J Nucl Med 1999;40:1935-46.
19. Rosenblat TL, McDevitt MR, Mulford DA, Pandit-Taskar N, Divgi CR, Panageas KS, et al. Sequential cytarabine and α-particle immunotherapy with bismuth-^{213}-lintuzumab (HuM195) for acute myeloid leukemia. Clin Cancer Res 2010;16:5303-11.
20. McDevitt MR, Finn RD, Sgouros G, Ma D, Scheinberg DA. An ^{225}Ac/^{213}Bi generator system for therapeutic clinical applications: Construction and operation. Appl Rad Isotopes 1999;50:895-904.
21. McDevitt MR, Ma D, Lai LT, Simon J, Borchardt P, Frank RK, et al. Tumor therapy with targeted atomic nanogenerators. Science 2001;294:1537-40.
22. Jurcic JG, Rosenblat TL, McDevitt MR, Pandit-Taskar N, Carrasquillo JA, Chanel SM, et al. Phase I trial of the targeted alpha-particle nano-generator actinium-225 (225Ac)-lintuzumab (anti-CD33; HuM195) in acute myeloid leukemia (AML). J Clin Oncol 2011;29:(suppl; abstr 6516).

ABOUT THE AUTHOR

Joseph G Jurcic

Professor, Department of Clinical Medicine; Director, Hematologic Malignancies, Columbia University Medical Centre, 177 Fort Washington 6-435 New York, NY-10032, USA, e-mail: jgj2110@columbia.edu

10.5005/jp-journals-10028-1052
REVIEW ARTICLE

^{68}Ge/^{68}Ga Generators and ^{68}Ga Radiopharmaceutical Chemistry on Their Way into a New Century

Frank Rösch

ABSTRACT

^{68}Ga faces a renaissance initiated by the development of new ^{68}Ge/^{68}Ga radionuclide generators, sophisticated ^{68}Ga radiopharmaceuticals, preclinical research and state-of-the-art clincial diagnoses via positron emission tomography/computed tomography (PET/CT). A new type of ^{68}Ge/^{68}Ga generator became commercially available in the first years of the 21st century, with eluates based on hydrochloric acid. These generators provided 'cationic' ^{68}Ga instead of 'inert' ^{68}Ga-complexes, and opened new pathways of Me^{III} radiopharmaceutical chemistry. The last decade has seen a ^{68}Ga rush. Increasing interest in generator-based ^{68}Ga radiopharmaceuticals in diagnostic applications has been accompanied by its potential use in the context of diease treatment planning, made possible by the inherent option expressed by theranostics. However, widespread acceptance and clinical application requires optimization of ^{68}Ge/^{68}Ga generators both from chemical and regulatory perspectives.

Keywords: ^{68}Ga, ^{68}Ge, Generator, Ligands.

How to cite this article: Rösch F. ^{68}Ge/^{68}Ga Generators and ^{68}Ga Radiopharmaceutical Chemistry on Their Way into a New Century. J Postgrad Med Edu Res 2013;47(1):18-25.

Source of support: Nil

Conflict of interest: None declared

INTRODUCTION

The ^{68}Ge/^{68}Ga radionuclide generator, with its secular equilibrium mathematics, offers a perfect combination of the nuclidic parameters in terms of half-lives and emission profiles: t½ = 270.95 days for ^{68}Ge and t½ = 67.71 minutes for ^{68}Ga, with no photon emission for ^{68}Ge and an 89.14% positron branching for ^{68}Ga.[10,46] This was known already in the middle of the 20th century, yet gallium-68 today sees a renaissance, with the development of new ^{68}Ge/^{68}Ga radionuclide generators, sophisticated ^{68}Ga radiopharmaceuticals, and state-of-the-art clincial diagnoses via positron emission tomography/computed tomography (PET/CT).[43] Current advances represent a 'renaissance' because ^{68}Ga is one of the very early radionuclides applied to PET imaging. Its application preceeds the use of fluorine-18 and even the term 'positron emission tomorgaphy'. Moreover, the availability of this positron emitter via the first ^{68}Ge/^{68}Ga generators,[16,17] lead to the development of the first positron scintillation camera which was created in the beginning of the 1960s.

With the availability of the first ^{68}Ge/^{68}Ga generators (which provided ^{68}Ga-EDTA eluates) and dramatically improved tomographic detection systems, several ^{68}Ga tracers for imaging of various diseases were investigated (mainly for imaging the human brain). Hundreds of patients were investigated in the USA using ^{68}Ga-EDTA, and others from 1963 on.

Despite several publications describing 'improved' ^{68}Ge/^{68}Ga radionuclide generators, the impact of ^{68}Ga imaging subsided in the late 1970s. This was primarily a consquence of two genertaor-related factors. Firstly, the generator design was inadequate for the versatile synthesis of ^{68}Ga radiopharmaceuticals. Secondly, in view of the parallel and rapid developments of the new classes of ^{99m}Tc- and ^{18}F-labeled diagnostics, the ^{68}Ge/^{68}Ga generators had only minor clinical relevance. Nevertheless, numerous papers in the 1970s and 1980s described the use of inorganic matrixes and organic resins, which allow for the isolation of ^{68}Ga from ^{68}Ge within hydrochloric acid solutions of weak (0.1-1.0 N) or strong (>1 N) concentrations respectively.

Pioneering achievement of radiochemists in Obninsk, Russia, resulted in the development of a new type of ^{68}Ge/^{68}Ga generator which became commercially available in the first years of the 21st century.[40] Generator eluates based on hydrochloric acid provided 'cationic' ^{68}Ga instead of 'inert' ^{68}Ga-complexes, opening new pathways of Me^{III} based radiopharmaceutical chemistry. Initially, the ^{68}Ga cation was introduced into existing ligands used for magnetic resonance imaging (MRI) and SPECT imaging probes, such as DTPA- or DOTA-based derivatives. The impressive results achieved using ^{68}Ga-DOTA-octreotides for PET/CT compared to ^{111}In-DTPA-octroescan paved the way toward the clinical acceptance of this particular tracer for imaging neuroendocrine tracers, and highlighted the great potential of the ^{68}Ge/^{68}Ga generator for modern nuclear medicine in general.

These advances intiated a ^{68}Ga rush in recent times (post 2002). However, the widespread acceptance and clinical application of ^{68}Ga radiopharmaceuticals requires optimization of ^{68}Ge/^{68}Ga generators both from chemical and regulatory points of view. Furthermore, dedicated chelators are required to broaden the possibilities of ^{68}Ga labeling to allow the use of more sensitive targeting vectors. Last but not least, this should also involve applying the concept of ^{68}Ga-radiopharmaceutical chemistry to an increasing number of targeting vectors, addressing the clinically most relevant diseases.

With current innovation and the favorable properties of the ^{68}Ga radionuclide, it is possible that in another decade from now ^{68}Ge/^{68}Ga generator-based ^{68}Ga diagnostics may approach a top three ranking in imaging (together with ^{99m}Tc- and ^{18}F-based tracer diagnostics).

This paper includes material which was presented at the 1st World Congress on Ga-68 and peptide receptor radionuclide therapy (PRRNT) theranostics-on the way to personalized medicine, Bad Berka, Germany, Junge 23-26, 2011, and which were published at a later stage.[5]

THE EARLY YEARS (1960-1970): THE SUNRISE OF ^{68}Ga

The First ^{68}Ge/^{68}Ga Radionuclide Generators

The first ^{68}Ge/^{68}Ga radionuclide generator was described in 1960[16] and entitled: 'A positron cow'. As the title elicits, the concept was to use a radionuclide generator for the production of a positron emitting radionuclide. The latter was a new entry for radiopharmaceutical chemistry and nuclear medicine molecular imaging *in vivo*. The generator chemistry involved a liquid-liquid extraction, and the whole processing protocol was considerably different to that of current radionuclide generator systems. Nevertheless, a variety of ^{68}Ga compounds were synthesized using this generator design.[2,7,44]

Further Generator Developments: Al_2O_3-based EDTA-Eluted Generators

Inherent disadvantages of the first generator lead to the development of two improved generator concepts soon after. The liquid-liquid extraction chemistry introduced by Gleason was substituted for a solid phase-based ion exchange system[17,50] (Fig. 1). In addition, a generator featuring an improved liquid-liquid extraction was described later.[15]

The original sketch, taken from the original publication by Yano and Anger (1964) for the second solid-phase based generator is reproduced in Figure 2. These solid-phase chromatographic generators offered excellent radiochemical characteristics. Using an alumina column and EDTA as eluent (10 ml 0.005 M EDTA), ^{68}Ga was easily eluted in a reproducible 95% yield without the need to introduce stable Ga^{III} as carrier. The eluate contained as little as 1.4×10^{-5}% of the parent ^{68}Ge. Prior to *in vivo* injection, 0.5 ml of 18% NaCl solution was added to the eluate.

^{68}Ge/^{68}Ga Generators and the Development of Positron Scintillation Cameras

This system served as a convenient and economical source of ^{68}Ga-EDTA. Effectively, this radionuclide generator was a synthesis unit of a relevant radiopharmaceutical; ^{68}Ga-

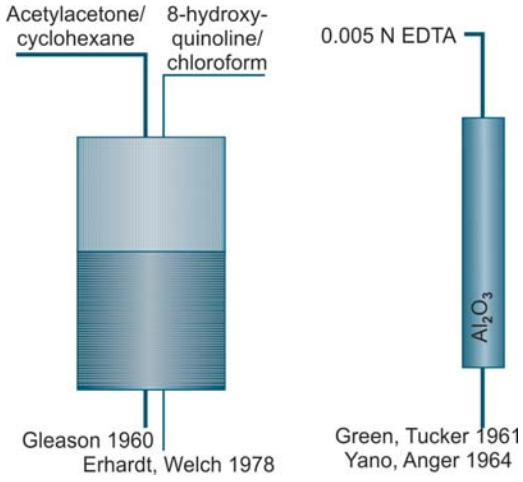

Fig. 1: Early progress in ^{68}Ge/^{68}Ga radionuclide generators II: From liquid-liquid extraction to solid phase-based elution

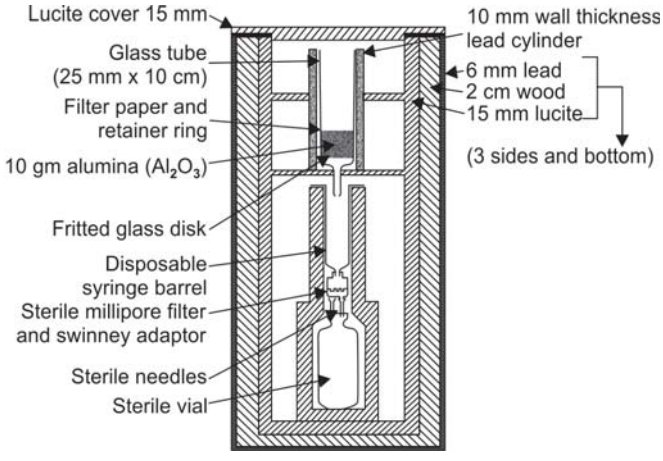

Fig. 2: Solid phase-based (alumina) ^{68}Ga elution (using an EDTA solution) reproduced from the original publication by Yano and Anger (1964)

EDTA (named 'veronate' at the time). ^{68}Ga-EDTA, and limited other ^{68}Ga-tracers, were adapted for human application quite quickly by various groups in the United States for early applications.[20,21,44] Systematic application for brain imaging was reported, with medical impact having significant dependence on the method of detection applied. Conventional imaging appeared to be relatively difficult, with relatively high dosage of ^{68}Ga-EDTA required for valuable medical information to be gained.

Anger thus, started to develop the basics of positron imaging tomography[2,22,23] (arguing as follows (Gottschalk and Anger 1964): … 'We seriously question whether satisfactory results can be obtained with the conventional positron scanner. Recent phantom studies indicate that the positron scintillation camera using ^{68}Ga-EDTA will detect lesions 1/2 the volume that can be detected by the conventional positron scanner using As74. The increase in sensitivity is obtained even though the phantom was set up to simulate our clinical condition where brain pictures are

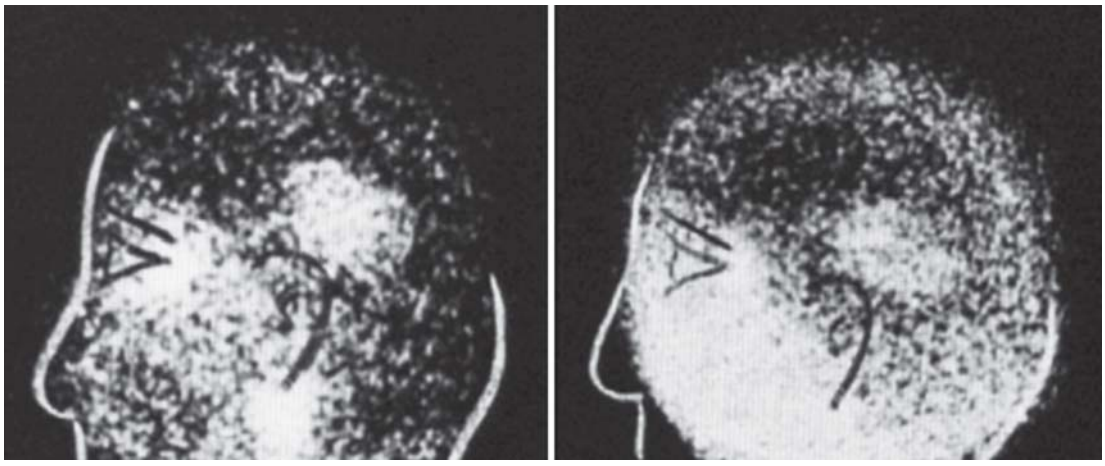

Fig. 3: A ^{68}Ga-EDTA brain scan acquired with the Anger positron camera circa 1962 showing the tomographic capability. The brain tumor is in best focus in the left image, taken at about the level of the temporal horn[2]

obtained in 4 to 10 minutes with a dose of 350 to 750 microcuries of ^{68}Ga-EDTA. Shealy et al, however, found that 2 to 3 millicuries of ^{68}Ga-EDTA was sometimes an inadequate dose with their positron scanner.' Images recorded with this new type of camera (Fig. 3)[2] paved the way for routine PET imaging.

^{68}Ga-EDTA: The Prototype PET-Pharmaceutical

Despite these new imaging features and the great success of ^{68}Ga-EDTA molecular imaging, the fact that in practice the generator was limited to ^{68}Ga-EDTA was a severe limitation. The extraction of ^{68}Ga from the thermodynamically very stable (log K = 21.7) ^{68}Ga-EDTA eluate species was not straightforward. Yano and Anger 1964 reported that, 'attempts are being made. .. to free ^{68}Ga ... from the EDTA complex'. A procedure was developed however; it was not user friendly and practical for ^{68}Ga. On a scale which uses 10 mg Ga carrier, the time required for extraction is 30 minutes, and the transfer yield of 60%.[50] The protocol was:

1. The cow is milked with 10 ml of 0.005 M EDTA solution, and the ^{68}Ga is collected in a 40 ml centrifuge tube.
2. The 10 to 20 mg of carrier $GaCl_3$ in HCl solution is added.
3. The 0.5 ml of saturated ammonium acetate solution is added.
4. Concentrated NH_4OH is added dropwise (about 1 ml) to precipitate $Ga(OH)_3$ at pH 6.0.
5. The solution is heated in a boiling water bath for 10 minutes to coagulate the $Ga(OH)_3$.
6. The solution is centrifuged, and the supernatant solution is discarded.
7. The $Ga(OH)_3$ is dissolved with a minimum volume of hot 20% NaOH.
8. The solution is acidified with about 1 ml of concentrated HCl.

HIBERNATING ^{68}Ga MEDICAL APPLICATIONS, BUT NEW CHEMISTRY AHEAD

The impact of ^{68}Ga imaging started to subside in the late 1970s, for two main reasons. Firstly, the generator design was inadequate in terms of the requirements for versatile synthesis of ^{68}Ga radiopharmaceuticals. Secondly, in view of the parallel and rapid developments of the new classes of ^{99m}Tc- and ^{18}F-labeled diagnostics, the generators available through the existing technology had only minor clinical relevance.

Despite this apparent decrease in interest, numerous basic radiochemical papers in the 1970s and 1980s described the use of inorganic matrixes as well as organic resins, selectively adsorbing ^{68}Ge and providing ^{68}Ga desorbtions within hydrochloric acid solutions of weak (0.1-1.0 N) or strong (>1 N) concentrations respectively.

Cationic ^{68}Ga eluates are required to facilitate the versatile radiolabeling chemistry with ^{68}Ga. Thus, the primary challenge is the development of separation systems which provide cationic ^{68}Ga species. Ga^{III} exists as cationic species (either pure water-hydrated aquocomplexes, such as the hexa-aqua cation $Ga(H_2O)_6^{3+}$, or similar monochloro or monohydroxo species). This speciation is easily achieved in solutions of hydrochloric acid of pH ranging between 0 and 2 (0.01-1.0 N HCl). For this purpose, $Me^{IV}O_2^-$ type matrixes (Me = Sn, Ti, Zr, Ce, etc.) appeared to be adequate, because they effectively adsorb the parent radionuclide $^{68}Ge^{IV}$.[1,25,26,33,39] Alternatively, organic resins have been developed which require more concentrated HCl soltuions for eluting the ^{68}Ga.[3,45] Figure 4 gives a schematic overview.

COMMERCIAL 'IONIC' GENERATORS

Generator Eluates Delivering the Gallium Cation

Thanks to the pioneering achievement of radiochemists in Obninsk (Russian Federation), a new type of ^{68}Ge/Ga

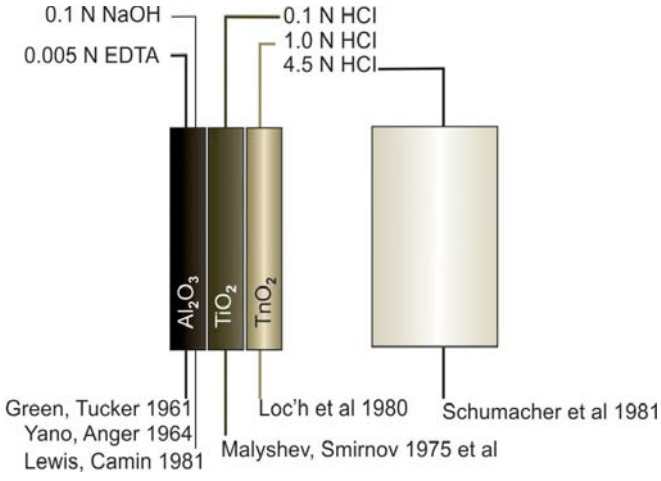

Fig. 4: ^{68}Ge/^{68}Ga radionuclide generator concepts developed in the 1970s and 1980s toward 'cationic' generators

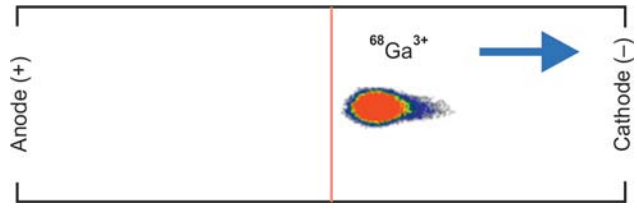

Fig. 5: Electrophoresis of a 0.1 N HCl ^{68}Ga generator eluate (EZAG Obninsk generator) demonstrating the presence of 'cationic' ^{68}Ga (parameters: 0.1 HCl, Whatman® paper strip, l = 19 cm, t = 5 minutes, 191 V, 210 mA, 40 W)

generator became commercially available in the first years of the 21st century.[40] These generators use eluting soltuions based on hydrochloric acid which provide 'cationic' ^{68}Ga, as opposed to 'inert' ^{68}Ga-complexes, opening new pathways of Me^{III}-based radiopharmaceutical chemistry (Fig. 5).

The ^{68}Ga cation was immediately introduced into existing ligand designs of MRI and SPECT imaging probes, namely DTPA- or DOTA-based derivatives. The impressive success of utilizing ^{68}Ga-DOTA-octreotides and PET/CT instead of, e.g. ^{111}In-DTPA-octroescan paved the way for clinical acceptance of this particular tracer for imaging neuroendocrine tumors, but also to the realization of the great potential of the ^{68}Ge/^{68}Ga generator for modern nuclear medicine in general. While commercial 'ionic' generators had successfully entered clinical environments, there were questions regarding its suitability, which became more relevant. In particular these related to its adequacy concerning radiation safety, legal requirements and labeling of medical tracers became more and more relevant. The most relevant concerns are outlined:

- *Problem 1:* The long physical half-life of the parent in principle should give a generator shelf-life of at least 1 year. However, the shelf-life of the generators did not necessarily parallel this long physical half-life due in particular to increasing breakthrough of ^{68}Ge, but also decreasing ^{68}Ga elution yield. ^{68}Ge breakthrough reduction and/or removal of ^{68}Ge from the eluates therefore remain an important radiochemical challenge.
- *Problem 2:* ^{68}Ga generator eluates are not chemically or radiochemically pure. Nonradioactive metals, such as $^{68}Zn^{II}$ (as generated on the generator as decay product of ^{68}Ga), Fe^{III} as general chemical impurity, and $^{68}Ge^{IV}$ as breakthrough represent metals, which may compete with $^{68}Ga^{III}$ for coordinative labeling of radiopharmaceutical precursors. Again, this illustrates the importance of minimizing the ^{68}Ge content in the eluate.[4,51]
- *Problem 3:* The new generation of ^{68}Ge/^{68}Ga radionuclide generators utilize hydrochloric acid solutions for ^{68}Ga elution. The relatively acidic environment created many protonated functional groups of ligands and bifunctional ligands needed for the labeling of ^{68}Ga, which may hinder efficient radiolabeling. Finally, minimizing the pH and volume of ^{68}Ga eluted prior to labeling should facilitate higher radiolabeling yields.

Generator Post-Processing

Three approaches have been developed to address one or more of these problems. Two processes include chemical separation strategies, which may be referred to as 'post-processing'.[35,51] The third technology involves a simple fractionation of the eluate, i.e. isolating eluate fractions with highest ^{68}Ga concentration.[11] The methods are schematically illustrated in Figure 6.

In most cases, commercial generators are used in direct connection with one of the three postelution processing technologies mentioned. The cation exchange-based post-processing[4,51] guarantees almost complete removal of the metallic impurities, in particular ^{68}Ge. Numerous modifications have been reported, including NaCl solutions instead of the solution no. 2 to desorb ^{68}Ga from the resin,[36] or by incorporating a subsequent anion exchange-based purification step[32] to remove organic solvent prior to labeling.

CURRENT STATE/OUTLOOK

Today, ^{68}Ge/^{68}Ga radionuclide generators are commercially available as TiO_2–, SnO_2– or organic resin-based columns. ^{68}Ga eluate yields range from about 70 to 80% for fresh generators, with a decrease overtime. ^{68}Ge breakthrough levels vary between 0.01 and 0.001% (or even less) for fresh generators, with these percentages increasing over extended periods of generator usage. Conjugated with post-processing

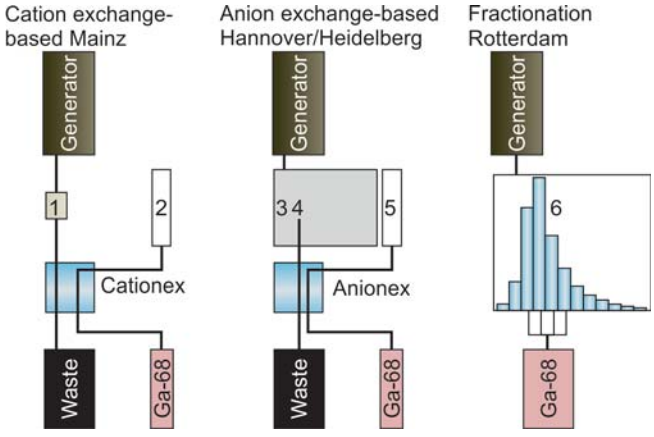

Fig. 6: Schematic representation showing an overview of post-processing technologies for commercial $^{68}Ge/^{68}Ga$ radionuclide generators: (1) Direct generator elution through cation-exchange cartridge, (2) desorption of purified ^{68}Ga using HCl/acetone or HCl/ethanol mixtures, (3) generator elution into HCl reservoir, (4) subsequently elution through anion-exchange cartridge, (5) desorption of purified ^{68}Ga using water, (6) identification of the eluate fraction representing at least two-third of the ^{68}Ga activity, and use without further purification

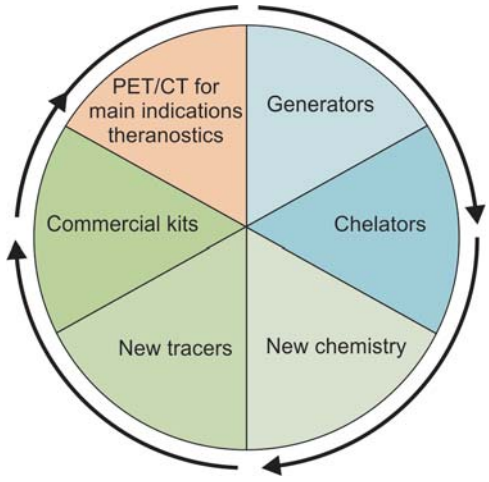

Fig. 7: Sketch of some future directions related to $^{68}Ge/^{68}Ga$ radionuclide generators and radiopharmaceuticals

technologies, ^{68}Ga radiopharmaceuticals are being synthesized routinely and safely. Thus, since the early $^{68}Ge/^{68}Ga$ radionuclide generator systems developed about half a century ago, significant advances have been made.

These generator improvements have allowed for the significant development of ^{68}Ga radiopharmaceutical chemistry within the last decade. Despite this, almost all the technological and chemical innovation involved belongs to the 20th century. There is room for further development, where several aspects of generator design and performance, labeling chemistry and clinical application need to be addressed. Figure 7 illustrates some of the potential future directions.

Generators

Concerning solid phase-based ion exchange chromatographic $^{68}Ge/^{68}Ga$ radionuclide generators, some improvements may be possible within the resin material itself. Recent publications hint at the potential of sophisticated nanoparticles, such as Zr^{IV} and Ce^{IV}-systems, which are classified as nanocomposites.[12,13] The rational is that these composites may provide effective adsorption of ^{68}Ge, effective release of ^{68}Ga, be more chemically stability and radiation resistant. In parallel, GMP-certified and licensed commercial generators are required to satisfy the increasing standards of legal authorities.

Generator Online Post-Processing

Elution of generators may be further integrated into faster and more efficient online post-processing procedures, which are managed by automated modules. A key issue in this regard, is to avoid the transfer of ^{68}Ge into ^{68}Ga-radiopharmaceuticals. Optionally, these post-processing technologies should also allow for versatile labeling protocols. For example, the transfer from aqueous to nonaqueous solutions for radiolabeling (addressing potential lipophilic ^{68}Ga tracers)[53] or onto resin for solid phase supported labeling reactions.

Post-processing technologies, which remove ^{68}Ge online from the eluate, are of utmost importance, as they avoid the transfer of critical ^{68}Ge levels into the radiopharmaceutical preparation. They also guarantee the safety, which is relevant from the legal point of view, i.e. addressing safety criteria of routine clinical use.[9] Although some of the ^{68}Ga radiopharmaceuticals used clinically, in particular ^{68}Ga-based peptides, are purified from uncomplexed ^{68}Ga, (which simultaneously removes ^{68}Ge present), the principal strategy should be to keep generator-derived ^{68}Ga solutions free of ^{68}Ge before labeling. Consequently, the monographs of the European Pharmacopoeia (Ph Eur) in its description of the gallium chloride (^{68}Ga) solution for radiolabeling, Monograph N°: 2464, Strasbourg, June 2012, adds, that '…the solution is intended for use in the preparation of gallium-68-labeled radiopharmaceuticals, including a procedure to reduce the level of germanium-68 below 0.001% of the total radioactivity.' This means that, necessarily, the procedure for preparation of a Ga-68 radiopharmaceutical has to include a procedure to remove germanium-68 up to a level below 0.001%.

Only this strategy will be suitable for a kit-type ^{68}Ga-labeling approach to parallel the ^{99m}Tc analog systems. This would allow for the direct synthesis and application of ^{68}Ga radiopharmaceuticals, such as ^{68}Ga chloride,[49] ^{68}Ga

citrate[28,37] (Rizello et al 2009), ^{68}Ga apotransferrin[27] or ^{68}Ga Schiff base complexes.[18,19] Radiotracers, such as these are otherwise not applicable due to the nonseparable content of ^{68}Ge.

Ligands

The future development of new ^{68}Ga radiopharmaceuticals may be facilitated by the development of new ligands and bifunctional derivatives for coordinating ^{68}Ga specifically, i.e. ideally discriminating Fe^{III} and Zn^{II}, or by allowing complex formation under a broader range of pH. Another relevant aspect is the development of ligands which complex ^{68}Ga at room temperature. Such radiolabeling characteristics approach the advantages of ^{99m}Tc kit-type labeling protocols. It is also desirable to speed up complex formation and minimize the amount of labeling precursor needed, thereby increasing the specific activities of the final radiolabeled product. Ideally new ligands should label more efficiently than that of established DOTA or NOTA derivatives, without detriment to complex stability. Important criteria (in addition to high radiochemical yields) are listed in Table 1. Several of the promising ligand candidates for ^{68}Ga radiolabeling are listed in Figure 8.

Current trends in bifunctional ligand design suggest a change in the paradigm that macrocyclic chelates are the ligands to go for. Recent developments describe modified acyclic ligands. In particular, recent ligands are derived from known Fe^{III} ligands, because the two metals have similar coordination chemistry. New classes of chelators currently under development, include acyclic ligands HBED,[14,48] H_2DEDPA[7,8,24] and tris(hydroxypyridinone) ligands,[6,53] but also research on deferoxamine[34] and on sulfur-based derivatives[30] continues.

New cyclic triazacyclononane-phosphinic acid chelators[38,39] have been developed, which complex ^{68}Ga very effectively. In case of the triazacyclononane-phosphinic acid chelators (TRAP), the idea is also to create an inert coordinating core leaving three linkable functionalities available for versatile chemistry, allowing for multimeric substitutions.

Table 1: Challenges for new ^{68}Ga ligand developments

Efficient labeling should occur:
- At temperatures below 100°, approaching room temperature
- Over a broad range of pH, i.e. covering the pH of the generator eluate up to physiological pH
- Within short periods, i.e. within 10 minutes or less
- At low amounts/concentration of the ligands (10 μM or less)
- In the presence of impurities, such as Fe^{III} (as a general impurity) and Zn^{II} (as decay product of ^{68}Ga), etc.

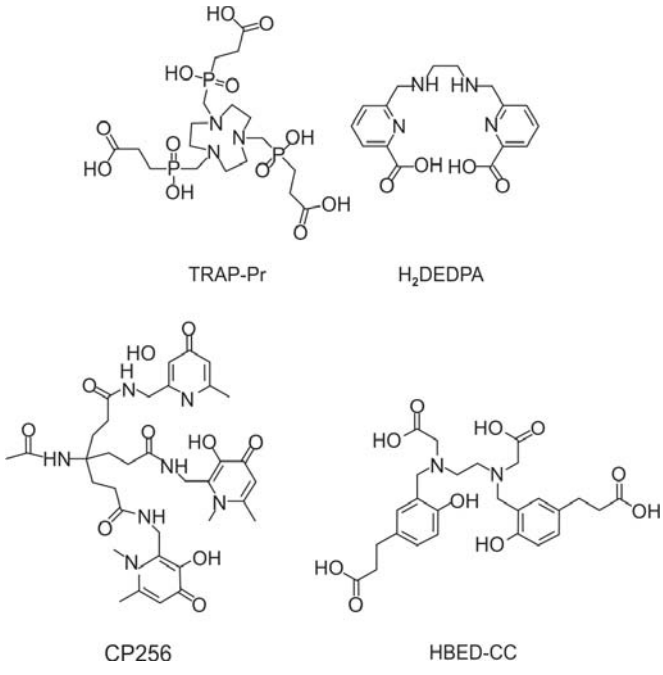

Fig. 8: Recent developments in ligand structures tailored for ^{68}Ga

^{68}Ga Radiopharmaceuticals

Novel ligand design presents the opportunity for a wide range of new tracers. The clinical application, however, will finally depend on the classes of targeting vectors attached, beyond peptidic and nonpeptidic targeting vectors available. Imaging will hopefully address tumors, infection and inflammation, but also a variety of clinical indications and almost all organs. This would mirror the ^{99m}Tc radiopharmaceuticals, e.g. brain, heart, etc. In the context of the similarity of generator based ^{99m}Tc and ^{68}Ga pharmaceuticals, the preparation of those ^{68}Ga radiopharmaceuticals should also be KIT-based if they are to find clinical application and widespread acceptance. These developments will contribute to a much more intense clinical use of ^{68}Ge/^{68}Ga generators and the corresponding ^{68}Ga pharmaceuticals for molecular imaging. Again, legal considerations apply to both the generator and the pharmaceuticals.[9]

Theranostics

Simultaneously to the further development of ^{68}Ga-PECT/CT diagnostics, it is one of the unique features of ^{68}Ga, that ^{68}Ga-PET/CT imaging may be directly linked to treatment options. For some classes of Ga^{III} bifunctional ligands, there should be an option to synthesize therapeutics analogs with trivalent radiometals, such as ^{90}Y, ^{177}Lu, ^{213}Bi, etc. The DOTA-conjugated octreotide derivatives represent a perfect example of the success of this theranostic concept.[42]

REFERENCES

1. Ambe S. Germanium-68-gallium-68 generator with alpha-ferric oxide support. Appl Radiat Isot 1988;39:49.
2. Anger HO, Gottschalk A. Localization of brain tumors with the positron scintillation camera. J Nucl Med 1963;4:326.
3. Arino H, Skraba WJ, Kramer HH. A new ^{68}Ge/^{68}Ga radioisotope generator system. Int J Appl Radiat Isot 1978;29:117.
4. Asti M, De Pietri G, Fraternali A, Grassi E, Sghedoni R, Fioroni F, et al. Validation of ^{68}Ge/^{68}Ga generator processing by chemical purification for routine clinical application of ^{68}Ga-DOTATOC. Nucl Med Biol 2008;35:721.
5. Baum RP, Roesch F (Eds). Theranostics, gallium-68, and other radionuclides. A pathway to personalized diagnosis and treatment. Recent results in cancer research. Springer, Heidelberg: New York, Dordrecut, London 2103;194:3-16.
6. Berry DJ, Ma Y, Ballinger JR, Tavaré R, Koers A, Sunassee K, et al. Efficient bifunctional gallium-68 chelators for positron emission tomography: Tris (hydroxypyridinone) ligands. Chem Commun 2011;47:7068.
7. Boros E, Ferreira CL, Patrick BO, Adam MJ, Orvig C. New Ga derivatives of the H_2dedpa scaffold with improved clearance and persistent heart uptake. Nucl Med Biol 2011;38:1165.
8. Boros E, Ferreira CL, Yapp DTT, Gill RK, Price EW, Adam MJ, et al. RGD conjugates of the H_2dedpa scaffold: Synthesis, labeling and imaging with ^{68}Ga. Nucl Med Biol 2012;39:785.
9. Breeman WA, Verbruggen AM. The ^{68}Ge/^{68}Ga generator has high potential, but when can we use ^{68}Ga-labelled tracers in clinical routine? Eur J Nucl Med Mol Imag 2007;34:978.
10. Burrows TW. Nuclear Data Sheets for A = 6.8. Nuclear Data Sheets 2002;97:1-127.
11. Breeman WAP, de Jong M, de Blois E, Bernard BF, Konijnenberg M, Krenning EP. Radiolabelling DOTA-peptides with ^{68}Ga. Eur J Nucl Med Mol Imaging 2005;32:478.
12. Chakravarty R, Shukla R, Ram R, Venkatesh M, Dash A, Tyagi AK. Nanoceria-PAN composite-based advanced sorbent material: A major step forward in the field of clinical-grade ^{68}Ge/^{68}Ga generator. Appl Mat Interfaces 2010;2:2069-75.
13. Chakravarty R, Shukla R, Ram R, Tyagi AK, Dash A, Venkatesh M. Development of a nano-zirconia based ^{68}Ge/^{68}Ga generator for biomedical application. Nucl Med Biol 2011;38:575.
14. Eder E, Wangler B, Knackmuss S, LeGall F, Little M, Haberkorn U, et al. Tetrafluorophenolate of HBED-CC: A versatile conjugation agent for ^{68}Ga-labeled small recombinant antibodies. Eur J Nucl Med Mol Imaging 2008;35:1878-86.
15. Erhardt GJ, Welch MK. A new germanium-68/gallium-68 generator. J Nucl Med 1978;19:925-29.
16. Gleason GI. A positron cow. Int J Appl Radiat Isot 1960;8:90.
17. Greene MW, Tucker WD. An improved gallium-68 cow. Int J Appl Radiat Isot 1961;12:62.
18. Hsiao YM, Mathias CJ, Wey SP, Fanwick PE, Green MA. Synthesis and biodistribution of lipophilic and monocationic gallium radiopharmaceuticals derived from N,N'-bis (3-aminopropyl)-N, N'-dimethylethylenediamine: Potential agents for PET myocardial imaging with ^{68}Ga. Nucl Med Biol 2009; 36:39.
19. Tarkia M, Saraste A, Saanijoki T, Oikonen V, Vähäsilta T, Strandberg M, et al. Evaluation of ^{68}Ga-labeled tracers for PET imaging of myocardial perfusion in pigs. Nucl Med Biol 2012; 39:715.
20. Gottschalk A, Anger HO. The sensitivity of the positron scintillation camera for detecting simulated brain tumors with gallium-68 EDTA. Am J Roentgen 1964;92:174.
21. Gottschalk A. Anger HO. Letter to the editor. J Nucl Med 1964;5:569.
22. Gottschalk A. The early years with Hal Anger. Sem Nucl Med 1996;26:171.
23. Gottschalk A. Hal Anger: Nuclear medicine´s quiet genius. J Nucl Med 2004;45:13N, 26N.
24. Koop B, Reske SN, Neumaier B. Radiochim Acta 2007;95:39.
25. Kopecky P, Mudrová B, Svoboda K. The study of conditions for the preparation and utilization of ^{68}Ge-^{68}Ga generator. Int J Appl Radiat Isot 1973;24:73.
26. Kopecky P, Mudrová B. ^{68}Ge-^{68}Ga generator for the production of ^{68}Ga in an ionic form. Int J Appl Radiat Isot 1974;25:263.
27. Kumar V, Boddeti DK, Evans SG, Roesch F, Howman-Giles R. Potential use of ^{68}Ga-apo-transferrin as a PET imaging agent for detecting Staphylococcus aureus infection. Nucl Med Biol 2011;38:393.
28. Kumar V, Boddeti DK, Evans SG, Angelides S. ^{68}Ga-Citrate-PET for diagnostic imaging of infection in rats and for intra-abdominal infection in a patient. Curr Radiopharm 2012;5:71.
29. Lewis RE, Camin LL. Germanium-68/Gallium-68 generator for the one step elution of ionic gallium-68. J Label Compds Radiopharm 1981;18:16.
30. Luyt LG, Katzenellenbogen JA. A Trithiolate tripodal bifunctional ligand for the radiolabeling of peptides with gallium(III). Bioconjugate Chem 2002;13:1140.
31. Loc´h C, Maziere B, Comar D. A new generator for ionic gallium-68. J Nucl Med 1980;21:171.
32. Loktionova NS, Belozub AN, Filosofov DV, Zhernosekov KP, Wagner T, Türler A, et al. Improved column-based radiochemical processing of the generator produced ^{68}Ga. Appl Radiat Isot 2011;69:942.
33. Malyshev KV, Smirnov VV. Gallium-68 yield from hydrated zirconium oxide-based generators. Sov Radiochem 1975;17:137.
34. Mathias CJ, Lewis MR, Reichert DE, Laforest R, Sharp TL, Lewis JS, et al. Preparation of ^{66}Ga- and ^{68}Ga-labeled Ga(III)-deferoxamine-folate as potential folate-receptor-targeted PET radiopharmaceuticals. Nucl Med Biol 2003;30:725.
35. Meyer GJ, Mäcke HR, Schuhmacher J, Knapp WH, Hofmann M. ^{68}Ga-labelled DOTA-derivatised peptide ligands. Eur J Nucl Med 2004;31:1097.
36. Mueller D, Klette I, Baum RP, Gottschaldt M, Schultz MK, Breeman WA. Simplified NaCl based ^{68}Ga concentration and labeling procedure for rapid synthesis of ^{68}Ga radiopharmaceuticals in high radiochemical purity. Bioconjug Chem 2012; 23:1712.
37. Nanni C, Errani C, Boriani L, Fantini L, Ambrosini V, Boschi S, et al. ^{68}Ga-citrate PET/CT for evaluating patients with infections of the bone: Preliminary results. J Nucl Med 2010;51:1932.
38. Notni J, Hermann P, Havlíèková J, Kotek J, Kubíèek V, Plutnar J, et al. A triazacyclononane-based bifunctional phosphinate ligand for the preparation of multimeric ^{68}Ga tracers for positron emission tomography. Chemistry 2010;16:7174-85.
39. Notni J, Šimeèek J, Hermann P, Wester HJ. TRAP, a powerful and versatile framework for gallium-68 radiopharmaceuticals. Chemistry 2011;17:14718-22.
40. Razbash AA, Sevastianov YuG, Krasnov NN, Leonov AI, Pavlekin VE. Germanium-68 row of products. Proceedings of the 5th International Conference on Isotopes, 5ICI, Brussels, Belgium April 25-29, Medimond, Bologna 2005;147-51.
41. Rizzello A, Di Pierro D, Lodi F, Trespidi S, Cicoria G, Pancaldi D, et al. Synthesis and quality control of ^{68}Ga citrate for routine clinical PET. Nucl Med Commun 2009;30:542.

42. Roesch F, Baum RP. Generator-based PET radiopharmaceuticals for molecular imaging of tumours: On the way to theranostics. Dalton Transactions 2011;40:6104-11.
43. Roesch F, Riss PJ. The renaissance of the $^{68}Ge/^{68}Ga$ radionuclide generator initiates new developments in ^{68}Ga radiopharmaceutical chemistry. Curr Top Med Chem 2010;10:1633-68.
44. Schaer LR, Anger HO, Gottschalk A. Gallium edetate ^{68}Ga experiences in brain-lesion detection with the positron camera. AMAM 1965;198:139.
45. Schumacher J, Maier-Borst W. A new $^{68}Ge/^{68}Ga$ radioisotope generator system for production of ^{68}Ga in dilute HCl. Int J Appl Radiat Isot 1981;32:31.
46. Schönfeld E. ^{68}Ge-^{68}Ga. Comments on evaluation–CEA 1999. ISBN 27272 02111 3.
47. Shealy CN, Aronow S, Brownell GL. Gallium-68 as a scanning agent for intracranial lesions. J Nucl Med 1964;5:161.
48. Sun Y, Anderson C, Pajeau T, Reichert D, Hancock R, Motekaitis R, et al. Indium (III) and gallium (III) complexes of bis(aminoethanethiol) ligands with different denticities: Stabilities, molecular modeling, and in vivo behavior. J Med Chem 1996;39:458-70.
49. Ujula T, Salomäki S, Autio A, Luoto P, Tolvanen T, Lehikoinen P, et al. ^{68}Ga-chloride PET reveals human pancreatic adenocarcinoma xenografts in rats-comparison with FDG. Mol Imaging Biol 2010;12:259.
50. Yano Y, Anger HO. A gallium-68 positron cow for medical use. J Nucl Med 1964;5:484.
51. Zhernosekov KP, Filosofov DV, Baum RP, Aschoff P, Bihl H, Razbash AA, et al. Processing of generator-produced ^{68}Ga for medical application. J Nucl Med 2007;48:1741.
52. Zhou Z, Neubert H, Liu DY, Liu ZD, Ma YM, Kong XL, et al. Iron binding dendrimers: A novel approach for the treatment of haemochromatosis. J Med Chem 2006;49:4171-82.
53. Zoller F, Riss PJ, Montforts FP, Rösch F. Efficient post-processing of aqueous generator eluates facilitates ^{68}Ga-labelling under anhydrous conditions. Radiochim Acta 2010;98:157.

ABOUT THE AUTHOR

Frank Rösch

Professor, Institute of Nuclear Chemistry, Johannes Gutenberg-University, University of Mainz, Fritz-Strassmann-Weg 2, D-55128 Mainz, Germany
Phone: +49-6131-3925302, e-mail: frank.roesch@uni-mainz.de

10.5005/jp-journals-10028-1053
REVIEW ARTICLE

An Increasing Role for ^{68}Ga PET Imaging: A Perspective on the Availability of Parent ^{68}Ge Material for Generator Manufacturing in an Expanding Market

Michael K Schultz, Patrick Donahue, Nannette I Musgrave, Konstantin Zhernosekov, Clive Naidoo, Anatolii Razbash Izabella Tworovska, David W Dick, G Leonard Watkins, Michael M Graham, Wolfgang Runde Jeffrey A Clanton, John J Sunderland

ABSTRACT

The use of gallium-68 for molecular imaging is gaining momentum world-wide. While our understanding of ^{68}Ga chemistry, generators, and associated synthesis modules appear to have advanced to a clinically-reliable stage, uncertainty in the supply of radiopharmaceutically-suitable parent is of significant concern. In this work, we examine the current supply of ^{68}Ge in an effort to better understand the potential for expansion of manufacturing to meet an increasing demand for ^{68}Ga. Although specific information on sales and demand of ^{68}Ge is highly business sensitive and thus guarded, our examination finds no shortage in the current supply of ^{68}Ge. On the other hand, increases in the use of ^{68}Ge generators for clinical applications in the United States point to the need for continued support for production at DOE laboratories in the United States to ensure a reliable supply and suggests that new commercial facilities may be needed to meet the increasing demand.

Keywords: Gallium-68, Germanium-68, Generators, PET imaging, Molecular imaging.

How to cite this article: Schultz MK, Donahue P, Musgrave NI, Zhernosekov K, Naidoo C, Razbash A, Tworovska I, Dick DW, Watkins GL, Graham MM, Runde W, Clanton JA, Sunderland JJ. An Increasing Role for ^{68}Ga PET Imaging: A Perspective on the Availability of Parent ^{68}Ge Material for Generator Manufacturing in an Expanding Market. J Postgrad Med Edu Res 2013;47(1):26-30.

Source of support: Nil

Conflict of interest: None declared

INTRODUCTION

The use of gallium-68 (^{68}Ga) for molecular imaging of disease has seen a marked increase over the last several years.[1-6] Applications for ^{68}Ga positron emission tomography (PET) are emerging across a broad spectrum of diagnostic imaging challenges including cancer, cardiovascular disease, infection and inflammation.[7-18] The increase in enthusiasm for ^{68}Ga use can be ascribed to several factors, including: Superiority in achievable image quality compared to other gamma-emitting radionuclides (e.g. indium-111);[19] nuclear decay characteristics (i.e. half life and positron emission branching ratio) that are considered favorable for clinical molecular imaging; and the potential for on-demand production via the introduction of maturing-competitive generator and fluid handling technologies that are now capable of providing reliable, high-purity, on-demand ^{68}Ga precursor in sufficient quantities for routine radiopharmaceutical production in the absence of cyclotron operations.[2,3,5,6,14,20] These characteristics promise an increasing role for ^{68}Ga PET imaging that has great potential to expand in the United States and throughout the world. The advances of generator technology for ^{68}Ga production, chemistry of gallium within the context of radiopharmaceuticals, and emerging applications for ^{68}Ga radiopharmaceuticals have been reviewed in detail by several authors recently.[2,3,5,6,21] The observations of these authors provide evidence that the future for ^{68}Ga appears bright. However, to accelerate the use of these exciting new diagnostic agents for clinical applications, concerted effort will be required to promote the 'promising' status of gallium-68, as alluded to by Breeman and Verbruggen,[22] to widespread routine clinical use in the United States.

One area of development that has the potential to significantly impact the trajectory of ^{68}Ga for clinical imaging in the United States revolves around uncertainty as to the supply of generators and parent radionuclide germanium-68 (^{68}Ge). A parallel can be made, in this context, to recent challenges to the use of the long-time dominant radionuclide technetium-99m (^{99m}Tc) with the loss of a single supplier of parent molybdenum-99 (^{99}Mo).[23,24] While the potential advantages of ^{68}Ga relative to ^{99m}Tc can be debated,[2] the need for a reliable source of parent radionuclide is critical to success. Thus, while ^{68}Ga chemistries and associated synthesis modules appear to have advanced to a clinically-reliable stage, uncertainty in the supply of radiopharmaceutically suitable parent is of significant concern. In this work, we examine the current supply of ^{68}Ge in an effort to better understand the potential for expansion of manufacturing to meet an increasing demand for ^{68}Ga.

MEETING AN INCREASED DEMAND FOR ^{68}Ga

As the potential for ^{68}Ga-labeled compounds has become evident, several commercial companies have advanced generator technologies to meet the demand for reliable

production of ^{68}Ga on a routine basis.[6] Several promising technological platforms have been applied for the development of these generators,[5] based on TiO_2,[2] SnO_2,[25] nano-zirconia,[26] and organic- or silica-based solid-phase materials.[27-29] The first generators documented in the literature were developed as early as the 1960s,[2,30,31] while the commercial alternatives available today were initially introduced in the early 1980s. The technology improvements of these commercial alternatives have played a large role in advancing the potential of ^{68}Ga. Significant advances included removing the need for complexing agents to selectively remove ^{68}Ga from the generator-column and reducing the acid concentration from as high as 1 M hydrochloric acid (HCl) to as low as 0.1 M HCl eluate concentration to remove ^{68}Ga as a cationic species. These improvements facilitated more reliable pH adjustments for the radiolabeling reaction with most chelator-modified peptides and small molecules. Importantly for smooth transition to routine clinical use, recently introduced commercial generators are demonstrating excellent elution yields (65-80%) and low initial breakthrough levels of ^{68}Ge parent on generator elution.[2,5,6]

While these findings and observations point to a maturing technology, which is increasingly recognized around the world as suitable for routine clinical operations,[6] one area of concern for expanding operations in the United States (US) is the availability of parent ^{68}Ge for manufacturing of generators and the potential for a shortfall. Specific information on the capability and capacity of current production of ^{68}Ge parent material is not entirely transparent. However, there is documented capacity from at least three major sources that lend confidence to the ability of current manufacturing to maintain a stable inventory of ^{68}Ge that can meet near-term projected demand. Four major centers which produce parent ^{68}Ge for generator manufacturing currently are: iThemba laboratories (South Africa), Brookhaven and Los Alamos National Laboratories (USA) and Cyclotron Co Ltd (Obninsk, Russia). According to a recent IAEA report, these facilities have production capacities of approximately 0.5 to 2 Ci per run.[32]

iThemba LABS (South Africa) has been producing chemically processed ^{68}Ge commercially for many years. The company reports production of unprocessed ^{68}Ge by standard irradiation of stable Ga targets (encapsuled in Nb) via a cyclotron proton irradiation (iThemba-provided communication). The raw ^{68}Ge material is then purified by way of volatilization and ion-exchange chemical processing techniques to produce radiochemically pure ^{68}Ge that is suitable for incorporation in ^{68}Ge/^{68}Ga generators. The manufacturing capacity under current capability at iThemba Labs is estimated to be approximately 4-5 Ci (148-185 GBq) ^{68}Ge per year, with the ability using current facilities to increase production to nearly 8 to 10 Ci (296-370 GBq) of process-purified ^{68}Ge per year.

The second major source of ^{68}Ge parent material is the United States, Department of Energy (DOE), which operates production facilities at Los Alamos National Laboratory (LANL; Los Alamos, NM) and Brookhaven National Laboratory (BNL; Brookhaven, NY), in the United States. Production facilities in the DOE have operated since 1954 with the inception of the US Atomic Energy Act, which specified a role for the US government in isotope production and distribution.[33] This program has grown to provide domestic supply of about 300 different isotopes (stable and radioactive), which the DOE sells for medical, commercial, research and national security applications. In fiscal year 2009, the DOE reports programmatic repositioning of isotope production to the Office of Science and revision of the program's mission to include maintenance of the infrastructure required to produce and supply isotopes (including ^{68}Ge) and related services. The revised mission of the program further included investigation and development of improved isotope production and processing techniques that can make new isotopes available. The DOE Isotope Program relies on appropriations and revenues from isotope sales to fund its operations. Yearly appropriations and sales revenues are deposited in a revolving fund that has flexibility for carryover from fiscal year to operate facilities, pay salaries, produce isotopes and fund other activities. The value of this flexibility to maintain operations in an unconstrained manner was evidenced recently with a steep decline in the use of strontium-82 (^{82}Sr) in 2010, which had accounted for over one-third of the programs total revenues.[34] The decrease in orders for ^{82}Sr declined steeply and unexpectedly as a result of a recall of the cardiac imaging device that represented the majority of the isotopes use. Through use of the revolving fund, the program demonstrated the ability to maintain continuous operations in spite of significant loss of current revenues. Further flexibility for production of ^{68}Ge by the DOE is related to the ability to produce at two independently operated sites (i.e. Brookhaven and Los Alamos).

The published funding appropriation for the DOE Isotope Program activities totaled nearly $20M US in fiscal year (FY) 2011, with total revenues exceeding $26M.[34] The program sold isotopes and provided related services to over 100 customers in FY 2011 domestically and internationally. Six of these customers account for more than 80% of sales in FY 2011. More than 95% of the program revenues were attributed to eight isotopes: Strontium-82, californium-252, helium-3, nickel-63, strontium-90, actinium-225, lithium-6 and germanium-68. According to these reports,

of total isotope sales, revenues for the DOE Isotope Program associated with ^{68}Ge production were nearly $2M US for FY 2011. Similar to the production route at iThemba LABS, the DOE has been irradiating Ga targets at its accelerator sites at BNL and LANL to produce and purify raw ^{68}Ge material. Published values for ^{68}Ge sales in radioactivity units from the US DOE were over 10 Ci (370 GBq) and 11 Ci (407 GBq) in FY 2009 and FY 2010 respectively. Interestingly, the modest increase in total ^{68}Ge revenues in radioactivity units contrasts the total number of shipments, which more than doubled from 26 in 2009 to 58 shipments of ^{68}Ge reported by the DOE in FY 2010. These sales are attributed, in these reports, to PET calibration sources, reflecting increased demand and economic dominance of solid ^{68}Ge/^{68}Ga calibration sources (in terms of total market need for ^{68}Ge), relative to generators for ^{68}Ga PET imaging applications. No documented shortages of ^{68}Ge could be found through our examination.[34] These observations suggest that the DOE has adopted strategies to increase production of ^{68}Ge in response to an growing market demand.

The third major source of parent ^{68}Ge material for generator production is the Cyclotron Co Ltd (Obninsk, Russia), which has operated production facilities for many years. Recent reports by the IAEA suggest that high specific activity material is routinely made available with capacity of approximately 2 Ci per run.[32,35] The company reports similar production methodologies, and produced over 6 Ci (222 GBq) in the calendar years 2010 and 2011. The company further reported a significant increase (up to 11 Ci or 407 GBq) in shipments for the calendar year 2012 (Cyclotron provided communication). The company reports that products were destined for generator manufacturing and calibration sources, although further breakdown of the use of the produced ^{68}Ge was not available at the time of this writing. The company further reports that in response to increased demand, the manufacturing facilities are currently capable of producing up to 15 Ci (555 GBq) per year, suggesting that the Obninsk operations are poised to respond to an increased market demand.

SUMMARY AND CONCLUSION

Gallium-68 generators are a promising, maturing technology, which is increasingly recognized around the world as suitable for routine clinical applications. In this brief perspective, the current production and availability of parent ^{68}Ge for manufacturing of generators has been examined. Currently, the vast majority of ^{68}Ge is produced in the Unites States, South Africa and Russia. In the United States, the Department of Energy has been using their accelerators at Brookhaven (BNL) and Los Alamos National Laboratories (LANL) for the production and distribution of ^{68}Ge for many years. The operating cycles at these facilities complement each other to enable continuous production and distribution of ^{68}Ge, with a current production level of approximately 11 Ci (407 GBq). In South Africa, iThemba LABS has been producing chemically processed ^{68}Ge for many years. The company reports current manufacturing capacity to be approximately 4 to 5 Ci (148-185 GBq) ^{68}Ge per annum, with ability using current facilities to increase production to nearly 8 to 10 Ci (296-370 GBq) of process-purified ^{68}Ge per year. Current production capacity of the third major supplier of ^{68}Ge (Cyclotron Co, Obninsk, Russia) is reported to be up to 15 Ci (555 GBq) per year, for a total estimated production capacity for the three major manufacturers of approximately 37 Ci (1369 GBq) per year. Although specific information on sales and demand of ^{68}Ge is highly business sensitive and thus guarded, currently there is no shortage in the supply of ^{68}Ge. On the other hand, increases in the use of ^{68}Ge generators for clinical applications in the United States point to the need for continued support for production at DOE laboratories in the United States to ensure a reliable supply and suggests that new commercial facilities may be needed to meet the increasing demand.

ACKNOWLEDGMENTS

Support for this work was provided by Nuclear Regulatory Commission (US NRC-HQ-12-G-38-0041; MKS), the Department of Homeland Security, Domestic Nuclear Detection Office and South Carolina University Research and Education Fund (2012-DN-130-NF0001; MKS), The National Institutes of Health (1R01CA167632-01; MKS), The US Department of Energy (Battelle Research Alliance; CR00131031), the University of Iowa Holden Comprehensive Cancer Center and the University of Iowa Dance Marathon.

REFERENCES

1. Breeman WA, de Jong M, de Blois E, Bernard BF, Konijnenberg M, Krenning EP. Radiolabelling DOTA-peptides with ^{68}Ga. Eur J Nucl Med Mol Imag 2005;32(4):478-85.
2. Decristoforo C. Gallium-68-A new opportunity for PET available from a long shelf-life generator-automation and applications. Curr Radiopharm 2012;5(3):212-20.
3. Fani M, Andre JP, Maecke HR. ^{68}Ga-PET: A powerful generator-based alternative to cyclotron-based PET radiopharmaceuticals. Contrast Media Mol Imag 2008;3(2):67-77.
4. Fani M, Maecke HR. Radiopharmaceutical development of radiolabelled peptides. Eur J Nucl Med Mol Imag 2012;39 Suppl 1:11-30.
5. Prata MI. Gallium-68: A new trend in PET radiopharmacy. Curr Radiopharm 2012;5(2):142-49.

6. Roesch F. Maturation of a key resource-the germanium-68/gallium-68 generator: Development and new insights. Curr Radiopharm 2012;5(3):202-11.
7. Afshar-Oromieh A, Haberkorn U, Eder M, Eisenhut M, Zechmann C. [^{68}Ga]Gallium-labelled PSMA ligand as superior PET tracer for the diagnosis of prostate cancer: Comparison with 18F-FECH. Eur J Nucl Med Mol Imag 2012 Jun;39(6): 1085-86.
8. Azad BB, Cho CF, Lewis JD, Luyt LG. Synthesis, radiometal labeling and in vitro evaluation of a targeted PPIX derivative. Appl Radiat Isot 2012;70(3):505-11.
9. Baum RP, Prasad V, Muller D, Schuchardt C, Orlova A, Wennborg A, et al. Molecular imaging of HER2-expressing malignant tumors in breast cancer patients using synthetic 111In- or ^{68}Ga-labeled affibody molecules. J Nucl Med 2010;51(6): 892-97.
10. De Decker M, Turner JH. Automated module radiolabeling of peptides and antibodies with gallium-68, lutetium-177 and iodine-131. Cancer Biother Radiopharm 2012;27(1):72-76.
11. Gemmel F, Van den Wyngaert H, Love C, Welling MM, Gemmel P, Palestro CJ. Prosthetic joint infections: Radionuclide state-of-the-art imaging. Eur J Nucl Med Mol Imag 2012 May; 39(5):892-909.
12. Ginj M, Maecke HR. Radiometallo-labeled peptides in tumor diagnosis and therapy. Met Ions Biol Syst 2004;42:109-42.
13. Gourni E, Demmer O, Schottelius M, D'Alessandria C, Schulz S, Dijkgraaf I, et al. PET of CXCR4 expression by a ^{68}Ga-labeled highly specific targeted contrast agent. J Nucl Med 2011;52(11): 1803-10.
14. Maecke HR, Hofmann M, Haberkorn U. ^{68}Ga-labeled peptides in tumor imaging. J Nucl Med 2005;46(Suppl 1):172S-78.
15. Persson M, Madsen J, Ostergaard S, Ploug M, Kjaer A. ^{68}Ga-labeling and in vivo evaluation of a uPAR binding DOTA- and NODAGA-conjugated peptide for PET imaging of invasive cancers. Nucl Med Biol 2012 May;39(4):560-69.
16. Simecek J, Schulz M, Notni J, Plutnar J, Kubicek V, Havlickova J, et al. Complexation of metal ions with TRAP (1,4,7-triazacyclononane phosphinic acid) ligands and 1, 4, 7-triazacyclononane-1, 4, 7-triacetic acid: Phosphinate-containing ligands as unique chelators for trivalent gallium. Inorg Chem 2012;51(1):577-90.
17. Tarkia M, Saraste A, Saanijoki T, Oikonen V, Vahasilta T, Strandberg M, et al. Evaluation of ^{68}Ga-labeled tracers for PET imaging of myocardial perfusion in pigs. Nucl Med Biol 2012 Jul;39(5):715-23.
18. Roivainen A, Jalkanen S, Nanni C. Gallium-labelled peptides for imaging of inflammation. Eur J Nucl Med Mol Imag 2012;39 (Suppl 1):68-77.
19. Buchmann I, Henze M, Engelbrecht S, Eisenhut M, Runz A, Schafer M, et al. Comparison of ^{68}Ga-DOTATOC PET and 111In-DTPAOC (Octreoscan) SPECT in patients with neuro-endocrine tumours. Eur J Nucl Med Mol Imag 2007;34(10): 1617-26.
20. Meyer GJ, Macke H, Schuhmacher J, Knapp WH, Hofmann M. ^{68}Ga-labelled DOTA-derivatised peptide ligands. Eur J Nucl Med Mol Imag 2004;31(8):1097-1104.
21. Zhernosekov KP, Filosofov DV, Baum RP, Aschoff P, Bihl H, Razbash AA, Jahn M, et al. Processing of generator-produced ^{68}Ga for medical application. J Nucl Med 2007;48(10):1741-48.
22. Breeman WA, Verbruggen AM. The ^{68}Ge/^{68}Ga generator has high potential, but when can we use ^{68}Ga-labelled tracers in clinical routine? Eur J Nucl Med Mol Imag 2007;34(7):978-81.
23. Maia S, Ayachi Hatit N, Paycha F. Situation of supply and boom of PET imaging: What is the future for technetium-99m in nuclear medicine? Ann Pharm Fr 2011;69(3):155-64.
24. Marcassa C, Campini R, Zoccarato O, Calza P. Technetium-99m supply shortage. Possible solutions in every day nuclear cardiology practice. Quart J Nucl Med Mol Img 2011;55(1): 103-04.
25. de Blois E, Sze Chan H, Naidoo C, Prince D, Krenning EP, Breeman WA. Characteristics of SnO_2-based ^{68}Ge/^{68}Ga generator and aspects of radiolabelling DOTA-peptides. Appl Radiat Isot 2011;69(2):308-15.
26. Chakravarty R, Shukla R, Ram R, Tyagi AK, Dash A, Venkatesh M. Development of a nano-zirconia based ^{68}Ge/^{68}Ga generator for biomedical applications. Nucl Med Biol 2011; 38(4):575-83.
27. Blom E, Koziorowski J. ^{68}Ga-autoclabeling of DOTA-TATE and DOTA-NOC. Appl Rad Isot 2012;70(6):980-83.
28. Nakayama M, Haratake M, Ono M, Koiso T, Harada K, Nakayama H, et al. A new ^{68}Ge/^{68}Ga generator system using an organic polymer containing N-methylglucamine groups as adsorbent for ^{68}Ge. Appl Rad Isot 2003;58(1):9-14.
29. Zhernosekov KP, Nikula T. Molecule for functionalizing a support, attachment of a radionuclide to the support and radionuclide generator for preparing the radionuclide and preparation process. US Patent Application Publication, 2010. US 2010/0202915 A1(August 12, 2010).
30. Gleason GI. A positron cow. Int J Appl Radiat Isot 1960;8: 90-94.
31. Yano Y, Anger HO. A gallium-68 positron cow for medical use. J Nucl Med 1964;5:484-87.
32. IAEA. Production of long lived parent radionuclides for generators: ^{68}Ge, ^{82}Sr, ^{90}Sr and ^{188}W. 2010. STI/PUB/1436.
33. The Atomic Energy Act. Science 1945;102(2653):441.
34. Office UGA. Managing critical isotopes: DOE's isotope program needs better planning for setting prices and managing production risks. GAO Report 2012;12-591.
35. Razbash AA, Krasnov NN, Sevastianov YG, Leonov AI, Pavlikhin VE. Germanium-68 row of products. 5th International Conference on Isotopes 2005;146-51.

ABOUT THE AUTHORS

Michael K Schultz (Corresponding Author)

Assistant Professor, Department of Radiology, Division of Nuclear Medicine, Carver College of Medicine, The University of Iowa, 500 Newton Drive MLB180 FRRB, Iowa City, Iowa-52242, USA Phone: +1 (319) 335-8017, e-mail: michael-schultz@uiowa.edu

Patrick Donahue

President, Blackthorn Associates, LLC, 32 Falcon Ridge Dr Hopkinton, Massachusetts, USA

Nannette I Musgrave

Manager, Department of Strategy and Portfolio Management Mallinckrodt, The Pharmaceutical Business of Covidien, Hazelwood Missouri, USA

Konstantin Zhernosekov

Research Scientist, ITG Isotope Technologies Garching GmbH Garching, Germany

Clive Naidoo

Head, Department of Radionuclide Production, iThemba LABS, Cape Town, South Africa

Anatolii Razbash

General Director, Cyclotron Co Ltd, Obninsk, Russia

Izabella Tworovska

Director, Department of Chemical Research and Drug Development RadioMedix, Inc, Houston, Texas, USA

David W Dick

Clinical Assistant Professor, Department of Radiology/Division of Nuclear Medicine, The University of Iowa, Iowa City, Iowa, USA

G Leonard Watkins

Clinical Professor, Department of Radiology/Division of Nuclear Medicine, The University of Iowa, Iowa City, Iowa, USA

Michael M Graham

Professor and Director, Department of Radiology/Division of Nuclear Medicine, The University of Iowa, Iowa City, Iowa, USA

Wolfgang Runde

Associate Director, National Isotope Development Center, US Department of Energy, Los Alamos, New Mexico, USA

Jeffrey A Clanton

RPH, Department of Radiology and Radiological Sciences, Vanderbilt University, Chattanooga, Tennessee, USA

John J Sunderland

Associate Professor, Department of Radiology, Division of Nuclear Medicine, The University of Iowa, Iowa City, Iowa, USA

10.5005/jp-journals-10028-1054
REVIEW ARTICLE

A Bridge not too Far: Personalized Medicine with the use of Theragnostic Radiopharmaceuticals

Suresh C Srivastava

ABSTRACT

This article deals primarily with the selection criteria, production, and the nuclear, physical, and chemical properties of certain dual-purpose radionuclides, including those that are currently being used, or studied and evaluated, and those that warrant future investigations. Various scientific and practical issues related to the production and availability of these radionuclides is briefly addressed. At brookhaven national laboratory (BNL), we have developed a paradigm that involves specific individual 'dual-purpose' radionuclides or radionuclide pairs with emissions suitable for both imaging and therapy, and which when molecularly (selectively) targeted using appropriate carriers, would allow pre-therapy low-dose imaging plus higher-dose therapy in the same patient. We have made an attempt to sort out and organize a number of such theragnostic radionuclides and radionuclide pairs that may thus potentially bring us closer to the age-long dream of personalized medicine for performing tailored low-dose molecular imaging (SPECT/CT or PET/CT) to provide the necessary pretherapy information on biodistribution, dosimetry, the limiting or critical organ or tissue, and the maximum tolerated dose (MTD), etc., followed by performing higher-dose targeted molecular therapy in the same patient with the same radiopharmaceutical. As an example, our preclinical and clinical studies with the theragnostic radionuclide Sn-117m are covered in somewhat greater detail.

A troublesome problem that remains yet to be fully resolved is the lack of availability, in sufficient quantities and at reasonable cost, of a majority of the best candidate theragnostic radionuclides in a no-carrier-added (NCA) form. In this regard, a summary description of recently developed new or modified methods at BNL for the production of five theragnostic radionuclide/radionuclide pair items, whose nuclear, physical, and chemical characteristics seem to show promise for therapeutic oncology and for treating other disorders that respond to radionuclide therapy, is provided.

Keywords: Radionuclide therapy, Personalized medicine, Theragnostics, Theragnostic radiopharmaceuticals, Tin-117m, Radionuclide production, Cancer therapy, Cardiovascular therapy.

How to cite this article: Srivastava SC. A Bridge not too Far: Personalized Medicine with the use of Theragnostic Radiopharmaceuticals. J Postgrad Med Edu Res 2013;47(1): 31-46.

Source of support: Nil

Conflict of interest: None declared

INTRODUCTION

Nuclear medicine has experienced an exponential resurgence of interest in radiotherapeutic procedures. Using unsealed sources for radionuclide therapy is not a new concept; it has been around for over 5 decades starting with the development of among others the treatment of thyroid disorders with radioiodine. However, recent advances in molecular biology have led to a better understanding of cancer and other disease states, and parallel research has shown promise for biological vehicles, such as monoclonal antibodies, specific proteins and peptides, and a variety of other intelligently designed molecules, to serve as specific carriers to deliver cell killing radiation into tumors in a highly localized fashion. These developments have led to a renewed interest in the exciting possibility of treating human malignancies with the systemic administration of radionuclides. A number of other relatively new modalities, such as the treatment of metastatic bone pain, radiation synovectomy, bone marrow ablation, and others, have given additional impetus to need for research on therapeutic radionuclides tailored for specific applications.

A major advantage of radionuclides is that they emit radiation of different radiobiological effectiveness and range of action. This offers the possibility of choosing a nuclide the physical and nuclear characteristics of which are matched with a particular tumor type, or the disease under treatment. In addition, certain dual-purpose ('theragnostic') radionuclides that seem to offer the exciting potential of pretherapy low dose imaging followed by higher dose treatment in the same patient, thus possibly bringing us a major step closer to personalized medicine, are discussed in somewhat greater detail in this article. We are reintroducing and reinforcing this relatively novel paradigm that involves specific individual theragnostic radionuclides or radionuclide pairs with emissions suitable for both imaging and therapy, and which when molecularly (selectively) targeted using appropriate carriers, would allow pretherapy low dose imaging plus higher dose therapy in the same patient. We have made an attempt to sort out and organize a number of such theragnostic radionuclides and radionuclide pairs that may thus potentially bring us a major step closer to the age-long dream of personalized medicine for performing tailored low dose molecular imaging (SPECT/CT or PET/CT) to provide the necessary pretherapy information on biodistribution, dosimetry, the limiting or critical organ or tissue, and the maximum tolerated dose (MTD), etc. followed by performing higher dose targeted molecular therapy in the same patient with the same radiopharmaceutical. Beginning in the 1980's, our work at

Brookhaven National Laboratory (BNL) with such a 'dual-purpose' radionuclide, tin-117m, convinced us that it is arguably one of the most promising theragnostic radionuclides and we have continued to concentrate on this effort. Our results with this radionuclide are therefore covered in somewhat greater detail in this paper.

THERAGNOSTIC RADIONUCLIDES

As mentioned above, certain radionuclides or radionuclide pairs have emissions that allow pretherapy information with low dose imaging, followed by higher dose therapy in the same patient.[1-4] Such dual-purpose theragnostic radionuclides, for example I-131, or the pair I-124/I-131 have been around and used for imaging followed by therapy, without consideration to the fact that the optimum radionuclide or the optimum radionuclide pair were not scientifically or methodically chosen with this requirement and/or with the particular disease in mind. Over 2 decades ago, when Y-90 began to be promoted for radio-immunotherapy and was undergoing rapid development, it was considered necessary to use In-111-monoclonal antibody (mAb) as a surrogate to carry out biodistribution and imaging studies in order to predict the dosimetry and toxicity prior to doing the therapy with Y-90-mAb, because of the lack of imageable photons in Y-90 emissions. After some very careful studies, the Julich group[5] and our own group at Brookhaven[6,7] showed that at best, it was hazardous to do so because these were two different elements whose biochemistry had many similarities but also many striking dissimilarities as well. Interestingly, this practice still continues, because of the lack of an alternate solution.[8] In such a situation, it would have been best to use the positron emitter Y-86, a congener of Y-90, and therefore with the same chemical and biochemical properties, to carry out pretherapy positron emission tomography (PET) imaging, so that imaging predicts biodistribution and dosimetry in a reliable, individualized fashion, and thus also predicts as to which patients will respond to the radionuclide therapy with Y-90 and which will not. However, Y-86 until very recently has not been available at all or only in insufficient quantities for this purpose. This situation is now changing and in many cases, if the therapeutic isotope has no photon emission, suitable congeners for imaging are becoming more and more available.

It is noteworthy that a number of such radionuclides or radionuclide pairs do exist[1-4] and it would make a lot of sense to direct their use for the development of 'theragnostic radiopharmaceuticals'. It is important to stress that ideally, for theragnostic use, the molecularly targeted radiopharmaceutical should constitute the same dual-purpose radionuclide with both imaging and therapeutic emissions. In the second best situation, as mentioned above for the Y-90 situation, a radionuclide pair (imaging photon emitter, either gamma or positron, and a congener of the therapeutic particle emitter, with the same electronic structure) can be used as well. One caveat here, which is a fact of life, is that even though many theragnostic PET/therapy radionuclide pairs may have the same electronic structure, their production and processing methodologies may be significantly different leading to the fact that their chemistry and in vivo behavior may be different as well due to differences in chemical species, charge, specific activity, etc. and/or the amount of chemical and radionuclidic and chemical impurities, which cannot be totally removed. Another caveat that one has to deal with is the issue of half-life of the imaging PET congener which in most cases might be much shorter than the usually (desirable) longer half-life of the therapeutic congener. In most situations, the determination of longer term biodistribution and dosimetry would be crucial but this information would not be achievable using the shorter lived PET congener for pretherapy imaging.

To re-emphasize, the theragnostic radionuclides or radionuclide pairs would initially allow molecular imaging (SPECT/CT or PET/CT) to provide the required and useful pretherapy information on biodistribution, dosimetry, the limiting or critical organ or tissue, and the maximum tolerated dose (MTD). If the imaging results then warrant it, it would be safe and appropriate to follow-up with dose ranging experiments to allow higher dose targeted molecular therapy with the greatest effectiveness. These factors are especially important in order to be able to do tailored imaging plus therapy (personalized medicine) in the same patient with the same radiopharmaceutical.[1-4]

There are indeed a number of individual radionuclides that emit both imaging photons and therapeutic electrons and which would be potentially excellent choices for theragnostic applications (Table 1). Some of the most promising PET/therapy radionuclide pairs are shown in Table 2. The lists included in both Tables 1 and 2 are not all-inclusive but consist of selected radionuclides and radionuclide pairs that are or could be made available in sufficient quantities to be of practical value, and which show the required combination of nuclear, physical and chemical properties, and thus the greatest promise. Some other criteria for inclusion were arbitrarily set at a minimum of 20% photon/positron emission for imaging, and a sufficiently abundant therapeutic particle emission consisting of medium (β^-) to high linear energy transfer (LET) electrons. It should be noted that there may be other suitable candidates from

Table 1: Selected theragnostic radionuclides[1]

Radionuclide	*t½ (days)*	*Principal y energy for imaging, keV (%)*	*Therapeutic particle(s) [Avg energy, keV (%) abundance]*
Scandium-47	3.35	159 (68)	β–(162)
Copper-67	2.58	186 (40	β–(141)
Gallium-67	3.26	93. 184, 296 (40, 24, 22)	15 Auger, 0.04-9.5 keV, 572% 10 CE, 82-291 keV, 30%
Indium-111	2.80	171, 245 (91, 94)	6 Auger, 0.13-25.6 keV, 407% 12 CE, 144-245 keV, 21%
Tin-117m	14.00	159 (86)	8 CE (141 keV avg, 114%)
Iodine-123	13.3 h	159 (83)	12 Auger, 23-30.4 keV, 1371% 7 CE, 0.014-32 keV, 17%
Iodine-131	8.0	365 (82)	β–(181)
Samarium-153	1.94	103 (30)	β–(280)
Astatine-211	7.2 h	79 (21)	α (5867, 42%)
Bismuth-213	46 min	441 (926)	β–(425); α (98%, from Tl-209 daughter, 2% from Bi-213)

Table 2: Selected theragnostic radionuclide pairs[1]

Radionuclide pair imaging/therapeutic	*T½ (d)*	*Imaging positron, keV (%)*	*Therapeutic particle(s) (avg energy, keV)*
Scandium-44/scandium-47	3.97/3.35	y ± 511 (99.9%)	β–(162)
Copper-64/copper-67	0.53/2.6	y ± 511 (38%)	β–(141)
Gallium-68/gallium-67	68 mins/3.26	y ± 511 (176%)	15 Auger, 0.04-9.5 keV, 572% 10 CE 82-291 keV, 30%
Yttrium-86/yttrium-90	0.61/2.7	y ± 511 (35%)	β–(935)
Iodine-124/iodine-131	4.2/8.0	y ± 511 (38%)	β–(181) i/mg of ^{67}Zn (mb)

the class of alpha and Auger electron emitters,[1-4,9-11] but these have not been included in this theragnostic group of radionuclides (except Ac-225/Bi-213) since their availability is either limited or not enough preclinical and clinical experimental data have thus far been available.

As mentioned above, a major problem that remains yet to be completely resolved is the lack of availability of a number of the best candidate therapeutic radionuclides, in particular the theragnostic radionuclides or PET/SPECT radionuclide pairs, in sufficient quantities and/or in a no-carrier-added (NCA) form. Methods have already been studied and developed for the production of research quantities of certain theragnostic radionuclides and radionuclide pairs listed in Tables 1 and 2 in particular Cu-64,[12] Y-86,[1-4,13,14] I-124,[15] and Sc-44.[16] Gallium-67, Y-90, In-111, I-123, Sm-153, Lu-177 and I-131 are routinely available from commercial sources. Close to sufficient quantities of Ge-68 (parent of Ga-68) are made available mainly from the Brookhaven Linac Isotope Producer (BLIP) at Brookhaven National Laboratory (BNL)[17] and from the Isotope Production Facility (IPF) at Los Alamos National Laboratory (LANL).

A summary description relating to the development of new or modified methods for the production of selected promising theragnostic radionuclides (Sc-47, Cu-67, Y-86, Sn-117m and Ac-225/Bi-213) is included in the following sections. Some of these have undergone through various stages of preclinical/clinical trials.

PRODUCTION OF SELECTED THERAGNOSTIC RADIONUCLIDES

Beta Emitters

Scandium-47

Two low energy reactions in the reactor that produce NCA Sc-47 are ^{47}Ti-47(n, p) ^{47}Sc and ^{46}Ca(n, γ)^{47}Ca(β$^-$) (t½ = 4.54 days).[18] The former reaction requires E_n >1 MeV, while the latter reaction uses thermal neutrons. Both types of neutrons are available in the fission neutron spectrum in the High Flux Isotope Reactor at Oak Ridge National Laboratory. The advantages of the ^{46}Ca(n, γ)^{47}Ca(β$^-$) reaction are: (i) The year-round availability of high flux thermal neutrons and (ii) use of a Ca-47/Sc-47 generator system to supply Sc-47 activity. The disadvantage of this route is the requirement of an enriched target. Calcium-46 is presently available with only 30% enrichment and at a very high price, which makes target costs prohibitive.

The ^{47}Ti(n,p) route also requires an enriched target though ^{47}Ti-O_2 is available with very high enrichment (94.53% Ti-47, 4.74% Ti-48, 0.35% Ti-46, 0.2% Ti-49 and 0.18% Ti-50) and at more reasonable cost. The hydraulic tube positions at HFIR at ORNL (with 4.6 × 10^{14}

neutrons cm^2s) have adequate flux in the high energy region of the neutron spectra to produce sufficient quantities of Sc-47 activity for theragnostic applications in radioimmunotherapy. The reported cross-section in a fission neutron spectrum is 18.9-26 mbarn, which is comparable to the cross-section value for proton-induced reactions, such as ^{nat}Ti(p, 2p) and ^{51}V(p, 3pn).[19]

Several $^{47}TiO_2$ targets were irradiated at HFIR for periods ranging from a few hours to several days.[19] The experimental results are lower than the theoretical ones, perhaps due to differences in the actual neutron spectrum when the irradiations occurred compared to the theoretical neutron spectrum. High production yields using the PTP positions at the HFIR were obtained. These results indicate that Sc-47 can be produced at a reactor using the ^{47}Ti(n,p) reaction in quantities sufficient for theragnostic applications. For example, at HFIR a 3.35 day (one half-life of Sc-47) irradiation of a 10g target would theoretically produce ~75 Ci of Sc-47 at EOB. Both the Sc-46/Sc-47 and Sc-48/Sc-47 impurity ratios are less than 0.4% at EOB (end of bombardment), leading to a product with greater than 99.5% radiopurity.[18,19]

The specific activity of Sc-47 depends essentially on the scandium content of the enriched target material. Scandium is not a ubiquitous contaminant, such as lead or copper, and would not be expected to be introduced during processing of the target. These expectations were borne out when several product samples were analyzed with ICP-AE and no stable Sc was detected.[19] Since scandium was not detected in batches of target material, stable scandium content can be assumed to be the reported detection limit. The specific activities are high enough for antibody labeling applications in radioimmunotherapy. Conservatively assuming that an average of two to three scandium-ligand complexes can be attached to each antibody molecule without loss of immunoreactivity, up to 30 mCi (1.16 GBq) of ORNL produced Sc-47 can be used to label 1 mg of a typical IgG antibody (mol. wt. ~150 kDa) given the measured specific activities.[19]

Finally, it is necessary to recycle the expensive enriched target material to defray the target cost over many production runs. A simple procedure was developed that recovers ~98.5% of the oxide based on precipitation of titanium at basic pH followed by conversion to the oxide using higher temperature.[19] Titanium may be recovered and easily reused since the only titanium activation product is the short lived Ti-51 ($t_{½}$ = 5.8 minutes) produced by the ^{50}Ti(n, γ) reaction using thermal neutrons. Other radionuclidic impurities that have been detected in recycled material are Ta-182 ($t_{½}$ = 114.4 days) and Zn-65 ($t_{½}$ = 244 days). These isotopes are also produced by (n, γ) reactions on minor target impurities of stable Ta and Zn. If required, these impurities could easily be separated from the target material using anion-exchange chromatography before precipitation of the titanium.[19]

Relative production yields were also determined using the (p, 2n) reaction on $^{48}TiO_2$ targets (98.5% $^{48}TiO_2$) at the BLIP in the energy region $48 < E_p < 150$ MeV.[18,19] These targets were irradiated to see whether the use of isotopically enriched Ti-48 would improve the Sc-47/Sc-44m, 46,48 radioimpurity ratios compared to using natural Ti targets. There is the expected improvement in the Sc-47/Sc-44 ratios using enriched targets since the ^{49}Ti(p, 2p)^{48}Sc and ^{50}Ti(p, 2 pn)^{48}Sc reaction pathways have been eliminated. The Sc-47/Sc-44m ratio is better at lower irradiation energies (Ep < 100 MeV); however, unfortunately the Sc-47/Sc-46 ratios are worse throughout the energy region measured. Thus, this production method would not be suitable for producing Sc-47 with sufficient purity for therapeutic use.[19]

Although Cu-67 has long been considered as one of the ideal therapeutic/theragnostic radionuclides (vide infra), its scaled up production with a sufficiently high specific activity is still an issue that has only partially been resolved and further improvements are difficult if not questionable, at this time. With this in mind, we have proposed Sc-47 as a possible replacement for Cu-67[20] as shown in Table 3.

Table 3: Sc-47 *vs* Cu-47 as a therapeutic radiolabel[20]

	Cu-67		*Sc-47*	
	Advantages	*Disadvantages*	*Advantages*	*Disadvantages*
Half-life	Good (2.58 d)	–	Good (3.35 d)	–
Beta energy, keV (total, weighted avg.)	Good (141)	–	Good (163)	–
Imageable photon (keV, %)	Good (185, 49%)	–	Good (159, 68%)	–
Specific activity	–	Low (2-18 mCi/μg)	High (no-carrier added)	–
Radiochemistry	–	Average	Good	–
Ease of production	–	Hard (accelerator)	Easy (reactor)	

Copper-67

Copper-67, with a 2.6-day half-life, is the longest lived radioisotope of Cu.[21] It provides medium energy emission of 0.6 MeV_{max} (average, 141 keV), photon emissions (184 keV, 48.7%; 93 keV, 16%; 91 keV, 7%), and facile labeling chemistry. It is a very attractive theragnostic radionuclide.[1-4] The half-life is suitable for imaging slow *in vivo* pharmacokinetics with agents, such as mAbs and other carrier molecules, and the beta particle energy is appropriate for therapy. The 185-keV gamma ray (49%) permits imaging of the uptake and biodistribution of the agent both before and during therapy administration. It can also be paired with the positron emitter Cu-64 to perform pretherapy biodistribution determinations and dosimetry by PET. However, as mentioned earlier in this article, the use of Cu-67 has been inhibited by a lack of regular availability of sufficient quantities at a cost that researchers can typically afford, as well as the low specific activity issue.[7,21] In the past several decades, the most typical source in the United States has been the high energy proton irradiation of natural Zn targets,[21] primarily irradiated at either the BLIP (Brookhaven Linac Isotope Producer) at BNL or at the Isotope Production Facility (IPF) at LANL (Los Alamos National Laboratory). These are both large accelerators operated and funded for physics research only part of each year. Thus, in the past, it has not been possible to provide Cu-67 on a time frame suitable to support clinical trials, with the attendant schedule fluctuations and changing patient status.[22,23] Additionally, the specific activity was at the low end of what was acceptable for antibody therapy, ranging from about 5 to 10 Ci (185-370 GBq) per mg of Cu at EOB. With the construction of a new target station at the IPF at LANL in 2004, the beam intensity and production have improved, but year-round availability still cannot be assured. Recent studies at BNL have tried to determine the causes of the low specific activity.[24] Exhaustive assays of all the reagents used in processing determined that these contribute only approximately 0.3 μg of Cu. Addition of the ZnO target to these blank experiments contributed only another 1.4 μg of Cu. This compares with the 25 μg of Cu typically measured in a batch of 80 to 380 (~3-14 GBq) of Copper-67. This result implies that most of the stable Cu found in each batch is produced directly by proton nuclear reactions on Zn, an often forgotten process. To investigate this hypothesis further, theoretical calculations of stable Cu isotopes were attempted using the well-known nuclear radiation transport code MCNPX. The predicted direct production of stable Cu-63 was approximately 11 μg, and 1μg of stable Cu-65, for every 200 mCi (~7.4 GBq) of Cu-67 produced. Therefore, this route is the major source of the reduction in specific activity and will be very difficult to remove. Because Cu-63 is likely produced by the $^{64}Zn(p, 2p)$ and $^{66}Zn(p, 3p)$ reactions, use of a highly enriched Zn-68 target containing minimal Zn-64, 66 may suppress the Cu-63 production. Recent accurate cross-section measurements on the $^{68}Zn(p, 2p)^{67}Cu$ reaction performed radiochemically over the energy range of 30 to 70 MeV showed that the yield of Cu-67 is fairly high.[24] Unfortunately, Zn-68 is rather expensive. Also, recycling the target material is considered difficult because of the unavoidable coproduction of long-lived Zn-65 in the target, unless the proton energy is kept around 70 MeV. To try to resolve these issues, BNL has recently been engaged in further research to develop the production of Cu-67 using high energy proton irradiation of enriched Zn-68 targets, followed by selective chemical separation of the pure product.[24] A number of specific challenges were addressed: (i) Development of very thick electroplated Zn-68 disks as targets, (ii) development of recovery/reuse technique of this expensive material after radiochemical processing, (iii) development of a target capsule that can be sealed and then opened remotely in a hot cell, (iv) development of a rapid highly selective chemical separation process for Cu-67 and (v) performing irradiations and measurements of product radiopurity, chemical purity and labeling efficiency. This research has allowed the prospect for the production capability for Cu-67, using a high beam-current accelerator or cyclotron, in sufficiently large quantities and with a greater than five times of the previously obtained specific activity, to support clinical trials.[24]

Yttrium-86

The popular beta-emitter therapeutic isotope Y-90, which is part of the Food and Drug Administration—approved radioimmunotherapy agent Zevalin (Spectrum Pharmaceuticals, Inc, Henderson, NV), has no imageable gamma photon in its emission. However, Y-86, a positron emitter ($E\beta^- = 660$ keV, 33%) with a t½ of 14.74 hours, could be a good choice as a surrogate pretherapy PET imaging congener for Y-90[2-5] for various Y-90 based therapeutic radiopharmaceuticals including Zevalin. Although there are several high energy gamma particles in its emission (Eγ, keV: 1076.6, 82.5%; 627.7, 32.6% and many others), which contribute to increased patient dose with no benefit, for cancer patients, who are candidates for radioimmunotherapy, the imaging dose would generally not be considered as a major issue of concern.

The possible production routes for Y-86 that have been considered are as follows: $^{86}Sr(p, n)^{86}Y$, Ep = 14.5 → 11.0 MeV; $^{natRb}(3He, xn)$, E ^{3}He =24 → 12 MeV; $^{88}Sr(p, 3n)^{86}Y$,

Ep = 45 → 37 MeV; and ^{90}Zr(p, 2p3n)^{86}Y, Ep = 40 → 30 MeV.[1,3-5] Out of these, it seems that the best method is the ^{86}Sr(p, n)^{86}Y reaction, but it requires enriched ^{86}Sr, which is rather expensive, and economy requires its recovery and reuse.[5,13,14] Recovered Sr-86 will contain radioactive Sr-85 after first irradiation if the proton energy is more than 14 MeV, which would mean that hot cell target assembly will be required. At BNL, we have designed such a target, both halves of which are aluminum for better conductivity, head screws are large enough for remote manipulator handling and silver-coated stainless steel C-rings are used to provide adequate seals.[14] Such a target design was successfully irradiated in the BLIP without any leakage and can be opened and sealed in a hot cell.

Modification to increase active area in beam may increase production levels but will require more enriched Sr-86 to be used. However, if really a low energy of 14 MeV is used, the amount of target material needed is not high. Targets of both natural $SrCl_2$ and enriched $SrCl_2$ were irradiated yielding 10-13 mCi/μAh of Y-86, giving an EOB batch yield of ~1,000 mCi in 1 hour, which is quite high.[14] Chemical yields of Y-86 ranged from 82 to 93%, and a further improvement is desirable. For labeling purposes, this chemical purity allowed for a labeling yield of 84%, and this needs to be improved further as well. The level of a major radionuclidic impurity, Y-87m, was a disappointing 34 to 55%. The low energy route on enriched Sr-86, which has previously been used[4,5] has allowed for better material and is now being pursued at BNL for larger-scale production. At BLIP, our first irradiation gave very low yield because the beam spot was larger than the target area. Also, the lowest tunable beam energy at the BLIP is 65.5 MeV, but the nuclear reaction cross-section peak is at ~14.5 MeV. The choice of degraders seems to have resulted in too high a target entrance energy. BLIP is not an ideal facility for this low energy reaction, but we carried out these investigations mainly to produce some material to develop a better and quicker radiochemical processing methodology that was short enough to allow for same-day irradiation and shipment, which has recently been accomplished.[14]

ALPHA, AUGER AND CONVERSION ELECTRON EMITTERS

Alpha Emitters

As mentioned earlier, targeted alpha radiation therapy can be a very potent treatment of cancer.[25] Due to comparatively short range of alpha particles in tissue and their high LET nature, radiation damage is mainly confined to targeted cells. The radiation burden to the surrounding healthy tissues is low when compared to beta emitters. By facilitating an efficient delivery of alpha-emitting isotope it is possible to achieve a very effective treatment regimen for the types of cancer where microscopic and small volume tumors are present. The effectiveness of alpha radioimmunotherapy has been confirmed in clinical and preclinical trials.[26,27]

A number of alpha emitting radioisotopes have been proposed as possible candidates. Among those are At-211, Bi-212, Bi-213, Ac-225, Pb-212, Ra-223, Tb-149 and Fm-255. Some of them (Bi-212, Bi-213, Ac-225, Pb-212, Ra-223) are produced from reactor irradiations, incorporated on generators and subsequently eluted. However, most of the clinical studies have been inhibited by a very limited supply of alpha-emitting isotopes, especially those that have theragnostic properties, for example, astatine-211, ^{213}Bi, radium-223 (223Ra) and ^{225}Ac. Three of these (213Bi, ^{225}Ac and 223Ra) are presently produced from reactor neutron irradiations, incorporated on generators and subsequently eluted. Their parent nuclides are often fissile materials and require special safeguard requirements due to nonproliferation concerns. On the other hand, production of At-211, Tb-149 and Fm-255 require alpha beam (At-211), 600 MeV protons (Tb-149) or neutron irradiation of Curium (Fm-255). Only a very few facilities in the world have such capabilities, and most of these because of their other primary missions are not generally available for isotope production.[1]

Astatine-211

Astatine-211 (t½ = 7.2 hours) decays through two paths, each emitting an alpha particle. The mean alpha energy is a potent 6.8 MeV. It is produced by the ^{209}Bi(α,2n) reaction and typically separated from the target by dry distillation into a chloroform solution.[28,29] A difficulty in this process is that the cyclotron energy must be carefully controlled to minimize the coproduction of astatine-210. This isotope (t½ = 8.1 hours) decays to Po-210 (t½ = 138 d) which is an alpha particle emitting bone seeker *in vivo* and could cause considerable hematological toxicity. The half-life of At-211 is relatively long compared to the other alpha emitters thus, allowing time for chemistry of labeling and use for molecular carriers with slower tumor uptake. However, it is more easily catabolized and shed after cell internalization of the labeled antibody/antigen complex than the metallic alpha emitters.[30] The main problem that inhibits clinical trials with this isotope is the relatively low nuclear yield and very limited number of cyclotrons capable of producing astatine-211. This situation may be somewhat improved in the coming years when the ARRONAX cyclotron in Nantes, France, as expected, goes into routine operations in early 2013.[31]

Actinium-225/Bismuth-213 System

Targeted alpha radiation therapy with alpha emitters Ac-225 and Bi-213, as is the case with astatine-211 (vide supra), is also a very promising treatment of cancer.[25] If selective efficient delivery of these alpha-emitting isotopes to tumor cells is achieved, they can become very effective for the treatment of the types of cancer where microscopic and small volume tumors are present. The effectiveness of alpha radioimmunotherapy using these isotopes has already shown promise in preclinical and clinical trials.[26,27] The results of the only human clinical trial involving an alpha-emitting isotope have demonstrated feasibility and antileukemic effects of Bi-213-HuM195, a humanized anti-CD33 mAb, specifically designed to target myeloid leukemia cells. In this study, 78 to 93% of the subjects showed reduction in circulating and bone marrow blasts.[28] A clinically approved Ac-225/Bi-213 generator capable of producing 25 to 100 mCi of Bi-213, suitable for antibody labeling, was developed[32] and continues to be improved upon. The antibodies and peptides labeled with the generated Bi-213 have successfully been used in numerous preclinical and clinical trials.[26,27,32,33] As mentioned above, most of the clinical studies have been inhibited by a very limited supply of these and other alpha-emitting isotopes, especially those that have theragnostic properties, for example, At-211, Bi-213, Ra-223 and Ac-225.

The *in vivo* use of targeted NCA Ac-225, in its own right, has received a great deal of attention as well.[34,35] Because of its ability to produce 4 alpha-emitting daughters, its overall potency to destroy cells is higher. The isotope has been referred to as an *in vivo* alpha particle nanogenerator because its power proliferates beyond the size of the atom.[35] In addition, the applications of Ac-225 were further extended to encapsulation in liposomes[36] and metallofullerenes.[37] At the Memorial Sloan–Kettering Cancer Center, a clinical trial for radioimmunotherapy of acute myeloid leukemia with both Bi-213 and Ac-225 has recently been carried out.[38] As mentioned earlier in the text, Ac-225 has been used for radioimmunotherapy both as a potent alpha emitter attached to an antibody and as a generator for the daughter alpha emitter Bi-213 (t½ = 45.7 minutes). The decay of Bi-213 is accompanied by emission of 440.45 keV (I = 25.9%) gamma photon, which allows SPECT imaging to study pretherapy biodistribution, pharmacokinetics and dosimetry of the labeled radiopharmaceuticals. The current availability of Ac-225 is very limited and insufficient to support ongoing and proposed clinical trials. Currently, there are two suppliers of Ac-225. One is the US Department of Energy's ORNL and the other is the Institute for Transuranium Elements in Karlsruhe, Germany. Both suppliers obtain thorium-229 from uranium-233 that was produced as part of US molten salt breeder reactor program. The current stock of purified Th-229 at ORNL is 150-mCi. In an 8-week period, about 100 mCi of Ac-225 grows in from that supply, separated and provided for clinical trials. Because Th-229 decays to Ac-225 through intermediate daughter Ra-225, Ra can be isolated to provide additional quantities (up to 20 mCi) of Ac-225.[39-41] Similarly, the Institute of Transuranium Elements can separate 43.2 mCi of Ra-225 and 39.4 mCi of Ac-225 from their stock.[40] It is widely acknowledged that the anticipated growth in demand for Ac-225 will soon exceed the levels extractable from the available uranium-233.[39]

At BNL, our intent is to carry out future investigations in an effort to increase the supply of Ac-225. This would involve using the high energy proton spallation reaction ^{232}Th(p, 2p6n)^{225}Ac on natural Thorium. This method has recently been studied and developed at other places, in particular, at the Institute of Nuclear Research (INR) in Troitsk, Russia, using accelerated protons at energies between 90 and 145 MeV in their 160-MeV proton accelerator.[41] This investigation has pointed out that the yield of Ac-225 increases monotonically with the proton energy. Therefore, the BLIP at BNL (200 MeV) would be capable of producing almost twice as much with an incident energy on the target of 192 MeV, with 110 μA beam intensity. The expected outcome of the BNL effort would be the method for Ac-225 production with quality (radionuclidic and chemical purity) suitable for applications both as a radiotherapeutic agent (Ac-225) and as a generator of Bi-213 (theragnostic use). The proposed work will involve development of an optimized Th-232 target for irradiation, development of the chemical procedure for dissolution and processing of irradiated target to selectively separate Ac-225, and carrying out preliminary labeling studies of conventional targeting molecules with Ac-225/Bi-213 to demonstrate the efficacy of the final purified radioisotope(s) for the eventual protein/antibody labeling applications.

At BNL, the method could potentially yield Curie amounts of Ac-225 in a 10-day irradiation period at the BLIP. The produced Ac-225 can be used for radio-immunotherapy as well as for generation of Bi-213 in a quality suitable for clinical trials. Shorter-lived radioisotopes Ac-228, 226, 224 will be coproduced in quantities comparable with those of Ac-225, but the activities of these isotopes will saturate out during the 10-day irradiation. The radionuclidic purity of the Ac-225 can be improved by

allowing a cool-off period for the target. Ten days (one t½ of Ac-225) after EOB, the coproduced Ac radionuclides will comprise 1% of the activity of Ac-225. Among these, Ac-227, because of its 21.77-year half-life, is the only radioimpurity that might be of some concern as far as noninvasive imaging is concerned but, in principle, of less concern for theragnostic use. However, this issue would require further investigation and additional studies.

Small quantities of Ac-225 can also be prepared by the reaction $^{226}Ra(p, 2n)^{225}Ac$ over an energy range of 13 to 20 MeV.[42] The cross-section for this reaction is calculated to reach a peak of 700 mb at 16 MeV but total yield is limited by the small energy range (and target thickness) where this reaction is favorable. Similarly the photonuclear reaction $^{226}Ra(\gamma, n)^{225}Ra$ (t½ = 14.9 days) followed by beta decay to Ac-225 is feasible but requires an extremely large Ra target (~40g) that represents radiological safety issues and availability concerns.

Thus, Ac-225, when produced by the BNL method, could substantially add to the very limited present supply of this promising alpha emitter. According to experimental and theoretical extrapolations, and assuming certain target dimensions, radiochemical processing losses, and so forth, the projected yields from a 10-day irradiation at the 5 high energy accelerators in the world are estimated (from the studies at INR) to be as follows (in Curies; experimental, and theoretical values within parentheses): BLIP at BNL, 3.1 (4.9); INR in Russia, 2.6 (4.1); IPF at LANL, 0.7 (1.3); Tri-University Meson Facility (TRIUMF) in Canada, 0.5 (0.7); and Arronax in France, 0.2 (0.7), giving a total of ~7 (11) curies.[41] This would allow detailed preclinical and clinical studies to determine the therapeutic potential of Ac-225 itself as well as of the theragnostic daughter Bi-213. Many of the presently available bifunctional chelating agents as well as those based on cyclohexylethyl-enediamine tetraacetic acid (CDTA) and 1,4,7,10-tetraazacyclo-dodecane-1,4,7,10-tetraacetic acid (DOTA) derivatives, developed earlier at BNL[43,44] should allow linking Ac-225 and Bi-213 with protein bifunctional chelating agent conjugates that will have high *in vivo* thermodynamic and kinetic stability. It would, of course, serve as a generator of Bi-213 similarly to Ac-225, produced by the decay from Th-229.

Auger and Conversion Electron Emitters

The production of metastable nuclei, such as conversion electron emitter Sn-117m and Auger electron emitter Pt-195m via neutron radiative capture reactions is characterized by small neutron cross-sections and, hence, low production rates. Metastable nuclei typically have excitation energies on the order of 100 keV, and large differences in angular momentum from ground states (most metastable nuclei have high angular momentum). An alternative route for producing these types of metastable nuclei is through neutron inelastic scattering where the cross-section of the $^{A}Z(n, n')^{Am}Z$ reaction is, in some cases, substantially higher than the cross-section for the $^{(A-1)}Z(n, \gamma)^{Am}Z$ route. As has been shown for the case of Sn-117m[45] the magnitude of gain in the cross-section may compensate for the relatively lower fast neutron flux from a well-moderated fission spectrum. Note that the excitation energy of metastable nuclei will represent the threshold for inelastic scattering. Large research reactors, such as HFIR at ORNL, and HFBR (now closed down) in the United States, and at the Research Institute of Atomic Reactors (RIAR) in Dimitrovgrad, Russia, with significant epithermal and fast neutron fluxes, have been well suited for these types of reactions.

A systematic study of the production of Sn-117m, and Pt-195m in the hydraulic tube facility of the HFIR was reported.[46] In all three cases, the yields from the [n, n'] reactions were higher than those obtained from the [n, γ] reactions. The relative gains in the specific activity of the unfiltered (no Cd filter) targets were 1.4, for Pt-195m, and 3.3 for Sn-117m. The excitation energies for Sn-117m and Pt-195m are 314.6 and 259.2 keV respectively. Since, the thresholds for these inelastic scattering reactions are well above the cadmium cutoff, Cd filters did not have any effect on the yield of these reactions. The corresponding cross-sections for the inelastic neutron scattering reactions for the production of Sn-117m, and Pt-195m are 222 ± 16, and 287 ± 20 mb respectively. A value of 176 ± 14 mb for the cross-section of Sn-117[n, n']Sn-117m reaction obtained at HFBR was reported earlier.[45]

Conversion Electron Emitter Tin-117m

The most common method for Sn-117m production is based on irradiation of tin with neutrons using the $^{117}Sn(n, n\gamma)^{117m}Sn$ reaction.[45] However, since this reactor production method is based on the inelastic neutron scattering reaction using enriched Sn-117 as a target, it results in Sn-117m with a low specific activity of about ≤20 Ci/g.[47] Stannic complexes with Sn-117m of such specific activity, particularly $Sn\text{-}117m^{4+}$-DTPA, effectively reduce pain from bone metastases without adverse reactions related to bone marrow, as demonstrated by the results presented in Tables 4 and 5.[48] However, such low specific activity does not allow scaling up the therapeutic doses for treating bone metastases. Also it is not acceptable for radioimmunotherapy and for many other applications.

Although it is not possible to achieve a higher than about 22mCi/mg of specific activity in the reactor-produced tin-

Table 4: Metastatic bone pain relief from Tin-117m DTPA: Phase II clinical[1] studies[48]

		Patients experiencing relief			
Dose group (MBq/kg)	*n*[2]	*Complete (100%)*	*Partial (>50%)*	*None (0-50%)*	*Total response (%)*
2.6	5	0	3	2	3 (60)
5.3	9	3	4	2	7 (78)
6.6	5	3	1	1	4 (80)
8.5	9	2	4	3	6 (67)
10.6	12	4	6	2	10 (83)
All doses	40	12	18	10	30 (75)

[1]Total patients 57; 54 received a single dose and 3 received 2 doses each; [2]A total of 40 therapeutic administrations were assessable

Table 5: Myelotoxicity levels[1] of radiopharmaceuticals for bone pain palliation[48]

Radiopharmaceutical	*Dose group*		*No. of patients with grade ≤ 2 toxicity*	
	(mCi/Kg)	*n*	*WBC*	*Platelets*
Sr-89 Cl_2	0.154	67	25 (37%)	41 (61%)
	0.040	161	48 (31%)[2]	
Re-186 HEDP	0.500-1.143	12	2 (17%)	3 (25%)
Sm-153 EDTMP	1.00	20	3 (15%)	5 (25%)
	1.50	4	3 (75%)	1 (25%)
	3.00	6	4 (100%)	2 (50%)
Sn-117m DTPA	0.143	9	1 (11%)	0 (0%)
	0.179	5	0 (0%)	0 (0%)
	0.286	12	1 (8%)	0 (0%)

[1]Using NCI criteria; [2]Only hematological toxicity at grade ≥ 2 mentioned

117m[47] NCA tin-117m can be produced by proton irradiation of antimony via nuclear reactions (p, 2p3n) or (p, 2p5n) in an accelerator.[45,49]

NCA Sn-117m can also be produced in an accelerator via a large number of other nuclear reactions. Using the ^{115m}In (α, pn)^{117m}Sn reaction over the energy range of 45 to 20 MeV, a relatively pure product is obtained; however, with very small yields.[50] In addition, the nuclear reaction ^{116}Cd(α, 3n)^{117m}Sn is also very useful for the production of NCA Sn-117m. The thick target yield over the energy range 47 → 20 MeV is about 150 μCi/μAh. Unfortunately, the present limiting factor for the scaled up production of Sn-117m via this route is the availability and power of existing alpha accelerators and targetry.[51] Using the BLIP at BNL, we have been producing NCA Sn-117m with the natural antimony$^{(natSb)}$(p, xn)^{117m}Sn reaction over the energy range of 38 to 60 MeV for quite some time.[45] This process, with a cross-section of 5 mb, was found enough to produce therapeutic quantities of Sn-117m with high specific activity. The specific activity when assumed to be wholly dependent on the amount of Sn impurity in the Sb target was calculated to be 30,000 mCi/mg for each part per million of Sn in the target. However, further theoretical cross-section calculations at the INR in Troitsk, Russia (*vide infra*) have demonstrated that the proton energy range should be much broader, perhaps 40 to 130 MeV.[49] The specific activity of Sn-117m depends mainly on the amount of stable tin, which is also generated during the irradiation of natural Sb, and the specific activity can vary from ~1000 to 3000 mCi/mg at EOB, a range that is quite suitable for radiolabeling molecules that bind to saturable *in vivo* receptors.

More recently, the larger-scale accelerator production and availability of NCA Sn-117m with high purity and high specific activity, targets based on natural or enriched Sb have been developed in our collaborative research between BNL and INR, along with other institutes, including the Institute for Physics and Power Engineering in Obninsk (IPPE) and Moscow State University (MSU), in the neighboring regions in Russia.[49] This project was initiated under a US Department of Energy/National Nuclear Security Administration/Global Initiative for Proliferation Prevention (DOE/NNSA GIPP) Program in 1999 and completed in 2009. Results from this 10-year BNL/INR collaborative study have demonstrated and fulfilled the promise for the high energy accelerator production of NCA Sn-117m in multi-Curie amounts for clinical theragnostic applications.[49]

Within this collaborative research program with BNL, investigations at INR dealt with the development of antimony as wells as antimony/titanium intermetallic targets suitable for the high energy production of NCA tin-117m. For irradiation with the high-intensity proton beam, targets consisting of Sb-monolith encapsulated into shells made of stainless steel or graphite were developed.[49] The shells were

filled with metallic antimony as follows. Powdered metallic antimony was inserted into the shells under inert nitrogen atmosphere, and the filled shell was heated at 645 to 660°C. It was found that at higher temperature liquid antimony reacts with iron and can destroy the stainless steel shell during the target preparation or irradiation. Graphite target shell is more reliable since there is no noticeable reaction between graphite and antimony, and graphite has higher heat conductivity than stainless steel [80-120 W/(m·K) *vs* 20 W/(m·K) at 300°C], providing effective target cooling. After antimony melting and shrinkage, the shell was again filled with powder of antimony and heated to melt again. The target with metallic shell containing a monolith of 29g metallic antimony (a cylinder 9 mm thick, 30 mm in diameter) was hermetically sealed with a threaded plug. The graphite shell targets (plates 32 × 76 × 5 mm, 3 mm of Sb thick each, 19g Sb each) were hermetically sealed with a cover by means of high temperature radiation resistant glue and electroplated outside with nickel in order to protect graphite from reaction with water radiolysis products during irradiation.[49]

The irradiated Sb-targets were chemically processed at the hot cell facility at IPPE in Obninsk. The stainless steel shell was dissolved in concentrated HCl while the graphite shell was opened mechanically. The freed Sb monolith was dissolved in concentrated HCl with gradual addition of small amount concentrated HNO_3. The major amount of Sb (in the form Sb^{5+}) was removed from the solution (10-11 M HCl) by extraction with dibutyl ether. Final purification of NCA Sn-117m from the rest of Sb, coproduced Te-118, 119m, 121m and In-111, 114m was achieved by chromatography on SiO_2 in 0.5 M sodium citrate (Na_3Cit) solution. Tin isotopes remained adsorbed on SiO_2 while Sb and radioisotopes of Te and In were washed out. Then the column was washed with 0.5 M Na_3Cit solution and water acidified by citric acid. Finally, tin was eluted from the column with 6 M HCl. Radionuclidic purity of the final solution and the specific activity of Sn-117m in the final product were determined using appropriate counting procedures (spectral emission analysis), and through inductively coupled plasma (ICP) spectrometry. Among other isotopes of tin coproduced with Sn-117m, Sn-113 is the most important impurity. It has a long half-life (115 d), relatively high energy γ-rays (392 keV) and cannot be chemically separated from Sn-117m. But it is possible to reduce Sn-113 impurity up to almost 1% by lowering the initial proton energy. The optimum range of between 55 and 20 MeV has been demonstrated to be most effective, although at the expense of somewhat reduced Sn-117m product.[52]

THERAGNOSTIC STUDIES WITH Sn-117m

Sn-117m ($t_{½}$ = 14.0 days; γ 159 keV, 86%) shows considerable promise as a theragnostic radionuclide due to its nuclear, physical and chemical characteristics. As mentioned earlier in this paper, it is certainly one of the best radionuclides for the development of theragnostic radiopharmaceuticals, in particular, for nuclear oncology. In contrast to most other therapeutic beta emitters, Sn-117m decays via isomeric transition, with the emission of three major mono energetic conversion electrons (127, 129 and 152 keV; abundance, 65, 12 and 26% respectively). These emissions with a very high LET have short discrete penetration ranges of between 0.22 (127 keV) and 0.29 mm (152 keV) in water. Therefore, Sn-117m when selectively targeted should be effective for therapy of metastatic disease and for certain other inflammatory conditions (e.g. atherosclerotic disease), causing much reduced myelo-suppression and greatly reduced dose to normal organs.[53] This is schematically represented in Figure 1 as well as in Figure 2[54] which shows whole-body autoradiographies performed in mice and rats after the administration of Sn-117m(4^+)-diethylenetriamine pentaacetic acid (DTPA), and the highly selective targeting and high uptake in bone by this agent, but not in bone marrow or other organs, suggesting the expected effectiveness of high-LET low energy conversion electrons to produce intense radiation dose within a very short distance without affecting normal tissues, in particular, the radiation-sensitive bone marrow.[53] Figure 3 shows whole body images in a prostate cancer patient, who had developed extensive bone metastases. Scan on the left was obtained using the standard Tc-99m MDP (methylene diphosphonate) imaging agent and the one on the right consists of scans obtained using tin-117m(4^+) DTPA, an agent which as mentioned above has shown great promise for treatment of metastatic pain in prostate and

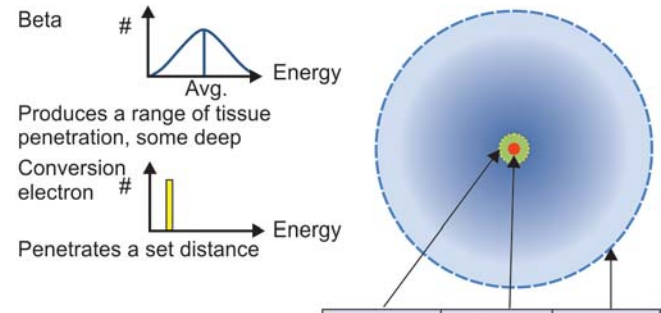

	Tin-117m	Alpha particles	Beta particles
Range in tissue (μm)	290	40-90	50-5000
Patient shielding for therapeutic doses/hospital stay requirement	No/No	No/Yes?	Yes/Yes

Fig. 1: A schematic comparison of energy types for therapeutic radionuclides[1]

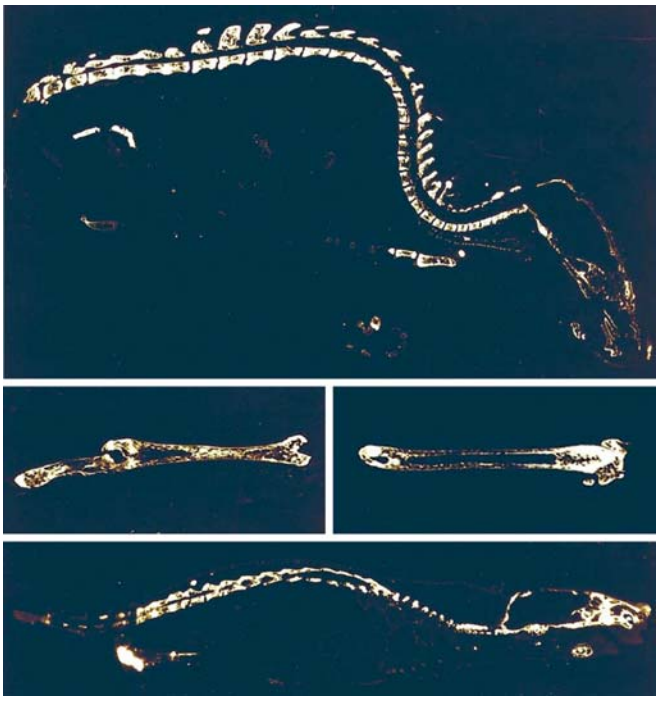

Fig. 2: Autoradiography in rats (top) and in mice (middle and bottom) demonstrates selective targeting and high uptake of tin-117m DTPA in bone and not in bone marrow or other organs[54]

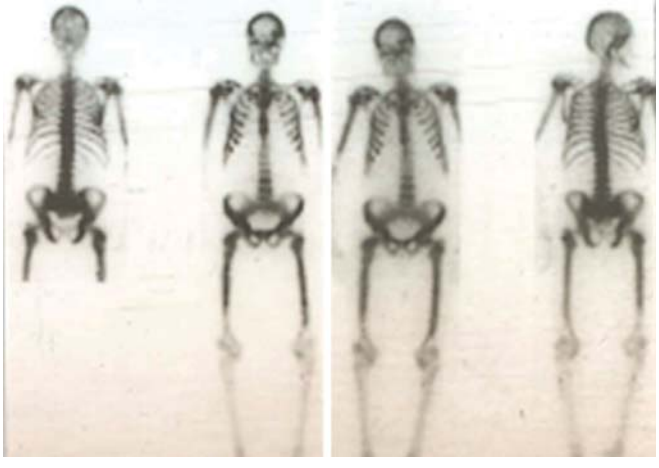

Fig. 3: Whole body images in a prostate cancer patient, who had developed extensive bone metastases. Scans on the left (posterior, anterior views) were obtained using the standard Tc-99m MDP bone imaging agent. Scans on the right are (anterior, posterior) obtained using tin-117m DTPA which is promising for treatment of metastatic bone pain and potentially of osseous metastases[48]

breast cancer patients.[48] These two scans are almost identical, demonstrating the specificity of tin-117m DTPA localization in bone and in much higher concentration in bone metastases, in fact quantitatively even much better than the Tc-99m MDP. Figures 4A and B,[55] which are from an actual sample of bone tissue from a prostate cancer patient, who was treated with Sn-117m DTPA for bone pain palliation and who donated his body for research after death corroborates the same result as in Figures 2 and 3. This latter patient had died of his primary cancer 47 days after therapy with 18.6 mCi (688 MBq) of Sn-117m DTPA, and the autopsy was carried out 6 hours after death.[55] Figures 5A and B displays both a picture and the bone scintigraphy of three longitudinal coronal slices (5 mm thick) of thoracolumbar vertebrae, again from the same patient as in Figures 4A and B. The uptake of Sn-117m DTPA is both diffuse (T8) and heterogeneous (L1). Partial involvement within a single vertebra indicates nonuniform distribution of radioactivity within the lesion, suggesting heterogeneous distribution of metastatic foci.[55] Thus, the unique therapeutic emissions of Sn-117m also imply that their therapeutic effectiveness will be highly localized and should be lesion-specific and thus more effective. The use of Sn-117m DTPA is also very worth considering for an early-stage disease at which time, there would be the possibility of slowing or even stopping the progression of further metastatic lesions. Moreover, having the 159-keV γ photon (86%), which is very similar to that of technetium-99m, Sn-117m is perfect for pretherapy imaging for dosimetry and for other information in the same patient as well as for monitoring the results of treatment.[55] All clinical studies thus, far for bone pain palliation using Sn-117m DTPA were carried out using reactor-produced Sn-117m, with a specific activity ranging between 8 and 20 Ci/g of Sn. More recently, several 50- to 150-mCi samples of NCA Sn-117m produced at INR as well as at the University of Washington alpha cyclotron, have successfully been used and evaluated at BNL, and in collaboration with the Saint Joseph's Translational Research Institute in Atlanta and at other institutions, for effectiveness for theragnostic applications in animal models.[56,57]

Tin-117m, in addition to being a good therapeutic agent for cancer, also shows promise for the noninvasive molecular imaging and treatment of active atheromatous disease [vulnerable plaque (VP), also known as thin-cap fibroatheroma (TCFA)], in the coronary arteries and other areas of vasculature through the use of (i) coronary stents electroplated with Sn-117m or (ii) specific Sn-117m-labeled molecules systemically targeted to VP components.

In the United States, there are, on an average, about 875,000 to 1,000,000 new heart attacks every year, and these are caused by two different types of atherosclerotic disease: Luminal calcified plaque and extraluminal active atheromatous disease leading to the formation of VP (Fig. 6). Vulnerable (unstable) plaque forms below the lumen in coronary artery walls, and inflammation is the main driver. VP is usually covered by a thin cap on the lumen side. When ruptured, the thin cap 'releases' highly thrombogenic material activating clotting cascade and inducing thrombosis. Approximately more than 120 substances are expressed in ruptured VP (including

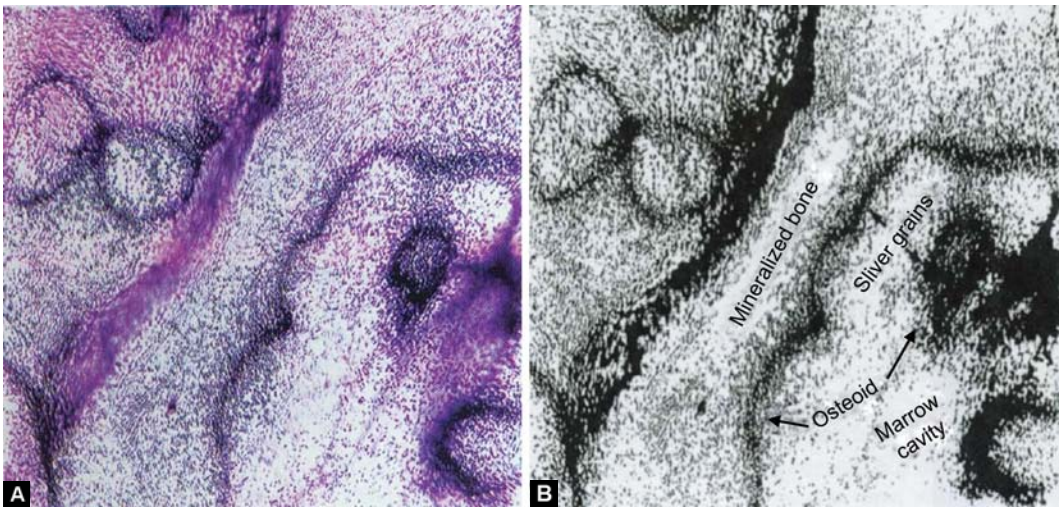

Figs 4A and B: Microautoradiographic demonstration of the deposition of Sn-117m DTPA in bone (A) and a schematic diagram (B) showing sites of localization from a sample of bone obtained following the autopsy of a patient treated with Sn-117m DTPA for bone pain palliation. There is high deposition in the actively mineralizing osteoid interface. Completely mineralized bone and the bone marrow space show very low deposition. Osteoid-to-marrow ratio is 11:1[55]

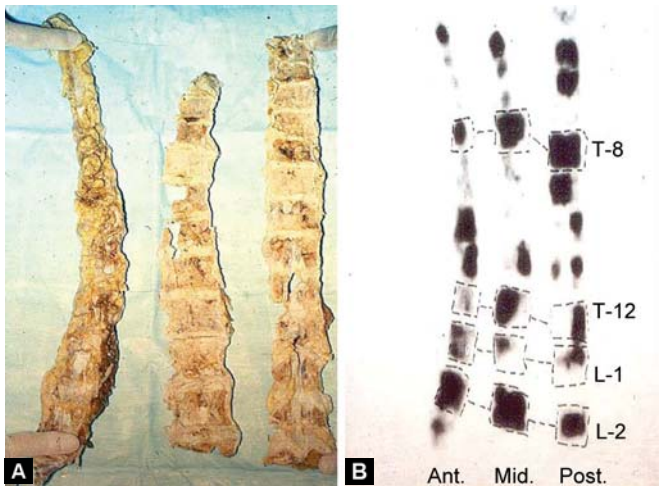

Figs 5A and B: Photographic picture (A) and bone scintigraphy (B) of three coronal slices (each 5 mm thick) of thoracolumbar vertebrae from the same patient as in Figures 4A and B. Partial involvement within a single vertebra indicates nonuniform distribution of radioactivity, within the lesion, suggesting heterogeneous distribution of metastatic foci. Note the uptake in diseased areas in various sections according to the range of the Sn-117m conversion electrons[55]

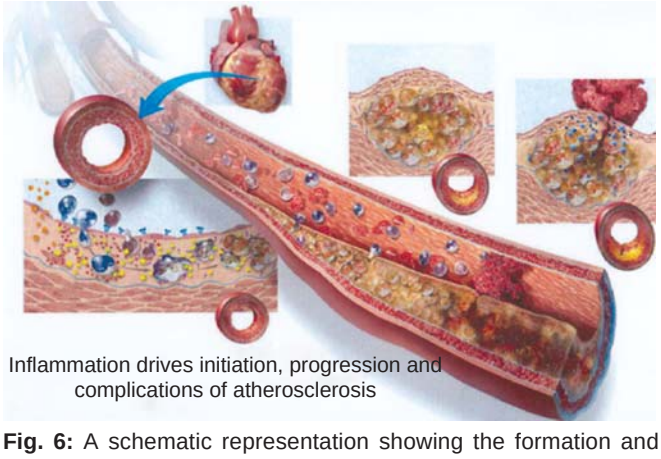

Fig. 6: A schematic representation showing the formation and positive remodeling of vulnerable plaque outside of the arterial lumen in the coronary artery walls

collagen) and this rupture then results in thrombosis, which can cause unstable angina, chest pain, acute MI, sudden coronary death and stroke. The luminal calcified plaques are easily detected by existing diagnostics, and the patient has a number of treatment options. However, VP develops and models positively outside the arterial lumen (Fig. 6) and cannot be detected by noninvasive imaging techniques. Unfortunately, a majority of all significant cardiac events (~70%) leading to MI, including sudden death, are caused by the rupture of these thin-cap fibroatheroma lesions, not lumen atherosclerosis.

The properties of Sn-117m as applied to vulnerable plaques are unique and significant.

At therapeutic doses, the conversion electrons from Sn-117m have been shown to reduce inflammation and, thus, are ideal for treating VP's as their range in tissue (~300 μm) is approximately the same as the VP thickness in human coronary arteries. Sn-117m-labeled Annexin effectively targets and binds to macrophage cells undergoing apoptosis, which are present in abundance in VP's. In relatively low doses, this agent can image the plaque using traditional SPECT gamma cameras with technetium-99m collimators and imaging protocols. Because of the longer half-life of Sn-117m combined with pretargeting techniques, gamma cameras can acquire images long after the nonspecifically bound tin—Annexin has cleared the blood pool thus improving the image quality.[58]

A clinical trial with Sn-117m–Annexin, begun in 2010, is currently in progress. At present, the phase IIa study (15 subjects) involves human carotid endarterectomy patients who are dosed and imaged for VP, with histology as the comparison. Further clinical trials (phase IIb and phase III) are in the planning stage. In recent studies in an

Apo-E mouse VP model, in doses that appear to be imaging doses, tin-117m-Annexin has demonstrated a significant anti-inflammatory therapeutic effect. The plaque composition showed significantly less expression of macrophages in the low, middle and high dose treatment groups as compared to the control group. In contrast, smooth muscle cell expression was greater in the middle and high dose groups as compared to the control, and in the low dose group, the difference was statistically significant between the low vs middle and high dose groups.[59]

Because inflammatory cells are more radiosensitive than other arterial wall cell types, the conversion electrons should exhibit a beneficial anti-inflammatory effect in diseased coronary arteries. Since 28 days, corresponding to two half-lives of Sn-117m, is believed to be roughly the optimum period for neoproliferative tissue suppression, including neointimal proliferation after angioplasty and other primary interventional treatments in the coronary arteries and other vasculature, radiotherapy with Sn-117m should provide highly effective treatment, with minimal collateral damage to adjacent, quiescent arterial wall cells because of its low energy conversion electron emission and short penetration in tissue. Furthermore, such limited energy delivery from a radioactive stent implant may circumvent the problem of cellular overgrowth at the implant edges, known as the 'candy wrapper' effect, which has been observed with previous forms of radioactive stents.

At BNL, a novel radioactive stent stably electroplated with Sn-117m was developed as a therapeutic tool for the treatment of atherosclerotic coronary arteries.[60] Effects on vessel wall inflammation from various doses of electroplated Sn-117m were studied in hyperlipidemic rabbits. Three days after stent implantation in the abdominal aorta [4 doses: 0- (cold tin), 30-, 60- and 150-μCi Sn-117m per 15-mm stent], the rabbits were sacrificed. Immunohistochemical analysis of proliferating macrophages and smooth muscle cells demonstrated that inflammatory cells in the Sn-117m-stented segments were dramatically reduced in a dose-dependent manner.[56,57] The anti-inflammatory therapeutic effectiveness of the tin-117m-stent implants was further demonstrated in a preliminary study in pigs (24 pigs, 72 bare metal stent implants: 0- to 400-μCi Sn-117m per 15-mm stent), which was carried out to investigate the effects on in-stent neointima formation. The electroplating process appeared benign because the response from 'cold' tin-plated stents was indistinguishable from what was observed for routinely used bare metal, 316L surgical stainless steel stents. A profound and unique radiation effect was consistently observed in the higher dose implants, which consisted of a discrete zone of dense connective tissue consolidation in the tunica adventitia, of ~0.25 to 0.30 mm thickness, corresponding to the anticipated tissue penetration of the Sn-117m conversion electron energy. Focal suppression of in-stent neointima formation was also observed, but further study will be needed to determine, with certainty, the therapeutic potential of Sn-117m-electroplated stents for prevention of in-stent restenosis.[61] To summarize, tin-117m shows great promise as a means to reduce inflammatory events following stent implantation, and when delivered systemically to atherosclerotic tissue using specific targeting molecules (e.g. Annexin-V), is effective in low doses to image and in higher doses to reduce the vulnerability for rupturing of unstable coronary artery plaques.

NCA Sn-117m is also being developed and tested for the therapy of bone metastases and for use in radioimmunotherapy. A phase I clinical trial for the imaging and treatment of bone metastases using Sn-117m DTPA in prostate cancer patients is in the planning stage for 2013.

CONCLUSION

There are a number of existing and potential future radionuclides for use as unsealed sources for targeted therapy of cancer and for other therapeutic applications in nuclear medicine. The various important therapeutic applications where radionuclide therapy would have an important role to play in, and the radionuclides best suited for that particular type of application, are summarized in Table 6. It should be noted that this listing is not meant to be exhaustive and additional radionuclides can be added based on present and future work as well as various other considerations. The substantial progress of investigations in areas, such as the treatment of cancer as well as of other inflammatory conditions, such as in bone pain palliation, radiosynovectomy, and of many other disorders that respond to radionuclide therapy, offers renewed hope and promise for the widespread use of internally administered radionuclides for a number of novel and effective therapeutic approaches.

Therapeutic nuclear medicine finally seems to be destined to find its rightful place in the 'personalized' therapy of patients with the use of a number of dual-purpose ('theragnostic') radionuclides or radionuclide pairs that are discussed and emphasized in this article. This paradigm, when properly enforced would constitute a major step forward to meet the challenges of enabling personalized medicine. Implementation of this regimen potentially creates a situation where treatments are better targeted, health systems save money by identifying therapies not likely to be effective for particular patients, and researchers have a better understanding of comparative effectiveness.

Table 6: Choice of radionuclides for principal therapeutic* applications[62]

Application	*Route of administration*	*Best-suited radionuclide(s)*
1. Tumor therapy		
(i) Solid tumors		
a. Large lesions	iv	Sc-47, Y-90, I-131, Lu-177, Re-188
	Intratumoral	Sc-47, Sm-153, Re-188
b. Micrometastases	iv	Sc-47, Sn-117m, Sm-153, other Auger, conversion electron, alpha and short range β-emitters
(ii) Leukemias, lymphomas	iv	Sc-47, Cu-67, Sn-117m, I-131, alpha emitters
2. Pain palliation		
(i) Soft tissue	iv	Y-90, I-131, Ho-166, Re-188
(ii) Metastatic bone pain	iv	Sr-89, Sn-117m, Sm-153, Lu-177, Re-187, Re-188, Ra-223
3. Nononcology		
(i) Synovectomy	Regional	P32, Y-90, Sn-117m, Re-186, Er-169
(ii) Marrow ablation	iv	Sn-117m, Ho-166
(iii) Microspheres	iv	Y-90, other radio-lanthanides
4. Receptor-binding tracers; cellular (intranuclear) antigens	iv	Auger, conversion electron, alpha and short-range β-emitters

*The isotopes in various categories are listed in order of increasing atomic mass and not necessarily based on their degree of their therapeutic effectiveness

Theragnostic radiopharmaceuticals have the power to drive advances in personalized medicine that will offer better-targeted diagnosis and treatments. Using this approach, it would be possible to envision a future where treatments are tailored to individual patients' specific disease parameters and where imaging data could be analyzed in real-time and in advance to predict likely effectiveness of therapy and learn what would or would not work. Oncology is just the beginning; in principle, we should be able to start scientific enquiries to apply this paradigm to other complex disease states, so that the potential for theragnostic radiopharmaceutical biomarkers as a bridge to help us better detect, understand, and treat diseases like CAD, diabetes, and Alzheimer's becomes a reality. However, an increased and continuously reliable availability at reasonable cost of some of the best theragnostic radionuclides has remained a major issue, which must be addressed before we can successfully put this paradigm into routine clinical practice. This issue has been discussed in this paper in some detail, and the evolving new methodologies for the production of a few of the very promising theragnostic radionuclides have been covered.

It is worth emphasizing that our nuclear medicine modality is the only modality that can fulfill the dream of carrying out tailored personalized medicine by way of enabling diagnosis followed by therapy in the same patient with the same radiopharmaceutical. This would be an exciting development with a very promising future, would be of invaluable benefit to patients with cancer, cardiovascular disease, and other disorders, and may very well mark the future of the field of nuclear medicine.

ACKNOWLEDGMENTS

This work was supported by the United States Department of Energy, Office of Science/Office of Nuclear Physics/ Isotope Development and Production for Research and Applications Program, and the NNSA-NA-24 GIPP Program, under Contract No. DE-AC02-98CH10886, at Brookhaven National Laboratory. Additional research grant support for part of this work by Clear Vascular Inc, including a Cooperative Research and Development Agreement (CRADA) with BNL, is gratefully acknowledged.

REFERENCES

1. Srivastava SC. Paving the way to personalized medicine: Production of some promising theragnostic radionuclides at Brookhaven National Laboratory. Semin Nucl Med 2012;42: 151-63.
2. Srivastava SC. Theragnostic radiopharmaceuticals: The 'Janus' approach to molecular diagnosis and therapy. CME session # 63 on Novel radiopharmaceuticals for molecular imaging and therapy–where are we headed next? Presented at 2009 SNM Annual Meeting, Toronto, Canada, June 15, 2009.
3. Srivastava SC. Theragnostic radiometals: Getting closer to personalized medicine. In: Mazzi U, et al (Eds). Technetium and other radiometals in chemistry and nuclear medicine. Padova, Italy, SG Editorial 2010;553-68.
4. Srivastava SC. Paving the way to personalized medicine: Production of some theragnostic radionuclides at Brookhaven National Laboratory. Radiochim Acta 2011;99:635-40.

5. Herzog H, Rösch F, Stöcklin G, et al. Measurement of pharmacokinetics of yttrium-86 radiopharmaceuticals with PET and radiation dose calculation of analogous yttrium-90 radiotherapeutics. J Nucl Med 1993;34:2222-36.
6. Srivastava SC. Radiolabeled monoclonal antibodies for imaging and therapy. New York: Plenum Press 1988;876.
7. Srivastava SC, Dadachova E. Recent advances in radionuclide therapy. Seminars in Nucl Med 2001;31:330-41.
8. Traub-Weidinger T, Raderer M, Uffman M, et al. Improved quality of life in patients treated with peptide radionuclides. World J Nucl Med 2011;10:115-21.
9. Kassis AI, Adelstein SJ, Haycock C, et al. Lethality of Auger electrons from the decay of Br-77 in the DNA of mammalian cells. Radiat Res 1982;90:362-73.
10. Adelstein SJ, Kassis AI. Radiobiologic implications of the microscopic distribution of energy from radionuclides. Nucl Med Biol 1987;14:165-69.
11. Feinendegen LE. Biological damage from the Auger effect: Possible benefits. Radiat Environ Biophys 1975;12:85-99.
12. Szelecsenyi F, Blessing G, Qaim SM. Excitation functions of proton induced nuclear reactions on enriched ^{61}Ni and ^{64}Ni: Possibility of production of no-carrier-added ^{61}Cu and ^{64}Cu at a small cyclotron. Appl Radiat Isotopes 1993;44:575-80.
13. Sadeghi M, Aboudzadeha M, Zali A, et al. Radiochemical studies relevant to Y-86 production via ^{86}Sr(p,n)^{86}Y for PET imaging. Appl Radiat Isot 2009;67:7-10.
14. Medvedev D, Mausner LF, Srivastava SC. Irradiation of strontium chloride targets at proton energies above 35 MeV to produce PET radioisotope Y-86. Radiochim Acta 2011;99: 755-61.
15. Aslam MN, Sudar S, Hussain M, Malik AA, et al. Evaluation of excitation functions of ^{3}He and α-particle induced reactions on antimony isotopes with special relevance to the production of iodine-124. Appl Radiat Isotopes 2001;69:94-104.
16. Huclier-Markai S, Sabatie A, Kubicek V, et al. Chemical and biological evaluation of scandium (III)-polyamino-polycarboxylate complexes as potential PET agent and radiopharmaceutical. Radiochim Acta 2011;99:653-62.
17. Meinken GE, Kurczak S, Mausner LF, Kolsky KL, Srivastava SC. Production of high specific activity Ge-68 at Brookhaven National Laboratory. J Radioanal Nucl Chemistry 2005;263:553-57.
18. Mausner LF, Kolsky KL, Mease RC, et al. Production and evaluation of Sc-47 for radioimmunotherapy. J Labelled Compds Radiopharm 1993;32:388-90.
19. Kolsky KL, Joshi V, Mausner LF, Srivastava SC. Radiochemical purification of no-carrier-added Scandium-47 for radioimmunotherapy. Appl Radiat Isot 1998;49:1541-49.
20. Mausner LF, Kolsky KL, Joshi V, Sweet MP, Meinken GE, Srivastava SC. Scandium 47: A replacement for Cu-67 in nuclear medicine therapy with beta/gamma emitters. In: Stevenson N (Eds). Isotope production and applications in the 21st Century. London: World Scientific 2000;43-45.
21. Mirzadeh S, Mausner LF, Srivastava SC. Production of no-carrier-added Cu-67. Int J Radiat Appl Instrum Part A, Appl Radiat Isot 1986;37:29-36.
22. DeNardo GL, DeNardo SJ, Kukis DL, O'Donnell RT, et al. Maximum tolerated dose of ^{67}Cu-2IT-BAT-LYM-1 for fractionated radioimmunotherapy of non-Hodgkin's lymphoma: A pilot study. Anticancer Res 1998;18:2779-88.
23. DeNardo SJ, DeNardo GL, Kukis DL, et al. ^{67}Cu-2IT-BAT-Lym-1 pharmacokinetics, radiation dosimetry, toxicity and tumor regression in patients with lymphoma. J Nucl Med 1999; 40:302-10.
24. Medvedev DJ, Mausner LF, Meinken GE, et al. Development of large scale production of Cu-67 from Zn-68 at the high energy accelerator: Closing the Zn-68 cycle. Int J Appl Radiat Isot 2012;70:423-29.
25. Dadachova E. Cancer therapy with alpha-emitters labeled peptides. Semin Nucl Med 2010;40:204-08.
26. Jurcic JG, Larson SM, Sgouros G, et al. Targeted particle immunotherapy for myeloid leukemia. Blood 2002;100:1233.
27. Miederer M, Henriksen G, Alke A, et al. Preclinical evaluation of the alpha-particle generator nuclide Ac-225 for somatostatin receptor radiotherapy of neuroendocrine tumors. Clin Cancer Res 2008;14:3555.
28. Larsen RH, Wieland BW, Zalustsky MR. Evaluation of an internal cyclotron target for the production of ^{211}At via the ^{209}Bi (alpha, 2n)211 at reaction. Appl Radiat Isot 1996;47: 135-43.
29. Zalutsky MR, Zhao XG, Alston KL. High-level production of alpha-particle-emitting (211)At and preparation of (211) At-labeled antibodies for clinical use. J Nucl Med 2001;42: 1508-15.
30. Yao Z, Garmestani K, Wong KJ, et al. Comparative cellular catabolism and retention of astatine-, bismuth-, and lead-radiolabeled internalizing monoclonal antibody. J Nucl Med 2001;42:1538-44.
31. Haddad F, Barbet J, Chatal JF. The arronax project. Current Radiopharm 2011;4:186-96.
32. McDevitt MR, Finn RD, Sgouros G, et al. An Ac-225/Bi-213 generator system for therapeutic clinical applications: Construction and operation. Applied Radiat Isot 1999;50:895.
33. Norenberg JP, Krenning BJ, Konings I, et al. Bi-213- DOTA(0), Tyr(3) octreotide peptide receptor radionuclide therapy of pancreatic tumors in a preclinical animal model. Clinical Cancer Res 2006;12:897.
34. Geerlings MW, Kaspersen FM, Apostolidis C, et al. The Feasibility of Ac-225 as a source of alpha-particles in radio-immunotherapy. Nucl Med Commun 1993;14:121.
35. Miederer M, Scheinberg DA, McDevitt MR, et al. Realizing the potential of the Actinium-225 radionuclide generator in targeted alpha particle therapy applications. Advanced Drug Delivery Reviews 2008;60:1371.
36. Sofou S, Kappel BJ, Jaggi JS, et al. Enhanced retention of the alpha-particle-emitting daughters of actinium-225 by liposome carriers. Bioconj Chem 2007;18:2061.
37. Akiyama K, Haba H, Tsukada K, et al: A metallofullerene that encapsulates Ac-225. J. Radioanal Nucl Chem 2009;280:329.
38. S Jurcic JG, McDevitt MR, Pandit-Taskar N, et al. Alpha-particle immunotherapy for acute myeloid leukemia (AML) with bismuth-213 and actinium-225. Cancer Biother Radiopharm 2006;21:40.
39. Boll RA, Malkemus D, Mirzadeh S. Production of actinium-225 for alpha particle mediated radioimmunotherapy. Appl Radiat Isot 2005;62:667.
40. Apostolidis C, Molinet R, Rasmussen G, et al. Production of Ac-225 from Th-229 for targeted alpha therapy. Analytical Chem 2005;77:6288.
41. Zhuikov BL, Kalmykov SN, Ermolaev SV, et al. Production of ^{225}Ac and ^{223}Ra by irradiation of Th with accelerated protons. Radiochemistry 2011;53:73-80.
42. Melville G, Allen BJ. Cyclotron and linac production of Ac-225. Appl. Radiat Isot 2009;67(4):549-55.
43. Mease RC, Mausner LF, Srivastava SC. Macrocyclic polyamino-carboxylates for radiometal antibody conjugates for therapy, SPECT and PET imaging. US Patent #5,639,879, June 17, 1997.

44. Sweet MP, Mease RC, Srivastava SC. Rigid bifunctional chelating agents. US Patent # 6,022,522, February 8, 2000.
45. Mausner LF, Mirzadeh S, Ward TE. Nuclear data for production of 117mSn for biomedical application. In: Proceedings of the International Conference on Nuclear Data for Basic and Applied Science. Santa Fe: New Mexico 1985 May;733-37.
46. Mirzadeh S, Knapp FF Jr, Alexander CW, Mausner LF. Evaluation of neutron inelastic scattering for radioisotope production. Appl Radiat Isot 1997b;48:441-46.
47. Srivastava SC, Toporov YuG, Karelin EA, Vakhetov FZ, Andreev OI, et al. Reactor production of high-specific activity tin-117m for bone pain palliation and bone cancer therapy. J Nucl Med 2004;45:475.
48. Srivastava, SC, Atkins HL, Krishnamurthy GT, et al. Treatment of metastatic bone pain with tin-117m(4+)DTPA: A phase II clinical study. Clinical Cancer Res 1998;4:61-68.
49. Ermolaev SV, Zhuikov BL, Kokhanyuk VM, Srivastava SC, et al. Production of no-carrier-added Tin-117m from proton irradiated antimony. J Radioanal Chem 2009;280:319-24.
50. Qaim SM, Döhler H. Production of carrier-free 117mSn. Int J Appl Radiat Isot 1984;35:645-50.
51. Yamazaki T, Ewan GT. Level and isomer systematics in even tin isotopes from Sn-108 to Sn-118 observed in Cd(α, xn) Sn reactions. Nucl Phys A 1969;134:81-109.
52. Zhuikov B, Srivastava SC, Ermolaev SV, et al. Production of no-carrier-added Sn-117m at medium energy cyclotrons. Publication in Progress (2012).
53. Bishayee S, Rao DV, Srivastava SC, et al. Marrow sparing effects of Sn-117m (4+) DTPA for radionuclide therapy of cancer in bone. J Nucl Med 2000;41:2043-50.
54. Oster ZH, Som P, Srivastava SC, et al. The development and in vivo behavior of tin containing radiopharmaceuticals II: Autoradiographic and scintigraphic studies in normal animals and in animal models of bone disease. Int J Nucl Med Biol 1985;12:175-84.
55. Swailem FM, Krishnamurthy GT, Srivastava SC, et al. In vivo tissue uptake and retention of Sn-117m (4+) DTPA in a human subject with metastatic bone pain and in normal mice. Nucl Med Biol 1998;25:279-87.
56. Li J, Mueller DW, Srivastava SC, et al. Intravascular stents electroplated with Sn-117m reduce arterial wall inflammation in hyperlipidemic rabbits. Atlanta, GA: Presented at the GLS 2007 Meeting, October 3, 2007 (abstr).
57. Li J, Mueller DW, Srivastava SC, et al. Intravascular stents electroplated with ^{117m}Sn reduce arterial wall inflammation in hyperlipidemic rabbits. Chicago, IL: Presented at the 2008 ACC Annual Meeting, May, 2008 (abstr).
58. Narula, J, Srivastava S, Petrov A, et al. Evaluation of tin-117m labeled Annexin V for imaging atherosclerotic lesions in a hyperlipidemic rabbit model. Publication in Progress (2013).
59. Srivastava SC, Gonzales G, Narula J, Strauss HW, et al. Development and evaluation of tin-117m labeled Annexin for the imaging and treatment of vulnerable plaques. Publication in Progress (2013).
60. Srivastava SC, Gonzales G, Adzic R, Meinken GE. Method of electroplating a conversion electron emitting source on implant. US Patent Application Serial No 11/758,914, Dec 22, 2011; Publication in Progress (2013).
61. Srivastava SC, Strauss HW, Narula J, et al. Theragnostic potential of Sn-117m for the molecular targeting and therapy of vulnerable plaque. Publication in Progress (2013).
62. Srivastava SC. Therapeutic radionuclides: Making the right choice. In: Mather SJ (Eds). Current directions in radiopharmaceutical research and development. Dordrecht, The Netherlands: Kluwer Academic Publishers 1996;63-79.

ABOUT THE AUTHOR

Suresh C Srivastava

Senior Medical Scientist and Head, Medical Isotope Research and Production Program, Collider-Accelerator Department, Building 801, Brookhaven National Laboratory, Upton, New York 11973; Research Professor of Radiology, Stony Brook University Medical Center, Stony Brook, NY, USA, e-mail: suresh@bnl.gov

10.5005/jp-journals-10028-1055
REVIEW ARTICLE

Molecular Imaging using PET/CT Applying ^{68}Ga-Labeled Tracers and Targeted Radionuclide Therapy: Theranostics on the Way to Personalized Medicine

Harshad R Kulkarni, Richard P Baum

ABSTRACT

Theranostics is an acronym, which exemplifies the togetherness of diagnostics and therapeutics in the individualized management of disease. The key to personalized medicine in cancer is to determine the molecular phenotypes of neoplasms, so that specific probes can be selected to target the tumor and its microenvironment. Molecular imaging and radionuclide therapy using a particular probe is based on this premise. Neuroendocrine neoplasms express somatostatin receptors, enabling the use of somatostatin analogs for molecular imaging, when labeled with the positron-emitter ^{68}Ga for receptor positron emission tomography/computed tomography (PET/CT), and targeted radionuclide therapy, when labeled with beta-emitters ^{90}Y and ^{177}Lu.

Keywords: Theranostics, Molecular imaging, Targeted radionuclide therapy, PRRNT, PET/CT.

How to cite this article: Kulkarni HR, Baum RP. Molecular Imaging using PET/CT Applying ^{68}Ga-Labeled Tracers and Targeted Radionuclide Therapy: Theranostics on the Way to Personalized Medicine. J Postgrad Med Edu Res 2013; 47(1):47-53.

Source of support: Nil

Conflict of interest: None declared

INTRODUCTION

Theranostics refers to the incorporation of diagnostics and therapeutics into the individualized management of disease. Molecular imaging with positron emission tomography/computed tomography (PET/CT) using the trivalent radiometal and positron-emitter ^{68}Ga, and its therapeutic counterpart for targeted radionuclide therapy (for e.g. ^{177}Lu, ^{90}Y), has paved the way to personalized medicine. The detection of molecular targets enables selection of the ideal ligand for both tumor-specific diagnosis and treatment. Molecular imaging provides useful diagnostic information concerning the metabolic or receptor status of a given tumor or its metastases for further selective targeting for therapy at the cellular/subcellular level.

Neuroendocrine neoplasms (NENs) originate from pluripotent stem cells or differentiated neuroendocrine cells and their endocrine metabolism [amine precursor uptake, and decarboxylation (APUD)] is characteristic. The overexpression of somatostatin receptors (SSTRs) provides the basis for the use of radiolabeled somatostatin (SMS) analogs. The successful application of molecular imaging using ^{68}Ga and targeted radionuclide therapy using ^{177}Lu/ ^{90}Y labeled SMS analogs has paved the way to state of the art theranostics.[1]

MOLECULAR IMAGING USING ^{68}Ga-LABELED PEPTIDES

The predominant overexpression in NENs of SSTR 2 forms the basis for peptide receptor imaging using ^{68}Ga-labeled SMS analogs.[2] The peptides used are small and have better pharmacokinetic characteristics and no antigenicity as compared to antibodies. ^{68}Ga is a trivalent radiometal with convenient labeling characteristics and an ideal positron emitter for PET imaging. It is derived from a ^{68}Ge/^{68}Ga generator system, which has a half-life of 271 days.[3] A simple sodium chloride (NaCl)-based ^{68}Ga eluate concentration and labeling technique (Müller's method) enables rapid and very efficient labeling of DOTA-conjugated peptides in high radiochemical purity (97 ± 2%).[4] The SMS analog DOTATOC (DOTA-D-Phe1-Tyr3-octreotide) was developed for imaging as well as for therapy.[5,6] DOTA-D-Phe1-Tyr3-Thr8-octreotide (DOTATATE) has a very high affinity for SSTR 2, higher than even natural somatostatin.[7] DOTANOC (DOTA-1-Nal3-octreotide) has a broader spectrum and binds to SSTR 2, SSTR 3 and SSTR 5.[8] SSTR antagonists are currently under investigation and have been shown to have higher tumor uptake (due to more binding sites on the tumor cell surface) and to deliver higher dose to the tumors.[9] The first radiolabeled SMS analog to be approved for scintigraphy was ^{111}In-DTPA-D-Phe1-octreotide (^{111}In-pentetreotide, Octreoscan) which has been in use worldwide in thousands of patients since 1999 for the scintigraphic localization of primary and metastatic NENs.[10] ^{99m}Tc-EDDA-HYNIC-TOC (or -TATE) has also been used in a large patient population and shown to be superior to ^{111}In-pentetreotide due to higher count rates (higher injected activity) and the use of SPECT or SPECT/CT enabling to finish the patient study within 1 day (whereas at least 2 days are necessary when using Octreoscan).[11]

The advantage of PET/CT is its ability to quantify the disease at a molecular level. Therefore, SSTR PET/CT using ^{68}Ga clearly has an edge over SPECT/CT using gamma-emitting radionuclides. Hofmann et al demonstrated this for the first time with ^{68}Ga-DOTATOC as compared to

^{111}In-octreotide SPECT (CT taken as reference) in detecting upper abdominal metastases.[12] In a more recent study by Gabriel et al, ^{68}Ga-DOTATOC PET was proven to be superior to ^{111}In-DOTATOC and ^{99m}Tc-EDDA-HYNIC-TOC in the detection of NEN metastases in the lung, bones, liver and brain.[13] In our own experience with more than 7,000 SSTR PET/CT studies (currently over 20 per week) performed at the Zentralklinik Bad Berka, ^{68}Ga-SSTR PET is able to detect many lesions which are not routinely detected by CT, magnetic resonance imaging (MRI), skeletal scintigraphy or ultrasonography. Our group (Kaemmerer et al 2011) demonstrated for the first time, a close correlation between SUV_{max} and immunohistochemical scores for the quantification of SSTR (particularly subtype 2A) in NEN tissue.[14] Thus the real power of molecular imaging using ^{68}Ga SSTR PET/CT, is in quantifying the SSTR density on tumor cells before planning of targeted radionuclide therapy, highlighting the principle of theranostics (Fig. 1).

In a bicentric study, ^{68}Ga DOTANOC PET/CT localized the primary tumor in 59% of cases with cancer of unknown provenience (CUP-NET), significantly higher than the detection rate (39%) reported in the literature for ^{111} In-Octreoscan.[15]

PET/CT is also useful in the early and accurate detection of response to therapy and to assess the prognosis of a patient. In a study involving 47 patients, the SUV_{max} of ^{68}Ga-DOTANOC was significantly higher in patients with well-differentiated pancreatic NENs, indicating a higher SSTR 2 expression.[16] SUV_{max}, therefore, has a prognostic value and correlates with the clinicopathologic features of well-differentiated NENs. ^{18}F-FDG PET has a role in comprehensive tumor assessment in intermediate and high-grade tumors: intense metabolic activity of the tumors/metastases indicates a poor prognosis due to the presence of aggressive tumor clones.[17]

Many new ^{68}Ga-labeled tracers including both peptides and nonpeptidic tracers are becoming available, thereby demonstrating the potential of ^{68}Ga to become the ^{99m}Tc for PET.[18] The biphosphonate-based agent BPAMD—4-{[bis-(phosphonomethyl)) carbamoyl]methyl}-7, 10-bis (carboxymethyl)-1, 4, 7, 10-tetraazacyclododec-1-yl acetic acid labeled with ^{68}Ga is one such option for the

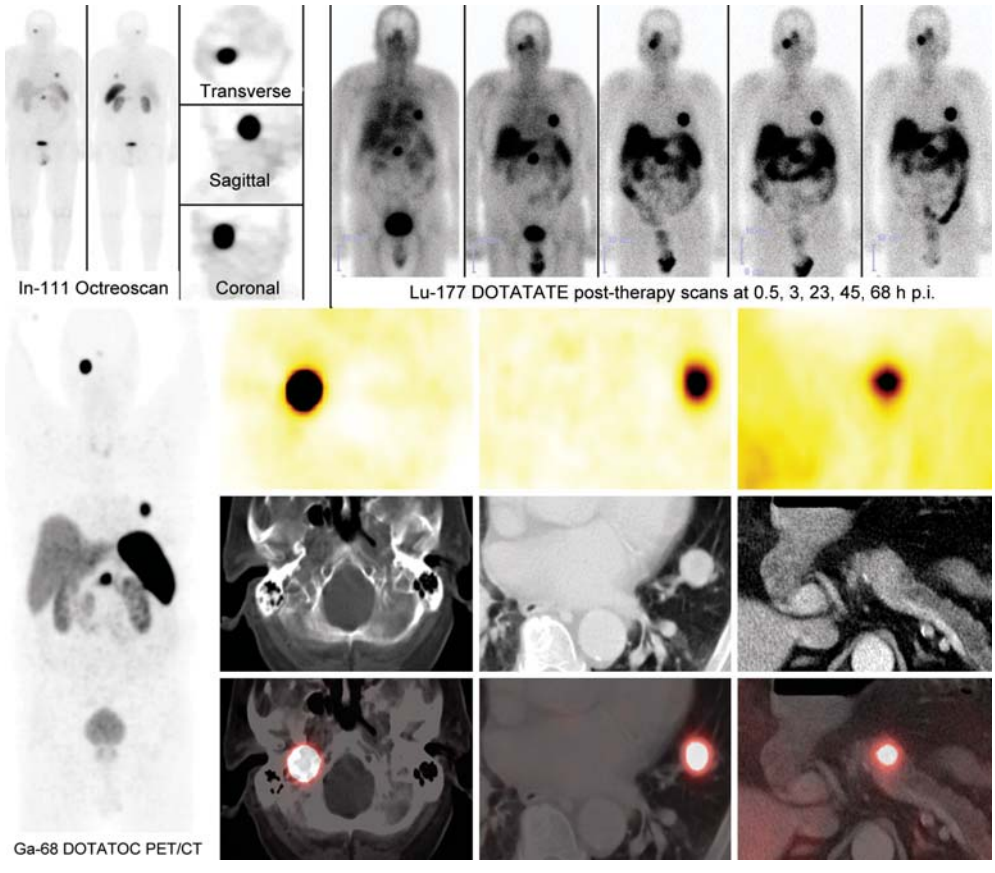

Fig. 1: A 74-year-old patient with three concurrent primary neuroendocrine neoplasms—a glomus tumor, a primary lung NET and a separate primary NEN in the pancreas. ^{111}In-octreotide scintigraphy (upper left) performed externally, showed focal uptake at the three sites, SPECT of the skull was reported to be suspicious for a brain metastasis. ^{68}Ga-DOTATOC PET/CT (below, maximum intensity projection image on the extreme left) demonstrated a very intense somatostatin-receptor positive lesion (SUV_{max} 148) in projection to the right carotid body (left), suggestive of a glomus tumor. The carcinoid tumor in the left lung and the pancreas NEN can be seen on the transverse PET/CT slices (successively toward the right). The patient underwent PRRNT with 7.9 GBq ^{177}Lu-DOTATATE. The ^{177}Lu-DOTATATE post-therapy planar scans at multiple time intervals (upper right) also showed intense uptake in the three tumors

personalized theranostics of skeletal lesions.[19] PET/CT with ^{68}Ga-BPAMD provides high-resolution and quantitative evaluation of osteoblastic bone metastases.

Newer radiolabeled peptides targeting the gastrin and cholecystokinin receptors have shown promising preclinical results in medullary thyroid cancer.[20] Exendin-3 and exendin-4, targeting the glucagon-like peptide-1 (GLP-1) receptors in insulinomas have been radiolabeled with ^{68}Ga for receptor PET/CT imaging.[21,22] ^{68}Ga-labeled arginine-glycine-aspartic acid (RGD) PET/CT (first in human use at our center) may be useful for noninvasive tumor detection and monitoring of expression of alpha v beta 3 {α(v)β(3)} integrins which are involved in angiogenesis as well as for monitoring the therapeutic response to antiangiogenic agents used for immunotherapy of tumors.[23] ^{68}Ga-PET imaging of the chemokine receptor CXCR4, which is expressed by many tumors, holds great promise for the future.[24]

Our group was the first to use the ^{68}Ga-labeled gastrin releasing peptide receptor (GRP-R) selective bombesin analog AMBA CH_2CO-G-4-aminobenzoyl-Q-W-A-V-G-H-L-M-NH_2) and the GRP-R antagonist demobesin in humans for imaging of metastatic breast, lung and prostate cancers.[25] Other ^{68}Ga-labeled tracers which have been applied by our group for the first time in humans are ^{68}Ga-labeled macroaggregates (MAA) for lung perfusion PET/CT, ^{68}Ga-DOTA-alpha-MSH (melanocyte stimulating hormone) for metastatic ocular melanoma, and the ^{68}Ga-labeled affibody molecule targeting human epidermal growth factor receptor 2 (HER2) as well as a ^{68}Ga-labeled growth hormone releasing hormone (GHRH) antagonist.[26-28] ^{68}Ga is therefore a very practical, affordable and a highly promising radionuclide for clinical use in PET/CT imaging.

TARGETED RADIONUCLIDE THERAPY

Radionuclide therapy can be specifically directed against molecular targets, utilizing the same probes as for molecular imaging, but labeled with a therapeutic (e.g. beta, alpha, auger emitters) radionuclide. The molecular basis of peptide receptor radionuclide therapy (PRRNT) is the receptor-mediated internalization and intracellular retention of the radiolabeled SMS analog. Upregulation of SSTR 2 in the peritumoral vessels is another target, accounting for antiangiogenic response after radionuclide therapy.[29]

^{90}Y- and/or ^{177}Lu-labeled DOTATATE or DOTATOC are the most frequently used peptides for PRRNT. ^{90}Y produces a 'cross-fire effect' due to the relatively high energy (935 keV) and tissue penetration range (up to 12 mm) of the emitted beta particles, and is therefore preferable for larger tumors. ^{177}Lu on the other hand, emits intermediate-energy beta particles (133 keV), having a relatively short tissue penetration range (up to 2 mm), which makes it preferable for smaller tumors. Due to additional two gamma peaks at 113 and 208 keV, ^{177}Lu is also suitable for imaging with a gamma camera for post-therapeutic dosimetry.

Several studies have shown promising results with PRRNT of well-differentiated NENs (Fig. 2). Objective response rates (complete and partial) were observed in 30% of the patients treated with ^{177}Lu-DOTATATE with very few adverse effects, and a significant benefit in median overall survival (median survival from start of treatment was 46 months).[30] In a study of a large cohort of patients treated with ^{90}Y-DOTATOC, though response was associated with longer survival, there was also a risk of significant nephro-

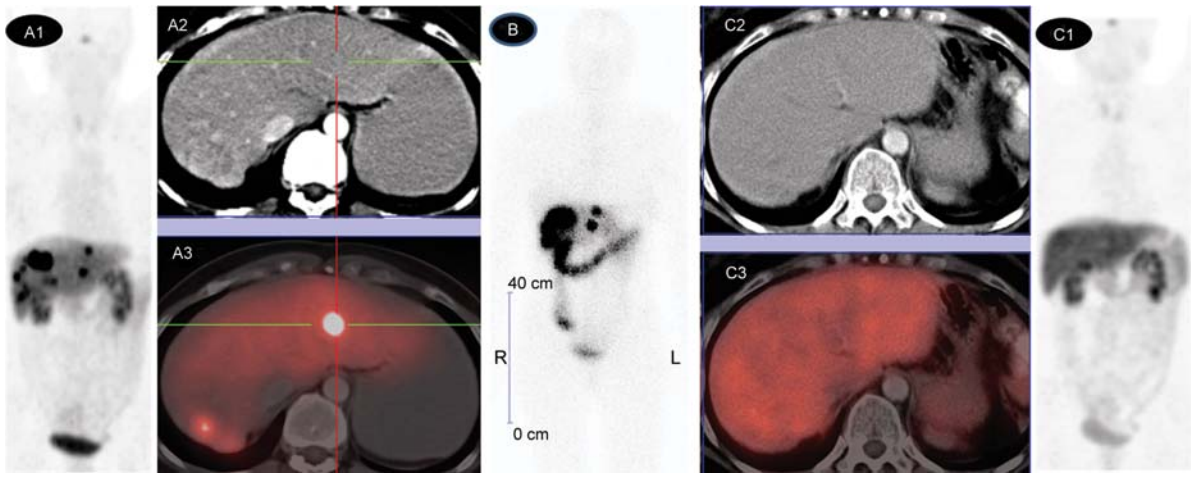

Fig. 2: A 44-year-old female patient with metastatic pancreatic NEN, initially diagnosed 10 years back, status post-distal spleno-pancreatectomy was treated with two cycles of DUO-PRRNT using 7.5 GBq of ^{177}Lu-DOTATATE (first cycle) and 3 months later administering ^{90}Y-DOTATATE for the second cycle. A complete remission was observed 2 years after the second cycle, possibly due to an additional delayed antiangiogenic effect. (A1, A2, A3: Pre-PRRNT SSTR PET/CT; B: ^{177}Lu-DOTATOC whole-body post-therapy scan 68 hours after the first PRRNT demonstrates intense uptake in the hepatic metastases; C1, C2, C3: SSTR PET/CT 2 years after the second PRRNT cycle; A1, C1: Maximum intensity projection images; A3, C3: transverse fused PET/CT images showing complete molecular response to PRRNT in the hepatic metastases; A2, C2: Corresponding CT images)

toxicity.[31] Neoadjuvant PRRNT can be administered in inoperable NENs so that the tumor is rendered operable by inducing radiation-induced necrosis with the possibility of complete cure after surgery.[32]

The aim of PRRNT is to deliver the highest possible dose to the tumor and at the same time prevent damage to normal organs. The different metabolism or receptor density in organs and tumor lesions accounts for interpatient differences in dose delivery. Therefore, individualized patient dosimetry is mandatory. The mean absorbed doses to normal organs and tumors are estimated using the MIRD scheme (OLINDA/EXM).[33] Pretherapeutic dosimetry for further personalizing PRRNT with SSTR PET/CT is possible using longer lived positron emitters, e.g. ^{44}Sc, ^{86}Y or ^{64}Cu. The first human study using the longer-lived, generator-derived, trivalent metallic positron emitter ^{44}Sc (scandium-44) coupled to DOTATOC was performed in Bad Berka in 2009. ^{44}Sc has a half-life of 3.9 hours and is derived from a titanium-44/scandium-44 generator, which has a half-life of approximately 60 years.[34,35]

Kidneys are the dose limiting organs for PRRNT since radiolabeled peptides (due to their small sizes) are filtered through the glomerular capillaries in the kidneys and subsequently reabsorbed by and retained in the proximal tubular cells.[36] Long range of the ^{90}Y beta particles increases the potential for kidney toxicity. The proximal tubular reabsorption of these radiolabeled peptides can be competitively inhibited by positively charged molecules, such as L-lysine and/or L-arginine. Plasma expanders like Gelofusine also help in preventing uptake in the tubules.

Acute reversible hematological toxicity is quite frequent, especially after ^{90}Y-labeled peptide therapy. The possibility of mild and progressive bone marrow toxicity exists after repeated cycles and the potential risk of development of myelodysplastic syndrome (MDS) or overt leukemia in patients receiving high bone marrow doses, especially in patients previously treated with alkylating chemotoxic agents must be considered.[37]

THE BAD BERKA EXPERIENCE

The Bad Berka Theranostics and Neuroendocrine Tumor Center was certified as ENETS Centre of Excellence in March 2011. At our center, a dedicated multidisciplinary

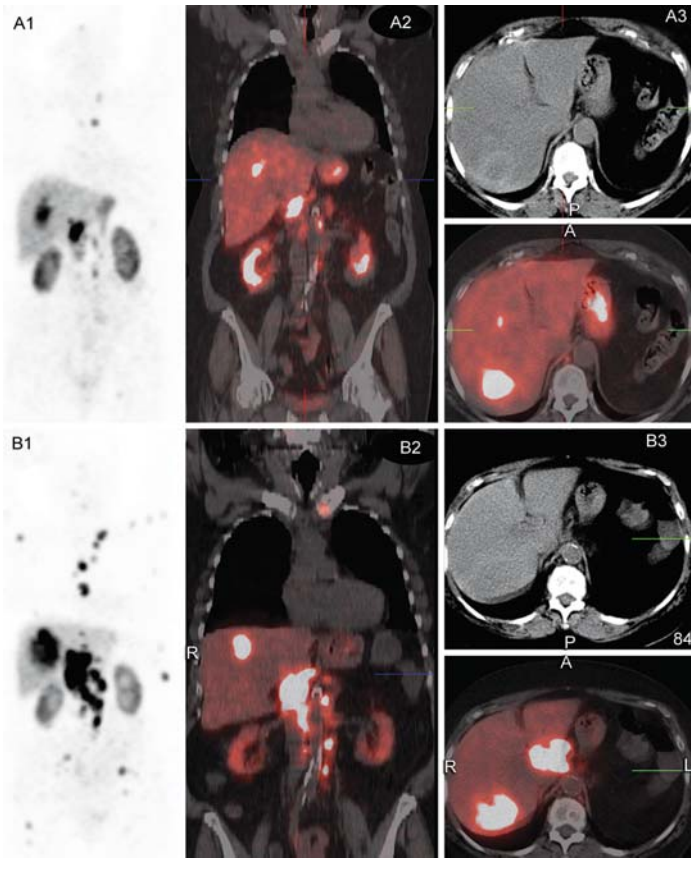

Fig. 3: A 77-year-old female patient with a well-differentiated, functioning (glucagonoma) neuroendocrine neoplasm of the pancreas (status post left pancreatectomy and splenectomy) developed progressive hepatic, peritoneal and lymph node metastases. The patient underwent five cycles of peptide receptor radionuclide therapy with a total administered activity of 30.3 GBq Lu-177. The follow-up Ga-68 DOTATOC PET/CT (6 months after the fifth cycle) showed stable disease (A1, A2 and A3). However, after 1 year, there was a significant progression of disease with new lesions and increase in the SUVmax (extremely intense somatostatin receptor expression—B1, B2 and B3). The renal function was normal. Hence, there was an indication for repeat PRRNT (A1, B1:Maximum intensity projection images; A2, B2: Coronal fused PET/CT images; A3, B3: Transverse fused PET/CT and the corresponding CT images) which resulted again in a very good therapy response

team of experienced specialists is responsible for the management of NEN patients (over 1,200 patient visits per year). We have been treating progressive well-differentiated NENs with PRRNT using ^{177}Lu and/or ^{90}Y since more than a decade, having treated around 1,100 patients (over 4,000 treatment sessions). Patient selection for PRRNT is based on the Bad Berka score, which takes several parameters into account, importantly the SUVs on SSTR PET (for referrals: Krenning's score on somatostatin receptor scintigraphy) for determining somatostatin receptor density, renal function and many other factors (Fig. 3).[38] Management of every patient is individualized, administering low or intermediate radioactivity by frequent therapy cycles (up to 9), i.e. applying the 'long-term low-dose' and not the 'short-term high-dose' concept (Figs 4A to F). Patients are well- hydrated and receive an amino acid infusion containing lysine and arginine over 4 hours beginning 30 minutes before PRRNT. Patients who are treated with Y-90 receive in addition Gelofusine over 3 hours. Applying these nephron-protective measures, end-stage renal insufficiency was observed in only 1 out of the 1,100 patients (less than 0.1%) treated at our center (>4,000 treatment sessions). Before each new treatment cycle, a complete restaging is performed both by morphologic (CT/MRI) and molecular imaging studies (particularly ^{68}Ga-SSTR PET/CT, and in selected cases ^{18}F-FDG or ^{18}F-fluoride PET/CT additionally), blood chemistry and tumor markers (CgA, serotonin, specific hormones). Renal function is serially determined by ^{99m}Tc-MAG3 scan/TER and by ^{99m}Tc-DTPA (GFR) measurements. All data are entered into a structured database containing 270 items per patient.

The systematic use of both ^{90}Y and ^{177}Lu labeled with SMS analogs in sequence (DUO-PRRNT) and concurrently (TANDEM-PRRNT) was also pioneered by our group. This

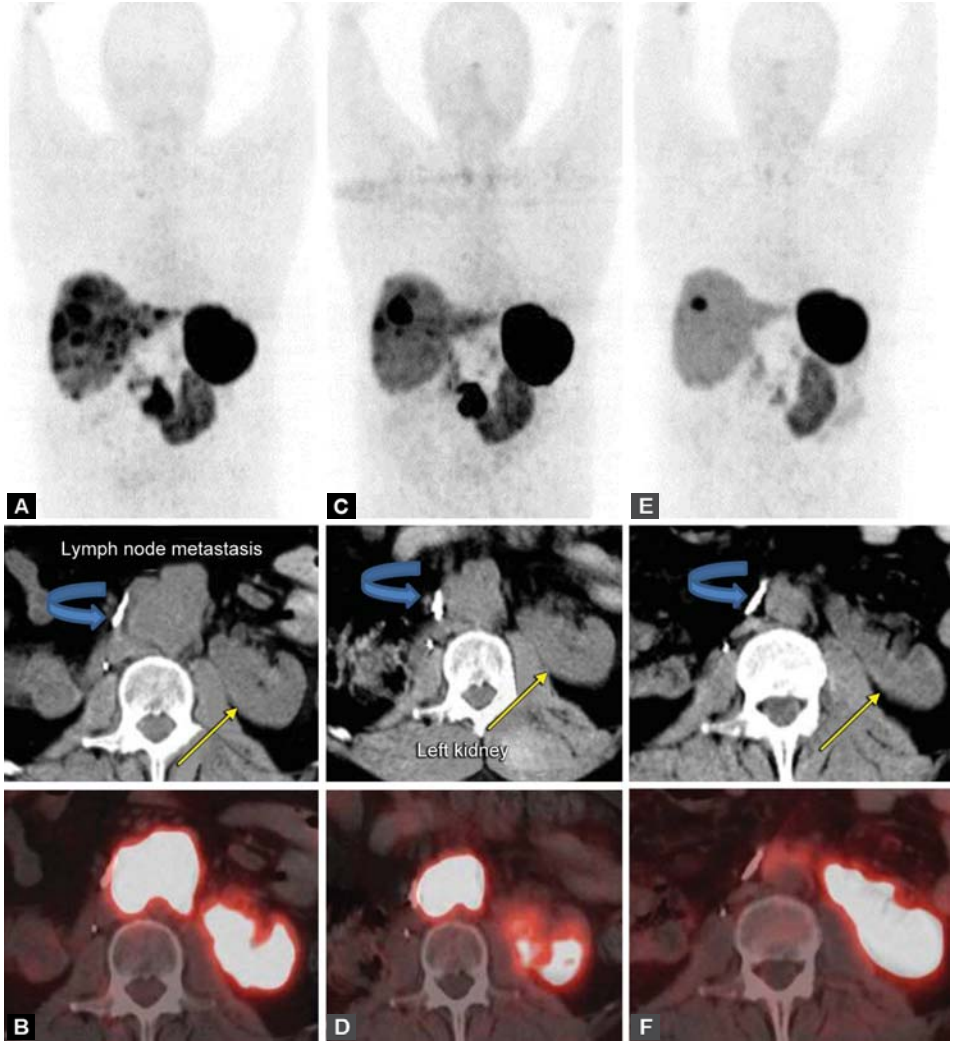

Figs 4A to F: A 60-year-old patient with NEN of the right kidney with extensive bilateral liver metastases (size 3.7 cm in S7) and retroperitoneal lymph node (size up to 6.5 cm) and bone metastases presented in a poor general condition, lymphedema and deranged renal function with a TER of 35% (A, B: ^{68}Ga-SSTR PET/CT before PRRNT). After two cycles of PRRNT, using 7 and 7.5 GBq of ^{177}Lu-labeled DOTA-SMS analogs respectively, there was a successive significant response according to molecular imaging criteria as well as a significant reduction in size of the lymph node metastases and an improvement in renal function, probably due to resolution of the lymphatic obstruction (C, D: SSTR PET/CT after first PRRNT cycle; E, F: SSTR PET/CT 4 months after second PRRNT cycle)

accounts for the variable sizes of tumors and inhomogeneous distribution of SSTRs. ^{177}Lu-DOTATATE is predominantly used for smaller metastases or in patients with impaired renal or hematological function. Intra-arterial use of ^{90}Y-labeled DOTATATE and DOTATOC, as a highly targeted therapy for hepatic metastases and large primary tumors was also inaugurated by our center. Recently, we performed for the first time a superselective intra-arterial PRRNT for treatment of a large meningioma with ^{90}Y-DOTATOC with evidence of partial response after the first cycle. An analysis of 416 GEP-NEN patients treated at the BBNETC showed a median overall survival from the time of first diagnosis of 210 months and a median survival after the first PRRNT of 59 months.

The theranostic potential of the bisphosphonate BPAMD has been explored using ^{177}Lu-BPAMD for the treatment of widespread, progressive and painful skeletal metastases refractory to conventional treatment.[39] Dosimetric studies showed that due to the very long half-life of the radiopharmaceutical in the metastases (>80 hours), high mean absorbed doses to the tumors, ranging from 2.4 to 209 mGy/MBq (the wide range was due to different sizes of the lesions) were observed. An excellent pain palliation could be achieved, corresponding with a significant reduction in osteoblastic activity of the bone metastases as seen on the follow-up ^{18}F sodium fluoride PET/CT. Only mild-to-moderate changes in blood cell counts were observed. Overall, the treatment was well-tolerated by all patients without any significant adverse effects.

^{177}Lu-demobesin therapy was administered in 2009 for the first time at our center and so was a novel GRP-R antagonist labeled with ^{177}Lu in a patient with metastatic prostate cancer. This is indeed an exciting future prospect for the theranostics of GRP-R positive tumors with ^{68}Ga-/^{177}Lu-labeled tracers.[40]

REFERENCES

1. Baum RP, Kulkarni HR, Carreras C. Peptides and receptors in image-guided therapy: Theranostics for neuroendocrine neoplasms. Semin Nucl Med 2012;42:190-207.
2. Krenning EP, Bakker WH, Kooij PP, Breeman WA, Oei HY, de Jong M, et al. Somatostatin receptor scintigraphy with indium-111-DTPA-D-Phe-1-octreotide in man: Metabolism, dosimetry and comparison with iodine-123-Tyr-3-octreotide. J Nucl Med 1992;33;652-58.
3. Rösch F, Baum RP. Generator-based PET radiopharmaceuticals for molecular imaging of tumours: On the way to theranostics. Dalton Trans 2011;40:6104-11.
4. Mueller D, Klette I, Baum RP, Gottschaldt M, Schultz MK, WAP Breeman. A simplified NaCl based ^{68}Ga concentration and labeling procedure for rapid synthesis of ^{68}Ga radio-pharmaceuticals in high radiochemical purity. Bioconjug Chem 2012;23:1712-17.
5. de Jong M, Bakker WH, Krenning EP, Breeman WA, van der Pluijm ME, Bernard BF, et al. Yttrium-90 and indium-111 labelling, receptor binding and biodistribution of [DOTA0, d-Phe1, Tyrc3] octreotide, a promising somatostatin analogue for radionuclide therapy. Eur J Nucl Med Mol Imaging 1997;24: 368-71.
6. Otte A, Mueller-Brand J, Dellas S, Nitzsche EU, Herrmann R, Maecke HR. Yttrium-90-labelled somatostatin-analogue for cancer treatment. Lancet 1998;351:417-18.
7. Kwekkeboom DJ, Bakker WH, Kooij PP, Konijnenberg MW, Srinivasan A, Erion JL, et al. [^{177}Lu-DOTAOTyr3] octreotate: Comparison with [^{111}In-DTPAo]octreotide in patients. Eur J Nucl Med 2001;28:1319-25.
8. Prasad V, Baum RP. Biodistribution of the Ga-68 labeled somatostatin analogue DOTA-NOC in patients with neuro-endocrine tumours: Characterization of uptake in normal organs and tumour lesions. Q J Nucl Med Mol Imag 2010;54:61-67.
9. Wild D, Fani M, Behe M, Brink I, Rivier JE, Reubi JC, et al. First clinical evidence that imaging with somatostatin receptor antagonists is feasible. J Nucl Med 2011;52:1412-17.
10. Krenning EP, Kwekkeboom DJ, Bakker WH, Breeman WA, Kooij PP, Oei HY, et al. Somatostatin receptor scintigraphy with [^{111}In-DTPA-D-Phe1]- and [^{123}I-Tyr3]-octreotide: The Rotterdam experience with more than 1000 patients. Eur J Nucl Med Mol Imag 1993;20:716-31.
11. Decristoforo C, Melendez-Alafort L, Sosabowski JK, Mather SJ. ^{99m}Tc-HYNIC-[Tyr3]-octreotide for imaging somatostatin-receptor-positive tumours: Preclinical evaluation and comparison with ^{111}In-octreotide. J Nucl Med 2000;41: 1114-19.
12. Hofmann M, Maecke H, Borner R, Weckesser E, Schöffski P, Oei L, et al. Biokinetics and imaging with the somatostatin receptor PET radioligand ^{68}Ga-DOTATOC: Preliminary data. Eur J Nucl Med Mol Imaging 2001;28:1751-57.
13. Buchmann I, Henze M, Engelbrecht S, Eisenhut M, Runz A, Schäfer M, et al. Comparison of ^{68}Ga-DOTATOC PET and ^{111}In-DTPAOC (Octreoscan) SPECT in patients with neuro-endocrine tumours. Eur J Nucl Med Mol Imaging 2007;34: 1617-26.
14. Kaemmerer D, Peter L, Lupp A, Schulz S, Sänger J, Prasad V, et al. Molecular imaging with ^{68}Ga-SSTR PET/CT and correlation to immunohistochemistry of somatostatin receptors in neuroendocrine tumours. Eur J Nucl Med Mol Imaging 2011;8:1659-68.
15. Prasad V, Ambrosini V, Hommann M, Hoersch D, Fanti S, Baum RP. Detection of unknown primary neuroendocrine tumours (CUP-NET) using ^{68}Ga-DOTA-NOC receptor PET/CT. Eur J Nucl Med Mol Imaging 2010;37:67-77.
16. Campana D, Ambrosini V, Pezzilli R, Fanti S, Labate AM, Santini D, et al. Standardized uptake values of ^{68}Ga-DOTANOC PET: A promising prognostic tool in neuroendocrine tumours. J Nucl Med 2010;51:353-59.
17. Kayani I, Bomanji JB, Groves A, Conway G, Gacinovic S, Win T, et al. Functional imaging of neuroendocrine tumours with combined PET/CT using ^{68}Ga-DOTATATE (Dota-DPhe1, Tyr3-octreotate) and ^{18}F-FDG. Cancer 2008;112:2447-55.
18. Pagou M, Zerizer I, Al-Nahhas A. Can gallium-68 compounds partly replace (18)F-FDG in PET molecular imaging? Hell J Nucl Med 2009;12:102-05.
19. Fellner M, Baum RP, Kubícek V, Hermann P, Lukes I, Prasad V, et al. PET/CT imaging of osteoblastic bone metastases

with (68)Ga-bisphosphonates: First human study. Eur J Nucl Med Mol Imag 2010;37:834.
20. Tornesello AL, Aurilio M, Accardo A, Tarallo L, Barbieri A, Arra C, et al. Gastrin and cholecystokinin peptide-based radiopharmaceuticals: an in vivo and in vitro comparison. J Pept Sci 2011;17:405-12.
21. Brom M, Oyen WJ, Joosten L, Gotthardt M, Boerman OC. ^{68}Ga-labeled exendin-3, a new agent for the detection of insulinomas with PET. Eur J Nucl Med Mol Imaging 2010;37:1345-55.
22. Wild D, Wicki A, Mansi R, Béhé M, Keil B, Bernhardt P, et al. Exendin-4-based radiopharmaceuticals for glucagon like peptide-1 receptor PET/CT and SPECT/CT. J Nucl Med 2010;51:1059-67.
23. Decristoforo C, Hernandez Gonzalez I, Carlsen J, Rupprich M, Huisman M, Virgolini I, et al. ^{68}Ga- and ^{111}In-labeled DOTA-RGD peptides for imaging of alphav beta3 integrin expression. Eur J Nucl Med Mol Imaging 2008;35:1507-15.
24. Gourni E, Demmer O, Schottelius M, D'Alessandria C, Schulz S, Dijkgraaf I, et al. PET of CXCR4 expression by a (68)Ga-labeled highly specific targeted contrast agent. J Nucl Med 2011;52:1803-10.
25. Schroeder RP, Müller C, Reneman S, Melis ML, Breeman WA, de Blois E, et al. A standardised study to compare prostate cancer targeting efficacy of five radiolabelled bombesin analogs. Eur J Nucl Med Mol Imaging 2010; 37:1386-96.
26. Kotzerke J, Andreeff M, Wunderlich G, Wiggermann P, Zöphel K. Ventilation/perfusion scans using Ga-68 labeled tracers. World J Nucl Med 2011;10:26-59.
27. Froidevaux S, Calame-Christe M, Schuhmacher J, Tanner H, Saffrich R, Henze M, Eberle AN. A gallium-labeled DOTA-alpha-melanocyte-stimulating hormone analog for PET imaging of melanoma metastases. J Nucl Med 2004; 45:116-23.
28. Baum RP, Prasad V, Müller D, Schuchardt C, Orlova A, Wennborg A, et al. Molecular imaging of HER2-expressing malignant tumors in breast cancer patients using synthetic ^{111}In- or ^{68}Ga-labeled affibody molecules. J Nucl Med 2010;51: 892-97.
29. Reubi JC, Horisberger U, Laissue JA. High density of somatostatin receptors in veins surrounding human cancer tissue: Role in tumour-host interactions? Int J Cancer 1994;56:681-88.
30. Kwekkeboom DJ, de Herder WW, Kam BL, van Eijck CH, van Essen M, Kooij PP, et al. Treatment with the radiolabeled somatostatin analog [^{177}Lu-DOTA 0,Tyr3]octreotate: Toxicity, efficacy, and survival. J Clin Oncol 2008;26:2124-30.
31. Imhof A, Brunner P, Marincek N, Briel M, Schindler C, Rasch H, et al. Response, survival, and long-term toxicity after therapy with the radiolabeled somatostatin analogue [^{90}Y-DOTA]-TOC in metastasized neuroendocrine cancers. J Clin Oncol 2011;29:2416-23.
32. Kaemmerer D, Prasad V, Daffner W, Hörsch D, Klöppel G, Hommann M, et al. Neoadjuvant peptide receptor radionuclide therapy for an inoperable neuroendocrine pancreatic tumour. World J Gastroenterol 2009;15:5867-70.
33. Wehrmann C, Senftleben S, Zachert C, Müller D, Baum RP. Results of individual patient dosimetry in peptide receptor radionuclide therapy with ^{177}Lu DOTA-TATE and ^{177}Lu DOTA-NOC. Cancer Biother Radiopharm 2007;22:406-16.
34. Majkowska-Pilip A, Bilewicz A. Macrocyclic complexes of scandium radionuclides as precursors for diagnostic and therapeutic radiopharmaceuticals. J Inorg Biochem 2011;105: 313-20.
35. Pruszyñski M, Loktionova NS, Filosofov DV, Rösch F. Post-elution processing of (44)Ti/ (44)Sc generator-derived (44)Sc for clinical application. Appl Radiat Isot. 2010;68:1636-41.
36. Valkema R, Pauwels SA, Kvols LK, Kwekkeboom DJ, Jamar F, de Jong M, et al. Long-term follow-up of renal function after peptide receptor radiation therapy with ^{90}Y-DOTA(0),Tyr(3)-octreotide and ^{177}Lu-DOTA(0), Tyr(3)-octreotate. J Nucl Med 2005;46:83-91.
37. Kwekkeboom DJ, Mueller-Brand J, Paganelli G, Anthony LB, Pauwels S, Kvols LK, et al. Overview of results of peptide receptor radionuclide therapy with 3 radiolabeled somatostatin analogs. J Nucl Med 2005;46:62-66.
38. Baum RP, Kulkarni HR. Theranostics: From molecular imaging using Ga-68 labeled tracers and PET/CT to personalized radionuclide therapy-The Bad Berka experience. Theranostics 2012;2:437-47
39. Baum RP, Kulkarni HR, Schuchardt C, Fellner M, Roesch F. First clinical experience using ^{177}Lu-BPAMD for the treatment of skeletal metastases in prostate cancer (Abstract). Eur J Nucl Med Mol Imaging 2011;38:225.
40. Maina T, Nock B, Baum RP, Krenning EP, de Jong M. Radiolabeled GRPR-antagonists: New promising tools in the diagnosis and therapy of GRPR positive tumours (Abstract). World J Nucl Med 2011;10:26-59.

ABOUT THE AUTHORS

Harshad R Kulkarni

Resident Physician, Department of Theranostics, THERANOSTICS Center for Molecular Radiotherapy and Molecular Imaging, ENETS Center of Excellence, Zentralklinik Bad Berka, Germany

Richard P Baum (Corresponding Author)

Chairman and Clinical Director, Department of Theranostics THERANOSTICS Center for Molecular Radiotherapy and Molecular Imaging, ENETS Center of Excellence, Zentralklinik Bad Berka Germany, e-mail: richard.baum@zentralklinik.de

10.5005/jp-journals-10028-1056
REVIEW ARTICLE

Role of Endoscopic Ultrasound in Gastroenteropancreatic Neuroendocrine Tumors and Update on Their Treatment

Surinder Singh Rana, Vishal Sharma, Deepak Kumar Bhasin

ABSTRACT

The gastroenteropancreatic (GEP) neuroendocrine tumors (NETs) are rare tumors and include all tumors arising from the gastrointestinal (GI) or pancreatic neuroendocrine cells. They can occur anywhere in the GI tract with the small intestine, pancreas and rectum being the common GI sites. Because of nonspecific symptoms they are difficult to diagnose and diagnosis is often delayed by years. Advancement in cross-sectional imaging techniques and advent of radionuclide-labeled somatostatin analogs have improved our accuracy of diagnosis and staging GEP NETs. Endoscopic ultrasound (EUS) with its unique combination of endoscopy and ultrasound provides high resolution images of GI tract wall as well as the surrounding solid parenchymal organs and therefore is an important investigation for the diagnosis and staging of GEP NETs. Surgery is the treatment of choice with good long-term results in patients with localized GEP-NETs. Control of symptoms in functional NETs is warranted to improve the quality of life of the patient. Somatostatin and its analogs like octreotide and lanreotide have been used to control symptoms because of functional NETs. The management of metastatic GEP NETs includes control of symptoms and therapy to decrease/stop tumor growth that includes somatostatin and its analogs and chemotherapy. Newer therapeutic modalities like peptide receptor radionuclide therapy (PRRT) and molecular therapy hold considerable promise.

Keywords: Endosonography, Pancreas, Carcinoids, Stomach, Computed tomography.

How to cite this article: Rana SS, Sharma V, Bhasin DK. Role of Endoscopic Ultrasound in Gastroenteropancreatic Neuroendocrine Tumors and Update on Their Treatment. J Postgrad Med Edu Res 2013;47(1):54-60.

Source of support: Nil

Conflict of interest: None

INTRODUCTION

The neuroendocrine tumors (NETs) are a heterogeneous group of relatively rare, but now being increasingly recognized and diagnosed tumors that are seen most commonly in the gastrointestinal (GI) and the bronchopulmonary system.[1] The gastroenteropancreatic (GEP) NETs, is an umbrella term which includes all tumors arising from the GI or pancreatic neuroendocrine cells and encompasses the earlier recognized categories of carcinoids and pancreatic neuroendocrine tumors (PNET).[2,3] They can occur anywhere in the GI tract with the small intestine, pancreas and rectum being the common GI sites and these tumors have varying biological behavior.[2,3] The diverse and sometimes nonspecific clinical syndromes associated with pancreatic NET can make these malignancies difficult to diagnose at an early stage. These tumors present with variable symptoms that may include functional symptoms due to overproduction of hormones or nonspecific symptoms due to nonfunctional tumors. Majority of the GEP NETs are nonfunctional and usually present with symptoms of mass effect of the tumor or distant metastasis that is usually in the liver.[4] Because of these nonspecific symptoms of GEP NETs are difficult to diagnose and diagnosis is often delayed by years. Advancement in cross-sectional imaging techniques and advent of radionuclide-labeled somatostatin analogs have improved our accuracy of diagnosis and staging GEP NETs.[4] Endoscopic ultrasound (EUS) with its unique combination of endoscopy and ultrasound provides high resolution images of GI tract wall as well as the surrounding solid parenchymal organs. These detailed high resolution images obtained by the EUS are much better than those obtained by other cross-sectional imaging modalities and this allows identification of small lesions that may be missed by other cross-sectional imaging techniques. Also the ability to do fine needle aspiration (FNA) from the lesion is an added advantage of the EUS. These qualities of EUS make it an important investigation for the diagnosis and staging of GEP NETs. This review discusses the role of EUS in diagnosis, staging and treatment of GEP NET and also a brief update on various therapeutic modalities for these rare but unique tumors will be provided.

EUS FOR DIAGNOSIS AND LOCALIZATION OF GEP NET

GEP NET occur either in the bowel or the pancreas and approximately 40% of these tumors are seen in pancreas with the rest being seen in the intestines with small bowel and the rectum being the common sites.[5] EUS is helpful in both of these clinical situations. Because of its ability to obtain high resolution images of the GI tract and adjacent organs, EUS is the most sensitive test for detection these lesions especially the ones that are small and especially localized in the pancreas. It has been shown to be particularly useful for identification of smaller lesions that have been missed by other cross-sectional imaging modalities.[5-7] Although the diagnosis of intestinal NET can be achieved by endoscopic studies, EUS helps to determine the depth and extension and this helps in planning appropriate therapy.[5]

Pancreatic NET

Despite the advances in imaging modalities, up to 30% of PNETs can be missed during a preoperative assessment. As majority of NETs have somatostatin receptors, octreotide scintigraphy has high sensitivity and specificity for localizing NET. However, tumors that lack somatostatin receptors and are small can be missed even on scintigraphy. EUS obtains high resolution images of the pancreas because the transducer is placed very close to the pancreas, being separated only by the thin GI tract wall (Figs 1 to 3). Because of this EUS is particularly well suited for detection of small pancreatic lesions. Studies have demonstrated that EUS with or without FNA has a sensitivity ranging from 77 to 93% for the diagnosis of pancreatic NETs.[8-11] Varas Lorenzo et al reported the diagnostic yield of various imaging modalities in 37 patients (16 males) with pancreatic NET by sequentially examining them with abdominal ultrasound, computed tomography (CT), magnetic resonance imaging (MRI), angiography, OctreoScan and radial and sectorial EUS. They found that the sensitivity, specificity and diagnostic accuracy of EUS to be 81, 80 and 78% and three pancreatic rumors of ≤1 cm size (all insulinomas) that were missed by other cross-sectional imaging modalities, were detected by EUS.[5] Versari et al compared the diagnostic yield of EUS, multidetector CT (MDCT) and Ga-68 DOTATOC PET/CT in patients with NETs and found that EUS, PET and MDCT correctly identified lesions in 13/13 (100%), 12/13 (92%) and 10/11 (91%) patients respectively.[12] De Angelis et al studied the role of EUS in PNET in 25 patients who underwent surgical resection and reported that EUS correctly localized 20/23 (87%) pancreatic tumors 11/12 (91.6%) insulinomas, 3/8 (37.5%) duodenal gastrinomas and 10/11 (90.9%) metastatic lymph nodes.[13] In contrast, correct localization was done on ultrasonography (US) in 17.4% patients, by CT in 30.4%, by MRI in 25%, by angiography in 26.6%, and by somatostatin receptor scintigraphy in 15.4% patients. EUS has been also found to be an excellent investigational modality for detecting pancreatic NETs in patients with multiple endocrine neoplasia (MEN) type 1 before the development of significant biochemical test abnormalities.[14]

On EUS, the pancreatic NET typically are well defined hypoechoic lesions with a homogeneous lesion appearance and majority of these lesions are solid.[2] Occasionally, these lesions may also have a cystic appearance. EUS may be falsely negative if the tumor has an isoechoic appearance, is very small in size, or is located at the tail end especially if it is pedunculated. A peripancreatic lymph node may mimic a PNET leading on to a false diagnosis of NET on

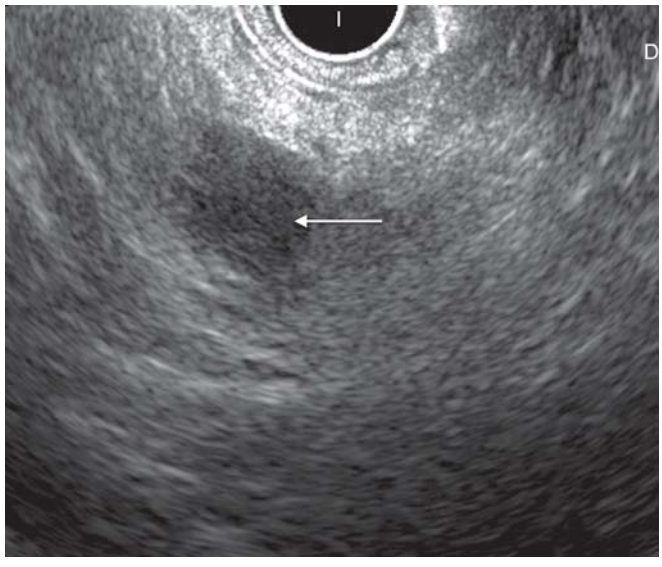

Fig. 2: EUS: A small pancreatic insulinomas localized on EUS (arrow)

Fig. 1: EUS: Large nonfunctional pancreatic NET

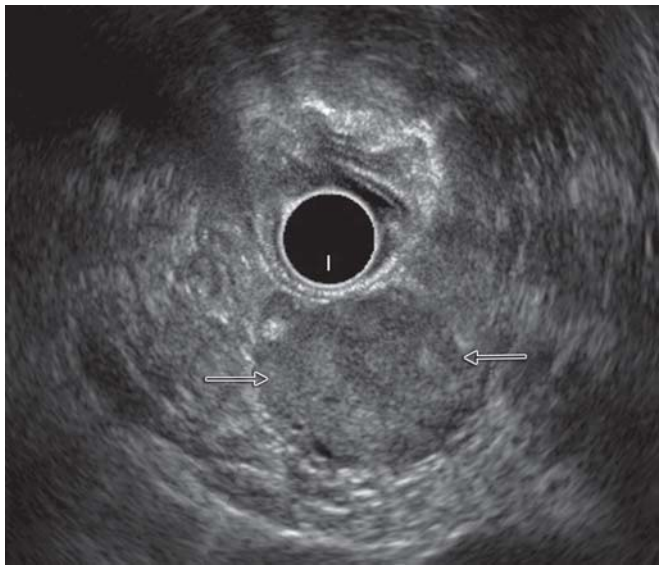

Fig. 3: EUS: Well-defined hypoechoic insulinomas (arrow)

EUS. Recently, contrast enhanced EUS (CEUS) has been used to detect small pancreatic tumors, differentiate between focal pancreatitis and pancreatic cancer as well as to differentiate and characterize various pancreatic tumors. Sakamoto et al[15] studied 156 patients of suspected pancreatic tumors by CEUS and they observed three types of vascular pattern: Hypovascular, isovascular and hypervascular lesions in comparison to the surrounding parenchyma. They observed that 96.2% of the hypovascular lesions were pancreatic carcinomas, 80% of the isovascular lesions were focal pancreatitis and 76% of the hypervascular lesions were NET. Ishikawa et al reported that heterogeneous ultrasonographic texture in the tumor, identified as filling defects in CEUS, was the most significant factor for malignancy and therefore concluded that CEUS has higher sensitivity in preoperative localization of PNETs and can also help in differentiating benign from malignant tumors.[16]

Thus, the available literature suggests that EUS is particularly able to localize gastrinomas and insulinomas. As most of the insulinomas are located in the pancreas, EUS is an excellent modality for diagnosing and localizing these lesions. The reported detection rates by EUS have ranged from 79 to 94%, with higher sensitivity in the head and lower sensitivity in the tail.[17] Similarly, pancreatic gastrinomas are also localized by EUS in 75 to 94% of cases. However, the extrapancreatic (duodenal) gastrinomas are less frequently detected by EUS possibly because of their generally smaller sizes.[3] CEUS is an upcoming promising new technique but more studies are needed.

EUS-GUIDED CYTOLOGICAL DIAGNOSIS OF PNET

EUS along with the localization of the tumor also allows FNA of the lesion (Fig. 4). This provides cytological material for cytology, histology and immunohistochemistry (IHC). Chatzipantelis et al reported that the helpful cytological findings for the diagnosis of NET on cytological material obtained via EUS FNA were a richly cellular sample with a monotonous, poorly cohesive population of small or medium-sized cells with granular chromatin (salt and pepper) and plasmacytoid morphology.[18] The IHC is commonly performed by using stains including chromogranin, synaptophysin, neuron specific enolase, CDX, and CD56 and various hormones like insulin, glucagon, etc.[2,18] Recently, attempts have been made to predict the biological behavior of the tumors by using the cytological or histological findings. Chatzipantelis et al retrospectively reviewed the cytopathological findings and proliferative activity (Ki-67) in EUS FNA specimens of 35 patients with PNET.[19] They found that 21/22 (95.4%)

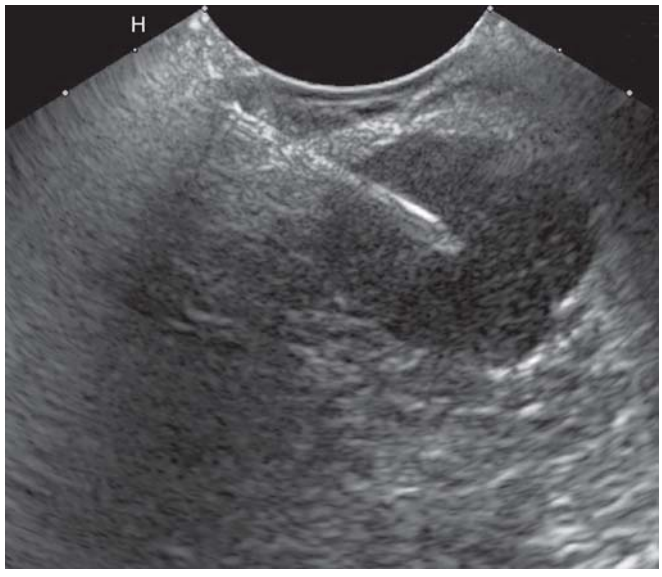

Fig. 4: EUS-guided FNA from pancreatic NET

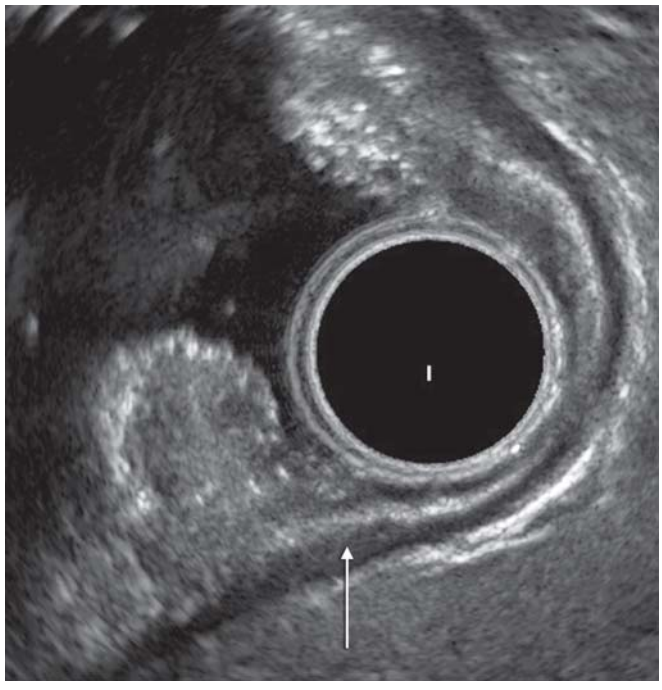

Fig. 5: EUS: Gastric carcinoid with muscularis propria intact (arrow)

malignant tumors had a high proliferative index (>2% Ki-67 cells) whereas Ki-67 was totally absent from tumors that were classified as WHO subgroup 1a (well-differentiated NETs confined to the pancreas) and was seen in a lesser proportion of tumors (42.86%) classified as WHO subgroup 1b (well-differentiated NETs of uncertain behavior confined to the pancreas). Thus, they concluded that Ki-67 evaluation in routine EUS-FNA cytology specimens can be used as a potential prognostic marker in pancreatic NET.

EUS for Staging of Luminal NET

NETs located in the stomach, duodenum and rectum can be diagnosed on endoscopy and if there is no extraintestinal

metastasis, the NETs can be resected endoscopically. But before proceeding on to the endoscopic resection, exact depth of the invasion of the NET needs to be determined so that appropriate therapeutic strategy can be planned. Yoshikane et al studied 29 patients with GI carcinoid tumors (five gastric, seven duodenal, and 17 rectal) by EUS and reported that accuracy of determining the depth of invasion using EUS was 75%. They concluded that EUS is useful for the staging of GI carcinoid tumors as it helps in determining depth of involvement as well as presence of perigastrointestinal lymph node involvement.[20] Kobayashi et al studied the depth of invasion of rectal carcinoids in 52 patients using EUS.[21] They found that the depth of invasion was correctly identified by EUS in all 52 patients with the tumors being localized to submucosa in 49 patients and infiltrating the muscularis propria in three patients. They concluded that rectal carcinoid tumors that are $\leq$ 10 mm in diameter with no invasion of the muscularis propria, and not having any depression or ulceration in the lesion can be resected endoscopically. Martinez-Ares et al resected 24 tumors in 21 patients endoscopically and found that EUS is the most precise diagnostic technique for evaluating tumor size, and showing the tumor-free state of the muscularis propria, the two most important factors that help in selecting the patients for endoscopic resection.[22] Also, endoscopic submucosal dissection (ESD) has also been described for rectal carcinoids and here also, EUS has been shown to be an useful technique for excluding muscularis propria invasion (Fig. 5).[23,24]

Although, EUS can also asses the depth of invasion in gastric NETs and thus help in selecting patients suitable for endoscopic resection, the therapy of gastric NETs is dependent upon multiple factors that include the type, size and number of NET and the readers are advised to consult other reviews on this topic.[25,26]

EUS-guided Antitumor Therapy

Because of its unique capability to simultaneously visualize both the pathological as well as normal structures in the real time along with the ability to avoid surrounding vascular structures, EUS has also been used to deliver therapeutic agents in to the tumor.[2] There are multiple reports of EUS-guided ablation of insulinomas.[27-31] Although, surgical resection is the preferred therapeutic approach in patients with insulinoma, some of the patients with insulinoma may not be good candidates for surgery because of comorbidities and therefore would need alternative minimally invasive treatment modalities for symptom control. EUS-guided alcohol ablation of the insulinomas has been described as case reports and although feasible and successful, its use has been associated with serious complications including life-threatening. A recent study by Levy et al in eight patients of insulinoma, used lower volumes of alcohol and repeated treatment sessions with the aim of symptom relief rather than complete ablation of the tumor.[32] In this study, EUS-guided injection was used in five patients and intraoperative ultrasound-guided alcohol injection in three patients. A volume of 0.8 ml (range: 0.12-3.0 ml) of alcohol was injected per session in small aliquots, typically 0.01 to 0.1 ml at a time using a 22 or 25G needle. The injections were repeated at the same site until a hyperechoic blush was seen expanding in the tumor and it was stopped when the blush was seen in close proximity to the edge of the tumor or whenever, there was concern for leakage beyond its border. Dependent upon the tumor size and pattern of spread after the initial injection, additional passes were made, avoiding the previous needle tracts. There were no peri- or postprocedural complications. In the first 24 hours after procedure, 3/5 patients needed intravenous glucose to control hypoglycemia whereas the remaining two patients did not need any intervention for control of blood sugars. On long-term follow-up, this treatment strategy effectively relieved symptoms and resulted in euglycemia without the need for medical therapy in two patients and with low dose diazoxide therapy in three patients. Thus, limited experience suggests that EUS-guided alcohol fine needle injection may be appropriate treatment modality for insulinomas requiring extensive resection and in patients who are poor surgical candidates.

Treatment of GEP NET: An Overview

NETs may manifest with symptoms related to the effects of hormone hypersecretion (carcinoid syndrome, gastrinoma, glucagonoma) or related to the mass effects associated with large lesions (nonfunctioning NETs) like pain, bowel obstruction and awareness of lump. The therapy for these tumors is decided on the site of disease and whether any distant spread has occurred or not. The therapy therefore needs to be individualized based upon the location, size, presence or absence of metastasis and the symptoms produced by it.[33]

Treatment of Nonmetastatic Disease

Surgical resection remains the therapy of choice for localized GEP-NET and is the only curative treatment.[4] As with all other tumors, the curative surgical resection depends upon the mode of presentation and the extent of the spread of the disease. If the lesion is less than 2 cm in diameter, the frequency of metastasis is usually low. The goals of the surgical therapy are to: (1) Prolong survival by resecting the primary tumor and any nodal or hepatic metastases, (2) control the symptoms related to hormonal secretion, (3) prevent or treat local complications.[34]

The usual approach for intestinal lesions is bowel resection with resection of draining lymph nodes. During surgery an attempt must be made to look for any synchronous lesions and to resect them. Concomitant cholecystectomy can be undertaken to prevent any gall bladder sludge formation that may accompany use of octreotide later. Smaller lesions may however be dealt with endoscopically.[2,34-37] For small duodenal lesions endoscopic resection may be done; larger lesions warrant transduodenal local excision or pancreatoduodenectomy. For lesions elsewhere in the small and the large intestine, surgical resection with lymphadenectomy is warranted. For appendiceal carcinoids, an appendectomy is sufficient for lesions smaller than 1 cm. The management of lesions between 1 and 2 cm is controversial with some advocating appendectomy and others preferring a right hemicolectomy. It is important to rule out lymphatic or distant metastasis in larger lesions. Rectal carcinoids smaller than 2 cm can be treated with endoscopic or transanal excision. However, examination under anesthesia and/or EUS before the procedure should be done for lesions larger than 1 cm. For lesions larger than 2 cm, or smaller lesions with invasion into the muscularis propria, or with lymph node involvement, low anterior resection or, in rare cases, an abdominoperineal resection is indicated. Close post-operative follow-up is needed in most of these patients to identify any recurrent disease early.

Gastric carcinoids are classified into three types.[4] The types I and II are associated with hypergastrinemia. Type I gastric carcinoids originate in the background of chronic atrophic gastritis while the type II carcinoids originate in the background of acid hypersecretion due to gastrinomas (Zollinger-Ellison syndrome). Type III carcinoids are sporadic lesions which occur in absence of hypergastrinemia and are usually larger and have more aggressive behavior. The frequency of metastasis increases from types I to III with rates of around 10, 10 to 30 and 50 to 60% respectively. Lesions in the stomach may be handled endoscopically or with surgical resection. For type I and II with lesions smaller than 2 cm the options include endoscopic resection of the lesions with biopsy of adjacent mucosa, or use of octreotide in gastrinoma and a policy of observation. Larger lesions (>2 cm) are usually resected surgically. In type III lesions, radical resection with locoregional lymphadenectomy is the therapy of choice.[33,38]

In nonfunctional PNETs, small tumors (<2 cm) can be enucleated, while larger lesions can be treated with a pancreaticoduodenectomy or a distal pancreatectomy with splenectomy depending on the site of the lesion. For functional PNETs which are localized, the therapy must attempt control of hormonal hypersecretion followed by surgical resection of lesion, if possible.[4,33,38]

Treatment of Metastatic GEP-NETs

The therapy of metastatic GEP-NETs must address two important issues: Control of symptoms due to secreted products and the control of the tumor load. Somatostatin and its analogs like octreotide and lanreotide can bind to the somatostatin receptor subtype (SSRT) 2 and 5.[39] They block the release and the synthesis of bioactive amines as also their peripheral actions. These analogs have a weak tumoricidal and a good tumoristatic effect.[39] Long acting formulations like lanreotide are preferred for the ease of use. A majority of patients will have some symptomatic response to therapy with a reduction in symptoms like flushing and diarrhea.[40] Side effects may include impaired blood sugar control, gallstone formation, steatorrhea, hypocalcemia, etc. Interferon-α, also, has a mild tumoricidal effect similar to somatostatin analogs.[41] Combination of interferon-α and octreotide has also been used especially in situations when one of the drugs becomes ineffective.[42,43] A number of chemotherapeutic agents have also been used but the response is dismal to most drugs. Various combinations of drugs which have been tried in treatment of metastatic disease include combination of streptozotocin with 5-flourouracil, or doxorubicin with 5-flourouracil.[44] Combination of etoposide and cisplatin may produce a significant antitumor response but their use is recommended only in patients advanced disease with high proliferative index.[45]

Newer therapeutic modalities have increased the armamentarium available for therapy in metastatic NETs. These include various molecularly targeted therapies and use of peptide receptor radionuclide therapy. Molecular targets are cellular molecules which have a role in cellular growth and division. Use of targeted approaches can stop the cells from abnormal proliferation and thus stop tumor growth. However, as multiple cellular pathways are involved in tumorigenesis, the benefits of targeted therapies do not last forever. Important molecules involved in tumorigenesis of NETs include mammalian target of rapamycin (mTOR), vascular endothelial growth factor (VEGF) for angiogenesis, insulin-like growth factor (IGF), transforming growth factor-alpha (TGF-α), platelet derived growth factor (PDGFR) and epidermal growth factor (EGFR) among others.[46]

Everolimus, an mTOR inhibitor, was compared with placebo in the RADIANT 3 trial in patients with NET. Everolimus (10 mg daily) prolonged the progression free survival in these patients.[47] A study has shown that Sunitinib, a multitarget tyrosine kinase inhibitor, in a dose of 37.5 mg daily improves survival in patients with NET vis-a-vis placebo.[48] Similarly bevacizumab, anti-VEGF monoclonal antibody, has been found superior to interferon in patients with NET who were already on octreotide.[49]

Table 1: Radionuclide agents used for PRRT

Radionuclide	*Mechanism*	*Utility*	*Half-life (in days)*	*Cons*
Indium-111	Gamma emitter, Auger electrons	Diagnostic	2.8	Minor therapeutic role
Yttrium-90	High energy pure beta emitter	Therapeutic, cross-fire effect to adjacent cells	2.7	Higher renal toxicity
Lutetium-177	Intermediate energy beta emitter, two gamma peaks	Therapeutic, less toxic, diagnostic utility also	6.7	—

Another therapeutic modality which has generated considerable interest is the use of radiolabeled somatostatin analogs. PRRT utilizes the high somatostatin receptor expression in NETs to ensure a targeted delivery of radiation to the tumor cells.[50] This has become possible with development of peptide with high receptor specificity (e.g. DOTA) and their tagging with various radionuclides (Table 1). The side effects of PRRT may include hematological, renal or hepatic effects. Usually the decrease in blood cells occurs due to bone marrow suppression and is transient. Renal toxicity may include thrombotic microangiopathy and tubular injury. Various approaches including amino acids infusion (lysine and arginine) to reduce renal toxicity are under evaluation. Hepatotoxicity is uncommon and usually mild. It manifests usually as an increase in transaminases but may result in significant toxicity in patients with large hepatic metastasis.[50]

TREATMENT OF LIVER METASTASIS

Liver is a common site of metastasis of the GEP-NETs due to the portal venous drainage of the GI tract and the pancreas where the primaries originate. The therapy of hepatic metastasis can be done using the previously mentioned systemic therapy or by using local ablative/resective approaches.[51,52] Local approaches include ablative therapy, surgical resection and hepatic transplantation for lesions of limited size and transarterial chemoembolization (TACE) for larger lesions. Local approaches to manage these lesions are done in cases where no other organs (except the primary lesion and the liver) are involved. Surgical resection is the preferred therapy in small resectable lesions and offers the best opportunity for long term survival. Ablation can be done using radiofrequency waves, microwaves or cryotherapy. Also, liver transplantation has been utilized as a therapeutic options in some patients but recurrence free 5-year survival has been less than 25%.[51,52]

REFERENCES

1. Maggard MA, O'Connell JB, Ko CY. Updated population-based review of carcinoid tumors. Ann Surg 2004;240:117-22.
2. Yao JC, Hassan M, Phan A, et al. One hundred years after 'carcinoid': Epidemiology of and prognostic factors for neuroendocrine tumors in 35,825 cases in the United States. J Clin Oncol 2008;26:3063-72.
3. Kim MK. Endoscopic ultrasound in gastroenteropancreatic neuroendocrine tumors. Gut Liver 2012;6:405-10.
4. Ramage JK, Ahmed A, Ardill J, et al. Guidelines for the management of gastroenteropancreatic neuroendocrine (including carcinoid) tumours (NETs). Gut 2012;61:6-32.
5. Varas Lorenzo MJ, Miquel Collell JM, Maluenda Colomer MD, Boix Valverde J, Armengol Miró JR. Preoperative detection of gastrointestinal neuroendocrine tumors using endoscopic ultrasonography. Rev Esp Enferm Dig 2006;98:828-36.
6. Othman MO, Wallace MB. The role of endoscopic ultrasonography in the diagnosis and management of pancreatic cancer. Gastroenterol Clin North Am 2012;41:179-88.
7. Fusaroli P, Kypraios D, Eloubeidi MA, Caletti G. Levels of evidence in endoscopic ultrasonography: A systematic review. Dig Dis Sci 2012;57:602-09.
8. Pais SA, Al-Haddad M, Mohamadnejad M, et al. EUS for pancreatic neuroendocrine tumors: A single-center, 11-year experience. Gastrointest Endosc 2010;71:1185-93.
9. Rosch T, Braig C, Gain T, et al. Staging of pancreatic and ampullary carcinoma by endoscopic ultrasonography. Comparison with conventional sonography, computed tomography and angiography. Gastroenterology 1992;102:188-99.
10. Fein J, Gerdes H. Localization of islet cell tumors by endoscopic ultrasonography. Gastroenterology 1992;103:711-12.
11. Muller MF, Meyenberger C, Bertschinger P, Schaer R, Marincek B. Pancreatic tumors: Evaluation with endoscopic US, CT, and MR imaging. Radiology 1994;190:745-51.
12. Versari A, Camellini L, Carlinfante G, et al. Ga-68 DOTATOC PET, endoscopic ultrasonography, and multidetector CT in the diagnosis of duodenopancreatic neuroendocrine tumors: A single-centre retrospective study. Clin Nucl Med 2010;35: 321-28.
13. De Angelis C, Carucci P, Repici A, Rizzetto M. Endosonography in decision making and management of gastrointestinal endocrine tumors. Eur J Ultrasound 1999;10:139-50.
14. Wamsteker EJ, Gauger PG, Thompson NW, Scheiman JM. EUS detection of pancreatic endocrine tumors in asymptomatic patients with type 1 multiple endocrine neoplasia. Gastrointest Endosc 2003;58:531-35.
15. Sakamoto H, Kitano M, Suetomi Y, Maekawa K, Takeyama Y, Kudo M. Utility of contrast-enhanced endoscopic ultrasonography for diagnosis of small pancreatic carcinomas. Ultrasound Med Biol 2008;34:525-32.
16. Ishikawa T, Itoh A, Kawashima H, et al. Usefulness of EUS combined with contrast-enhancement in the differential diagnosis of malignant versus benign and preoperative localization of pancreatic endocrine tumors. Gastrointest Endosc 2010;71:951-59.
17. Sotoudehmanesh R, Hedayat A, Shirazian N, et al. Endoscopic ultrasonography (EUS) in the localization of insulinoma. Endocrine 2007;31:238-41.
18. Chatzipantelis P, Salla C, Konstantinou P, Karoumpalis I, Sakellariou S, Doumani I. Endoscopic ultrasound-guided fine-needle aspiration cytology of pancreatic neuroendocrine tumors: A study of 48 cases. Cancer 2008;114:255-62.
19. Chatzipantelis P, Konstantinou P, Kaklamanos M, Apostolou G, Salla C. The role of cytomorphology and proliferative activity

in predicting biologic behavior of pancreatic neuroendocrine tumors: A study by endoscopic ultrasound-guided fine-needle aspiration cytology. Cancer 2009;117:211-16.
20. Yoshikane H, Tsukamoto Y, Niwa Y, et al. Carcinoid tumors of the gastrointestinal tract: Evaluation with endoscopic ultrasonography. Gastrointest Endosc 1993;39:375-83.
21. Kobayashi K, Katsumata T, Yoshizawa S, et al. Indications of endoscopic polypectomy for rectal carcinoid tumors and clinical usefulness of endoscopic ultrasonography. Dis Colon Rectum 2005;48:285-91.
22. Martínez-Ares D, Souto-Ruzo J, Varas Lorenzo MJ, et al. Endoscopic ultrasound-assisted endoscopic resection of carcinoid tumors of the gastrointestinal tract. Rev Esp Enferm Dig 2004;96:847-55.
23. Hamada Y, Tanaka K, Tano S, Katsurahara M, Kosaka R, Noda T, et al. Usefulness of endoscopic submucosal dissection for the treatment of rectal carcinoid tumors. Eur J Gastroenterol Hepatol 2012;24:770-74.
24. Yamaguchi N, Isomoto H, Nishiyama H, Fukuda E, Ishii H, Nakamura T, et al. Endoscopic submucosal dissection for rectal carcinoid tumors. Surg Endosc 2010;24:504-08.
25. Zhang L, Ozao J, Warner R, Divino C. Review of the pathogenesis, diagnosis, and management of type I gastric carcinoid tumor. World J Surg 2011;35:1879-86.
26. Massironi S, Sciola V, Spampatti MP, Peracchi M, Conte D. Gastric carcinoids: Between underestimation and overtreatment. World J Gastroenterol 2009;15:2177-83.
27. Scott A, Hinwood D, Donnelly R. Radio-frequency ablation for symptom control in a patient with metastatic pancreatic insulinoma. Clin Endocrinol (Oxf) 2002;56:557-59.
28. Jurgensen C, Schuppan D, Neser F, Ernstberger J, Junghans U, Stolzel U. EUS-guided alcohol ablation of an insulinoma. Gastrointest Endosc 2006;63:1059-62.
29. Vleggaar FP, Bij de Vaate EA, Valk GD, Leguit RJ, Siersema PD. Endoscopic ultrasound-guided ethanol ablation of a symptomatic sporadic insulinoma. Endoscopy 2011;43 (Suppl 2) UCTN:E328-29.
30. Deprez PH, Claessens A, Borbath I, Gigot JF, Maiter D. Successful endoscopic ultrasound-guided ethanol ablation of a sporadic insulinoma. Acta Gastroenterol Belg 2008;71:333-37.
31. Muscatiello N, Nacchiero M, Della Valle N, et al. Treatment of a pancreatic endocrine tumor by ethanol injection (PEI) guided by endoscopic ultrasound. Endoscopy 2008 Sep;40(Suppl 2):E83.
32. Levy MJ, Thompson GB, Topazian MD, Callstrom MR, Grant CS, Vella A. US-guided ethanol ablation of insulinomas: A new treatment option. Gastrointest Endosc 2012;75:200-06.
33. Modlin IM, Oberg K, Chung DC, et al. Gastroenteropancreatic neuroendocrine tumours. Lancet Oncol 2008;9:61-72.
34. Kianmanesh R, O'toole D, Sauvanet A, Ruszniewski P, Belghiti J. Surgical treatment of gastric, enteric, and pancreatic endocrine tumors Part 1. Treatment of primary endocrine tumors. J Chir (Paris) 2005;142:132-49.
35. Falconi M, Bettini R, Boninsegna L, Crippa S, Butturini G, Pederzoli P. Surgical strategy in the treatment of pancreatic neuroendocrine tumors. JOP 2006;7:150-56.
36. Akerström G, Hellman P. Surgery on neuroendocrine tumours. Best Pract Res Clin Endocrinol Metab 2007;21:87-109.
37. Azimuddin K, Chamberlain RS. The surgical management of pancreatic neuroendocrine tumors. Surg Clin North Am 2001;81: 511-25.
38. Kulke MH, Benson AB 3rd, Bergsland E, et al. Neuroendocrine tumors. J Natl Compr Canc Netw 2012;10:724-64.
39. Eriksson B, Oberg K. Summing up 15 years of somatostatin analog therapy in neuroendocrine tumors: Future outlook. Ann Oncol 1999;10(Suppl 2):S31-38.
40. Ruszniewski P, Ducreux M, Chayvialle JA, et al. Treatment of the carcinoid syndrome with the longacting somatostatin analogue lanreotide: A prospective study in 39 patients. Gut 1996;39:279-83.
41. Oberg K. Chemotherapy and biotherapy in the treatment of neuroendocrine tumours. Ann Oncol 2001;12(Suppl 2): S111-14.
42. Tiensuu Janson EM, Ahlstrom H, Andersson T, Oberg KE. Octreotide and interferon alfa: A new combination for the treatment of malignant carcinoid tumours. Eur J Cancer 1992; 28A:1647-50.
43. Frank M, Klose KJ, Wied M, Ishaque N, Schade-Brittinger C, Arnold R. Combination therapy with octreotide and alpha-interferon: Effect on tumor growth in metastatic endocrine gastroenteropancreatic tumors. Am J Gastroenterol 1999; 94:1381-87.
44. Sun W, Lipsitz S, Catalano P, Mailliard JA, Haller DG. Eastern Cooperative Oncology G. Phase II/III study of doxorubicin with fluorouracil compared with streptozocin with fluorouracil or dacarbazine in the treatment of advanced carcinoid tumors: Eastern Cooperative Oncology Group Study E1281. J Clin Oncol 2005;23:4897-904.
45. Mitry E, Baudin E, Ducreux M, et al. Treatment of poorly differentiated neuroendocrine tumours with etoposide and cisplatin. Br J Cancer 1999; 81:1351-55.
46. Yao JC. Neuroendocrine tumors. Molecular targeted therapy for carcinoid and islet-cell carcinoma. Best Pract Res Clin Endocrinol Metab 2007;21:163-72.
47. Yao JC, Shah MH, Ito T, et al. Everolimus for advanced pancreatic neuroendocrine tumors. N Engl J Med 2011;364: 514-23.
48. Raymond E, Dahan L, Raoul JL, et al. Sunitinib malate for the treatment of pancreatic neuroendocrine tumors. N Engl J Med 2011;364:501-13.
49. Yao JC, Phan A, Hoff PM, et al. Targeting vascular endothelial growth factor in advanced carcinoid tumor: A random assignment phase II study of depot octreotide with bevacizumab and pegylated interferon alpha-2b. J Clin Oncol 2008;26:1316-23.
50. Forrer F, Valkema R, Kwekkeboom DJ, de Jong M, Krenning EP. Neuroendocrine tumors. Peptide receptor radionuclide therapy. Best Pract Res Clin Endocrinol Metab 2007;21:111-29.
51. Lewis MA, Hobday TJ. Treatment of neuroendocrine tumor liver metastases. Int J Hepatol 2012:973-946.
52. Lehnert T. Liver transplantation for metastatic neuroendocrine carcinoma: An analysis of 103 patients. Transplantation 1998;66: 1307-12.

ABOUT THE AUTHORS

Surinder Singh Rana (Corresponding Author)

Assistant Professor, Department of Gastroenterology, Postgraduate Institute of Medical Education and Research, Sector-12, Chandigarh India, Phone: +91-172-2749123, Fax: +91-172-2744401 e-mail: drsurinderrana@yahoo.co.in

Vishal Sharma

Senior Resident, Department of Gastroenterology, Postgraduate Institute of Medical Education and Research, Chandigarh, India

Deepak Kumar Bhasin

Professor, Department of Gastroenterology, Postgraduate Institute of Medical Education and Research, Chandigarh, India

10.5005/jp-journals-10028-1057
REVIEW ARTICLE

^{90}Yttrium Microsphere Radioembolization for Liver Malignancies: A Technical Overview

Sandeep T Laroia

ABSTRACT

The incidence of the liver tumors is increasing worldwide; concurrently liver directed therapies are also evolving rapidly. Management of these complex disease processes involves a multidisciplinary approach, hence it is imperative to understand the underlying management principles thoroughly. This overview is intended to provide an easy, step by step approach to transcatheter brachytherapy, also known as radioembolization (RE). A brief overview of the anatomical issues, transcatheter technique and intraarterial RE will be provided.

Keywords: Liver malignancy, Transarterial brachytherapy, Radioembolization, ^{90}Yttrium, Liver directed therapy.

How to cite this article: Laroia ST. ^{90}Yttrium Microsphere Radioembolization for Liver Malignancies: A Technical Overview. J Postgrad Med Edu Res 2013;47(1):61-64.

Source of support: Nil

Conflict of interest: None declared

INTRODUCTION

Liver malignancies have been and continue to be a scourge of mankind. Hepatocellular carcinoma (HCC) is one of the most common forms of cancers. Overall incidence is more than a million cases every year. The worrisome thing is that incidence is increasing over the last decade.[1] The increasing incidence of hepatitis C, alcoholic and nonalcoholic liver disease all probably are contributing to the increasing incidence of this particular tumor. Liver involvement from secondary malignancies especially from gastrointestinal tract, breast cancer is also on the rise both in the developing and developed countries. In colorectal carcinoma, more than 60% of the patients will have liver dominant secondaries in the course of the disease. Similarly neuroendocrine tumors with hepatic secondaries have significant morbidity and mortality. HCC traditionally had few treatment choices, hence was one of areas of intense research for the alternate treatments. The curative options for HCC include surgical resection and liver transplantation. Unfortunately only a minority of patients (10-15%) are candidates for surgery.[2,4] For metastatic disease systemic chemotherapy is the standard of treatment. However, if standard first- and second-line treatments have failed, which happens in many patients, other therapies need to be considered. Presently, a whole gamut of these options is available.[3] The most common ones are enlisted below:

- Transcatheter arterial chemoembolization (TACE)
- Radiofrequency ablation (RFA)
- ^{90}Yttrium radioembolization (90YRE)
- Drug eluting microspheres (DEM), etc.

In this article, we will focus on radioembolization with particular emphasis on technical and clinical considerations.

Pathological and diagnostic considerations: Before we embark on the ^{90}YRE, it is important to briefly review the pertinent pathology and diagnostic characteristics of the liver malignancies:

HCC: These patients usually have cirrhosis of viral, alcoholic, nonalcoholic or uncertain cause. So in patients with cirrhosis, any hepatic mass should be considered a HCC unless proven otherwise. In appropriate clinical reference there is no need to biopsy these lesions,[5] as biopsy may lead to the seeding of the tract.[5] Alpha fetoprotein level of 400 nanogram/ml has aided the diagnosis. Based on the institutional expertize and facilities available, triple-phase computed tomography (CT) or magnetic resonance imaging (MRI) are the imaging modalities of choice.[6-8] Ultrasound, because of already altered echotexture of the liver may not be reliable. As many of these tumors are hypervascular, special attention is paid to the arterial phase and subsequent washout on both CT and MRI. Recently, liver imaging-reporting and data system (LI-RADS) of describing liver lesions has been advocated. This should be incorporated in the reporting systems to encourage standardization of the reporting of the liver masses. Another unique feature of HCC is arteriovenous shunting. If the disease is multifocal different masses may show different levels of arteriovenous shunting. This pathological feature has important implications as therapeutic particles can get shunted to the lungs and cause undesirable effects.[22] Portal vein thrombosis is another feature of the HCC. The thrombosis can be tumor or bland.

It is also relevant to briefly introduce the staging systems for the liver malignancies. Various systems have been proposed with Child-Pugh, MELD, Okuda, Cancer of Italian Liver Program, Barcelona Clinic Liver Program, etc.[9] Underlying principle is that as the liver involvement by the tumor becomes extensive, liver's synthetic and excretory functions get affected to a larger extent which gets reflected in various lab and clinical parameters.[10] In short bilirubin levels, ascites, presence of encephalopathy, etc. are taken into account. As the liver is responsible for synthesis of albumin and procoagulant proteins, their levels also are taken into consideration.

Patient's performance status and Karnofsky score are also taken into account. For ^{90}YRE, ideal patient will have following parameters:

- Tumor load less than 50%

- Normal bilirubin level
- Albumin level 3 gm/dl or greater
- No ascites
- Good functional status.

In clinical practice, patients may not be presenting early enough to fulfill all or any of these criteria. In such cases, different approaches can still be used which will be discussed in special situations section.

Metastatic Disease

Patients with metastatic disease have different pathological characteristics than HCC. They usually have better laboratory parameters; bilirubin may not be as deranged as in HCC, they are most likely to have completed first or second-line chemotherapy. So in these patients performance status is an important determinant of the suitability for liver directed therapy, other than liver dominant disease.[11] Also unlike HCC, whenever a liver mass is discovered in a patient with some primary tumor, it needs pathological confirmation. Positron emission tomography (PET) provides an excellent modality both for initial staging and post therapy follow-up in these cases. For ^{90}YRE, an ideal patient with liver metastasis will have following parameters:[20]

- ECOG performance status of 0 to 2.
- Karnofsky score of above 60%
- Liver dominant metastatic disease
- Hypervascular tumor.

Laboratory Evaluation

Many other laboratory tests having a role in liver directed therapy either for diagnostic, prognostic or follow-up purposes are:[12]

- INR
- Alpha fetoprotein
- Carcinoembryonic antigen
- Cancer antigen 19-9
- Serotonin/Chromogranin A
- Liver function profile including AST and ALT
- Complete blood count with differential
- LDH
- C-reactive protein.

Anatomical and Technical Considerations

It is imperative that a detailed and meticulous vascular anatomy examination be performed prior to actual delivery of ^{90}Y.[13] The following vessels should be checked invariably before therapy:

- Celiac axis
- Common hepatic artery
- Lobar hepatic arteries
- Gastroduodenal artery
- Superior mesenteric artery (SMA).

Aortogram may be added to this protocol to look for any other variant anatomy or additional supply to the liver.

The angiographic goal is to get the following information:

- To outline the normal and variant anatomy of the liver vascular bed.
- To do prophylactic embolization of nontarget vascular beds to prevent inadvertant delivery of the radiopharmaceutical to these areas.
- To plan whether lobar or segmental delivery is possible.
- To estimate the number of treatments based on the vascular.

Normal and common variants of the hepatic vascular supply:

The arterial supply to the liver broadly can follow one of these anatomies:

- Common hepatic artery from the celiac axis and dividing into right and left hepatic arteries.
- Common hepatic artery from the celiac axis and dividing into right left and middle hepatic arteries.
- Replaced common hepatic artery arising from SMA and following any of the above two branching pattern.
- Accessory hepatic artery arising from SMA.
- Left hepatic artery arising from the left gastric artery.

Things to remember are:

Accessory hepatic artery usually supplies segment 6 and 7.

Segment 4 can have either right or left or middle hepatic arteries supplying it.

Right hepatic artery in the presence of accessory hepatic artery usually supplies segment 5 and 8.

This vascular information gleaned from the angiogram is then correlated with the extent of disease seen on cross-sectional imaging.

Prophylactic Embolization

This concept is based on the fact that the ^{90}Y particles will cause irreversible damage to the gastrointestinal tract if it gets injected inadvertently to the gastrointestinal blood supply.

Resin spheres are more embolic compared to glass spheres, so resin spheres cause more pronounced slowing of normal antegrade blood flow to the liver. Hence, theoretically chances of reflux to nontarget visceral vessels is higher when resin sphere-based therapy is used, compared to the glass spheres during therapy. The threshold for embolizing GDA, right gastric artery, supraduodenal, retroduodenal, and accessory left gastric artery should be low, especially when the vehicle to deliver ^{90}Y is resin spheres. The clinical sequelae of prophylactic embolization of these vessels are insignificant in the carefully studied patient population. Recent development of flow directing devices, to protect nontarget vessels is also being studied; however cumulative experience in the use of these devices is not much.

Some groups have also advocated altering hepatic vascular anatomy to optimize treatment delivery, e.g. embolizing a small middle hepatic artery to increase blood flow to the diseased right or left lobes, however in the majority of cases, this is not warranted.

The basic principal of ^{90}YRE is to treat target vascular bed at 30 to 60 days interval. So in more common dichotomous branching of the common hepatic artery (into right and left hepatic arteries) this goal can be achieved in two treatment sessions. For each additional vascular bed an additional session is generally required.

Issues related to Pulmonary Shunting

After arterial anatomy is established, the next step is to calculate the pulmonary shunt fraction. This is done with the help of 99m-Tc macroaggregated albumin (MAA).[14] The logic is that, as the size of MAA closely mimics that of ^{90}Y spheres, so the distribution of MAA will closely mimic the distribution of the spheres.[15] The dose injected is usually 4 to 5 mCi. The imaging can be done with planar or SPECT gamma camera systems. The imaging should quickly follow the injection of MAA. Gastric mucosa and the salivary gland uptake should be looked carefully. Isolated gastric mucosa uptake indicates true gastrointestinal shunting.

As discussed earlier liver tumor, HCC in particular has varying degrees of arteriovenous shunting. In metastatic tumors, significant shunting is rare. There is important implication of this difference:

- In HCC, if the disease is multilobar, then each lobe must be injected with MAA, prior to the treatment session. So the lobar or segmental branch needs to be cannulated and lung shunt fraction is calculated. This increases the number of angiographic sessions. However observational studies have demonstrated this to be of little clinical importance and many institutions do only one MAA injection at the beginning. If significant shunting (more than 10%) is found in that study, then lobar administration of MAA is undertaken.
- In metastatic disease, the proper hepatic artery may be injected once to calculate the shunt fraction and ^{90}Y administration can follow in a sequential manner for each lobe involved.
- In cases of variant anatomy like accessory hepatic artery arising from SMA or left hepatic artery arising from left gastric artery, etc. fractionated injection of MAA is done.

The MAA injection also provides adjunctive information like extrahepatic gastrointestinal uptake. One should look carefully for this on the nuclear scan.

Types of ^{90}Y: ^{90}Y is available as either glass or resin spheres.[16,17] There are important differences among them which a practioner needs to know.

- Glass bead particle size is little smaller than the resin spheres: 20 to 30 micron *vs* 20 to 60 microns.
- Glass beads are less in number per vial than resin spheres: 1.2 to 8.0 million *vs* 40 to 80 million.
- Glass beads have more activity per sphere: 2500 Bq *vs* 50 Bq for resin spheres.
- Resin spheres are more embolic.
- Body excretion through urine is more of a concern with resin spheres.
- Both have half-life of 64.2 hours.
- Near complete decay (3% residual activity) is also the same, 13 days each.

Dose calculation: Glass bead dose is dependent upon the volume of the liver being infused; resin spheres dose depends on the percentage of the tumor load.

The lung dose is also calculated with the help of lung shunt fraction. Lungs tolerate ^{30}Gy in a single session and ^{50}Gy cumulative doses.

Treatment process: The patient should have undergone a planning diagnostic and prophylactic embolization as already discussed. The room needs to be prepared with suitable disposable flooring coverings in the event of inadvertent spill of ^{90}Y microspheres. Dose calibrator is used to measure the activity before and after the procedure and also to check for activity due to any spillover or leakage. The patient is prepared in the usual way and an initial angiogram obtained to select the spot where ^{90}Y will be injected. A 3 Fr system catheter is preferred for the delivery as 5 Fr system increases the chances of reflux; also the chances of vessel injury may be higher with deep placement of these catheters. Smaller catheter systems like 0.018 inch have too much resistance for adequate delivery. Infusion set is now carefully prepared as there are many connections. As resin spheres are more embolic than glass spheres, so chances of reflux are higher. The rate of infusion should be matched to the rate of arterial flow in the hepatic artery being injected. The estimation of dose administered at any particular point can be easily measured with the help of ionization chamber (minimum detection 1 mrem/h). In HCC patients who are usually cirrhotic and significantly hypervascular, a segmental approach is recommended.

Safety concerns: Once the dose administration is completed, all the catheters and tubings must be carefully disposed off. Special care should be taken for any backflow of blood through the catheters as it can cause the reflux of ^{90}Y. ^{90}Y is a beta-emitter so the main concern is exposure to the eyes, hands and skin. Hence, all personnel involved in the procedure must be checked for any contamination at the end of the procedure. Technically both the glass and the resin microspheres are sealed sources. However, since both are delivered in a liquid medium, all precautions for handling radiopharmaceuticals should be undertaken. The post administration exposure from the patient is within 4 to 12 mrem/h, which is within the acceptable range, so no special precautions are necessary. However, since resin spheres are excreted in the urine so during first 24 hours precautions are needed for urine disposal.[21]

Post-treatment care and follow-up: Major concerns are reflux of the microspheres through unrecognized

gastrointestinal channels.[18] As mucosa of the stomach and proximal duodenum are primarily involved, nonhealing ulcers can cause major morbidity and even mortality, we start antiulcer medications right after the procedure. Some authorities recommend use of steroids for postembolization fatigue. Noninfective fever usually responds to acetaminophen. Nausea, vomiting can happen which responds to conservative measures.[19]

The patient is seen within the next 2 to 3 weeks, mainly for the assessment of the functional status. Post-treatment liver function is checked at this time. A transient increase in liver enzymes and tumor markers may be seen at this time; however massive increase in the liver enzymes should be investigated further.

Further treatments: If the disease is confined to one lobe of the liver, above-mentioned protocol is followed. As the disease may be bilobar or the patient may have aberrant vascular anatomy, then more than one session of therapy may be required. Typically the second session is done 30 days after the first one. Before undertaking the second session, imaging of the liver tumor either with MR or PET must be undertaken.[20] For HCC, this scan may show shrinkage and necrosis of the tumor. For metastatic tumors, this scan is important as it may show either failure or progression of the disease. For this reason functional imaging like PET is important as it may show the spread of extrahepatic disease, thereby precluding any further liver treatments. A complete blood count may also be obtained at 30 days to look for any radiation-related cytopenias. On the other hand, any progression in the nontreated lobe of the liver is actually an indication for the treatment. Repeated treatment in the previously treated lobe or segment of the liver should be undertaken for definitely hypervascular tumors. In cases where multiple sessions of therapy are required, cumulative radiation dose to the lungs may become a limiting factor. A scrupulous log of radiation dose received by the patient should be maintained in all cases of radioembolization.

REFERENCES

1. American Cancer Society, Cancer Facts and Figures 2004. Atlanta: American Cancer Society 2004.
2. Llovet JM. Treatment of hepatocellular carcinoma. Curr Treat Options Gastroenterol 2004;7:431-41.
3. Messersmith W, Laheru D, Hidalgo M. Recent advances in the pharmacological treatment of colorectal cancer. Expert Opin Investig Drugs 2003;12:423-34.
4. Sasson AR, Sigurdson ER. Surgical treatment of liver metastases. Semin Oncol 2002;29:107-18.
5. Llovet JM, Vilana R, Bru C, et al. Increased risk of tumor seeding after percutaneous radiofrequency ablation for single hepatocellular carcinoma. Hepatology 2001;33:1124-29.
6. Kim TK, Jang HJ, Wilson SR. Imaging diagnosis of hepatocellular carcinoma with differentiation from other pathology. Clin Liver Dis 2005;9:253-79.
7. Lim JH, Choi D, Kim SH, et al. Detection of hepatocellular carcinoma: Value of adding delayed phase imaging to dual-phase helical CT. AJR Am J Roentgenol 2002;179:67-73.
8. Cortez-Pinto H, Camilo ME. Non-alcoholic fatty liver disease/non-alcoholic steatohepatitis (NAFLD/NASH): Diagnosis and clinical course. Best Pract Res Clin Gastroenterol 2004;18:1089-104.
9. Toyoda H, Kumada T, Kiriyama S, et al. Comparison of the usefulness of three staging systems for hepatocellular carcinoma (CLIP, BCLC and JIS) in Japan. Am J Gastroenterol 2005;100:1764-71.
10. Okuda K, Ohtsuki T, Obata H, et al. Natural history of hepatocellular carcinoma and prognosis in relation to treatment: Study of 850 patients. Cancer 1985;56:918-28.
11. Yu AS, Keeffe EB. Management of hepatocellular carcinoma. Rev Gastroenterol Disord 2003;3:8-24.
12. Hashimoto K, Ikeda Y, Korenaga D, et al. The impact of preoperative serum C-reactive protein on the prognosis of patients with hepatocellular carcinoma. Cancer 2005;103:1856-64.
13. Liu DM, Salem R, Bui JT, et al. Angiographic considerations in patients undergoing liver-directed therapy. J Vasc Interv Radiol 2005;16:911-35.
14. Mounajjed T, Salem R, Rhee TK, et al. Multi-institutional comparison of 99mTc-MAA lung shunt fraction for transcatheter Y-90 radioembolization. New Orleans, LA: Presented at the Annual Meeting of the Society of Interventional Radiology, 2005.
15. Hung JC, Redfern MG, Mahoney DW, et al. Evaluation of macroaggregated albumin particle sizes for use in pulmonary shunt patient studies. J Am Pharm Assoc (Wash) 2000;40:46-51.
16. Murthy R, Nunez R, Szklaruk J, et al. Yttrium-90 microsphere therapy for hepatic malignancy: Devices, indications, technical considerations and potential complications. Radiographics 2005;25 (suppl 1):S41-S55.
17. Sato K, Lewandowski RJ, Bui JT, et al. Treatment of unresectable primary and metastatic liver cancer with yttrium-90 microspheres (TheraSphere): Assessment of hepatic arterial embolization. Cardiovasc Intervent Radiol 2006;9:522-29.
18. Yip D, Allen R, Ashton C, et al. Radiation-induced ulceration of the stomach secondary to hepatic embolization with radioactive yttrium microspheres in the treatment of metastatic colon cancer. J Gastroenterol Hepatol 2004;19:347-49.
19. Goin JE, Dancey JE, Roberts CA, et al. Comparison of post-embolization syndrome in the treatment of patients with unresectable hepatocellular carcinoma: Trans-catheter arterial chemo-embolization versus yttrium-90 glass microspheres. World J Nucl Med 2004;3:49-56.
20. Kosmider S, Tan TH, Yip D, Dowling R, Lichtenstein M, Gibbs P. Radioembolization in combination with systemic chemotherapy as first-line therapy for liver metastases from colorectal cancer. J Vasc Interv Radiol 2011 Jun;22(6):780-86.
21. Gaba RC, Riaz A, Lewandowski RJ, Ibrahim SM, Ryu RK, Sato KT, et al. Safety of yttrium-90 microsphere radioembolization in patients with biliary obstruction. J Vasc Interv Radiol 2010 Aug;21(8):1213-18.
22. Chen JH, Chai JW, Huang CL, et al. Proximal arterio portal shunting associated with hepatocellular carcinoma: Features revealed by dynamic helical CT. AJR 1999;172:403-07.

ABOUT THE AUTHOR

Sandeep T Laroia

Assistant Professor, Department of Radiology, University of Iowa Hospitals and Clinic, Iowa, USA, e-mail: sandeep-laroia@uiowa.edu

10.5005/jp-journals-10028-1058
REVIEW ARTICLE

Dosimetry in Targeted Radionuclide Therapy: The Bad Berka Dose Protocol—Practical Experience

Christiane Schuchardt, Harshad Kulkarni, Carolin Zachert, Richard P Baum

ABSTRACT

Aim: Calculating the absorbed dose is important for the determination of risk and therapeutic benefit of internal radiation therapy. Optimal dose estimations require time-consuming and sophisticated methods, which are difficult due to practical reasons. To make dosimetry available for each of the patients, we developed a specific dosimetry procedure used in daily clinical routine.

Materials and methods: Dosimetry has been performed according to the MIRD scheme and adapted to the special conditions at our department (which we have called as the Bad Berka Dose protocol, BBDP): Conjugated planar whole-body scintigraphies at 0.5, 3, 24, 48 and 72 hours postinjection are analyzed by regions of interest with 'HERMES WHOLE-BODY DISPLAY™ and the time-dependent organ and tumor activities are determined with Microsoft EXCEL™. The cumulated activity is calculated using the software ORIGIN PRO 8.1G™ and a mono- or biexponential fit of the time-activity curves. Mean absorbed doses are finally estimated using the software OLINDA EXM™.

Results: We found a compromise between the calculation model and practical conditions. It has ensured dose estimation in daily clinical routine with a reasonable effort and within acceptable time. In consequence, the dosimetry method developed for Bad Berka allows each of our patients to undergo dosimetry after therapy using Lu-177-labeled peptides (peptide receptor radionuclide therapy). Additionally, this approach can be used for any internal radiotherapy using a gamma-emitting radionuclide.

Conclusion: The BBDP is a practicable dosimetric approach, which can be used in daily clinical routine. It not only helps in identifying patients who would benefit most from the treatment, but also those with unfavorable dosimetry. Additionally, the analysis of dosimetric data from peptide receptor radionuclide therapy (PRRNT) could help in predicting possible toxicity.

Keywords: Dosimetry, Peptide receptor radionuclide therapy, DOTATATE, DOTATOC.

How to cite this article: Schuchardt C, Kulkarni H, Zachert C, Baum RP. Dosimetry in Targeted Radionuclide Therapy: The Bad Berka Dose Protocol—Practical Experience. J Postgrad Med Edu Res 2013;47(1):65-73.

Source of support: Nil

Conflict of interest: None declared

INTRODUCTION

Currently, various radiolabeled therapeutic agents are used against different forms of cancer. The challenge of internal targeted radionuclide therapies is to deliver the highest possible dose to the tumor while sparing normal organs from damage. For the determination of the risk and therapeutic benefit of such internal therapies, patient-specific dosimetry is an essential prerequisite.

Dosimetry represents meanwhile a precious guide for the selection of radionuclides and peptides as well as for therapy optimization. There exist various methods to estimate internal doses and recent studies promise new perspectives to come.[1] Furthermore, a recent publication presents guidelines regarding optimal practice of internal dosimetry which would also enable researchers to use the information for possible improvements to the approach.[2]

Dose estimations could be based on either two-dimensional (2D) planar gamma camera imaging or three-dimensional (3D) imaging using SPECT/CT or positron emission tomography/computed tomography (PET/CT).[3,4] The 3D techniques to enable the absorbed dose calculation are however not routinely available. In fact, the MIRD scheme provides a more conventional method for calculating absorbed doses of radionuclides.[5] The optimal dose estimation requires time-consuming and sophisticated methods, including pharmacokinetic biodistribution as well as washout studies using the same radionuclide as is used for therapy. This may be difficult owing to practical (e.g. the patients' status) and physical reasons.

Due to encouraging clinical results, peptide receptor radionuclide therapy (PRRNT) with radiolabeled somatostatin analogs (SSTA) is now established as a treatment modality in gastroenteropancreatic (GEP) neuroendocrine tumors (NETs) and therefore one of the most frequently used targeted radiotherapies. Because of an increasing number of PRRNTs, we aimed to make dosimetry available for most of the patients and developed a specific dosimetry procedure. The Bad Berka Dose protocol (BBDP) is based on planar whole-body scintigraphies and used in our daily clinical routine. The estimated mean absorbed doses to organs and tumor lesions obtained from these dosimetric calculations can be used to evaluate therapy response as well as possible adverse effects.

Bad Berka Dose Protocol

The dose estimation requires an accurate determination of the time-dependent activity of the source regions. Thus, most important is the correct evaluation of the distribution and

the kinetics of the administered radiopharmaceutical.[6,7] For dose estimations we developed a convenient procedure which is based on the MIRD scheme, using the OLINDAEXM^{TM} software by adapting the calculation model to our special conditions. The main objective was to establish a method which is practicable in our daily clinical routine for a huge number of patients.[8,9] Flow Chart 1 show the BBDP.

The following camera parameters were used for planar whole-body imaging: MEDISO spirit DH-V dual-headed gamma camera (Medical Imaging Systems, Budapest, Hungary), MeGP collimator, 15% energy window, peak at 208 keV, scan speed 15 cm/min. Whole-body scintigraphies were acquired at 5 time points postinjection: 0.5 hours (immediately after administration of therapeutic activity) followed by 3, 20, 44 and 68 hours postinjection.

The dose estimation consists of four main steps:

1. *ROI analysis*: Manual drawing of regions of interest (ROI) using the HERMES^{TM} whole-body display (Hermes Medical Solutions, Stockholm, Sweden).
2. *Determination of activity*: Analysis of ROI statistics using Excel sheet.
3. *Fit*: Fit of the time-activity graph using ORIGIN PRO 8.1G^{TM}.
4. Dose estimation using OLINDAEXM 1.1^{TM}.

The organs showing tumor involvement or overlaying with other source regions were excluded from dosimetric evaluation. For this reason, normal liver was not included in the analysis in this study because nearly all patients had extensive liver metastases. Some patients had liver lesions superimposing on the right kidney, allowing only analysis of the left kidney. In these cases, it was assumed that the mean absorbed dose would be identical for both kidneys (which were also checked and confirmed by prior ^{99m}Tc MAG3 scintigraphy proving that there was no significant difference in the differential renal function). Also, kinetics and mean absorbed dose to the spleen were not estimated in several patients, who had undergone splenectomy.

To estimate the mean absorbed dose to red marrow (RM), blood sampling was performed. After the administration of the therapeutic dose, venous blood samples were obtained at different time points postinjection. The radioactivity in 0.5 ml blood samples was measured using a high-purity germanium detector and the activity in MBq/ml was plotted against time. Depending on the degree of correlation, the curves were fitted to bi- or triexponential functions to determine the cumulated activity in blood. Assuming that there was no specific uptake in the blood cells, a uniform distribution in the blood, and that clearance from RM was equal to that from the blood, the mean absorbed dose to RM was estimated by using the S-values from the software OLINDA EXM^{TM}.[10,11]

All data as well as dosimetric parameters and results were documented. The database also contains additional data (e.g. concerning pretherapy examinations) which facilitates comprehensive individual and/or interindividual analysis.

A possible drawback of the BBDP may be that it is based only on 2D planar imaging. It is known, that there are intrinsic limitations of these 2D approaches, especially regarding attenuation and scatter correction as well as background and organ overlay.[12] Sandstöm et al analyzed the feasibility and reliability of individualized dosimetry based on SPECT/CT in comparison with conventional planar imaging in patients treated with ^{177}Lu DOTATOC. Their results showed that planar and SPECT doses were comparable in areas free of tumors, but that planar dosimetry overestimated the absorbed dose in tumor lesions.[13] Furthermore, Garkavij et al compared three different quantification methods to evaluate the absorbed dose to the kidneys. They found that patients evaluated according to the conventional planar-based dosimetry may have been undertreated when compared to the evaluation according to other methods using SPECT/CT, because the mean absorbed dose to the kidneys was overestimated.[14] Even though the kidney dose is overestimated with planar imaging, it is definitely better to be on the safer side than to underestimate and overtreat. In conclusion, in spite of the availability of more accurate methods for dose estimation, planar imaging continues to be the most feasible option.

Dosimetry in Peptide Receptor Radionuclide Therapy

Most frequently applied targeted radiotherapy at our department is PRRNT using ^{177}Lu- or ^{90}Y-labeled SSTA. Because the nuclide ^{177}Lu, in contrast to ^{90}Y, is not a pure β-emitter and has also a certain amount of gamma emission, it can be directly used for imaging and dosimetry during the therapy cycle. Therefore, the BBDP is mainly used for patients receiving ^{177}Lu-labeled peptides for therapy.

Since, different subtype receptor affinity profiles of the various SSTA result in different uptake and kinetics in normal tissues and tumors, we compared dosimetric parameters in PRRNT using DOTATATE, DOTATOC and DOTANOC.

To describe differences between the various radiolabeled peptides, the following parameters were chosen: Uptake at 20 hours postinjection (maximum uptake for tumor lesions), effective half-life and mean absorbed dose. To describe differences among the peptides, nonparametric tests were

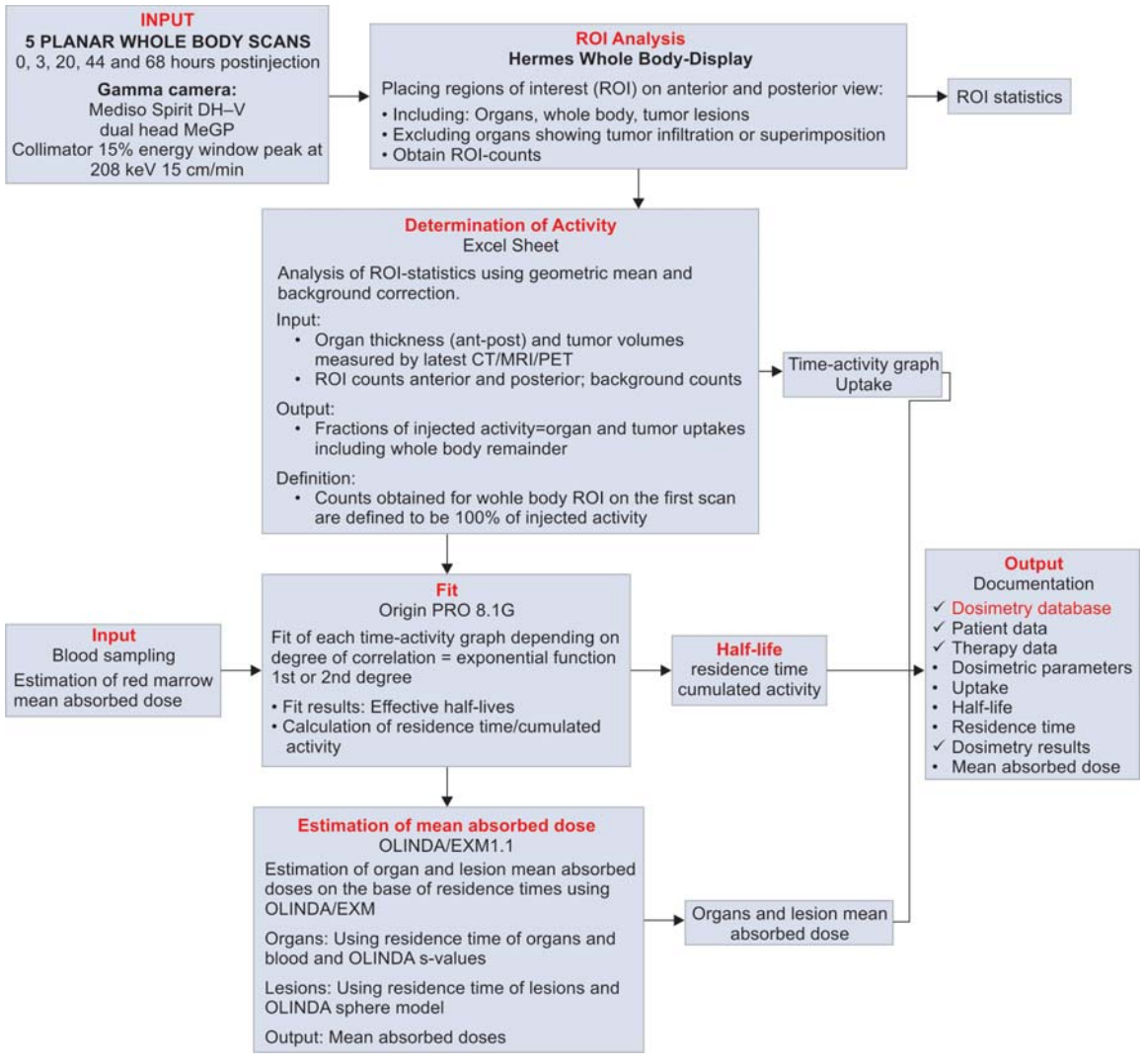

Flow Chart 1: Bad Berka dose protocol

used. All statistical tests were performed on ORIGINPRO 8.1 G™; p-values ≤ 0.05 were considered to be significant.

All patients enrolled in studies concerning PRRNT were suffering from metastatic NETs with liver, lymph node, bone or other organ involvement. Intense somatostatin receptor expression of (inoperable) primary tumors and metastases had been verified before therapy by using ^{68}Ga DOTANOC, DOTATOC or DOTATATE PET/CT. Before PRRNT, each patient was extensively informed about the therapeutic procedure and possible adverse effects. All patients provided written informed consent to undergo treatment and follow-up. The studies were approved by the local Ethics Committee and performed in accordance with German regulations concerning radiation safety.

Dosimetry in Peptide Receptor Radionuclide Therapy using ^{177}Lu-DOTATATE, DOTATOC and DOTANOC

The dosimetric parameters from 253 patients, treated with 1 to 6 cycles of ^{177}Lu-labeled DOTATATE, DOTANOC or DOTATOC were compared. Differences with respect to kinetics, biodistribution and mean absorbed dose, between the three different peptides were analyzed on the basis of dosimetric data obtained in this group.

For normal organs (whole-body, kidneys, spleen), DOTATOC shows the lowest and DOTANOC, the highest uptake. The mean absorbed organ doses and half-lives were observed to be the lowest for DOTATOC. In contrast, the highest uptake in tumor lesions was found for DOTATATE and the lowest, for DOTANOC. The resulting mean absorbed lesion doses were the highest for DOTATATE, followed by DOTATOC and DOTANOC. DOTATOC was found to have the best tumor to kidney ratio compared to DOTATATE and DOTANOC, apart from the lowest absolute mean absorbed renal dose.

Dosimetry in Peptide Receptor Radionuclide Therapy using ^{177}Lu-DOTATATE and DOTATOC in the Same Patient

For intraindividual comparison, 25 patients who received PRRNT, first using ^{177}Lu-DOTATATE, and in a following

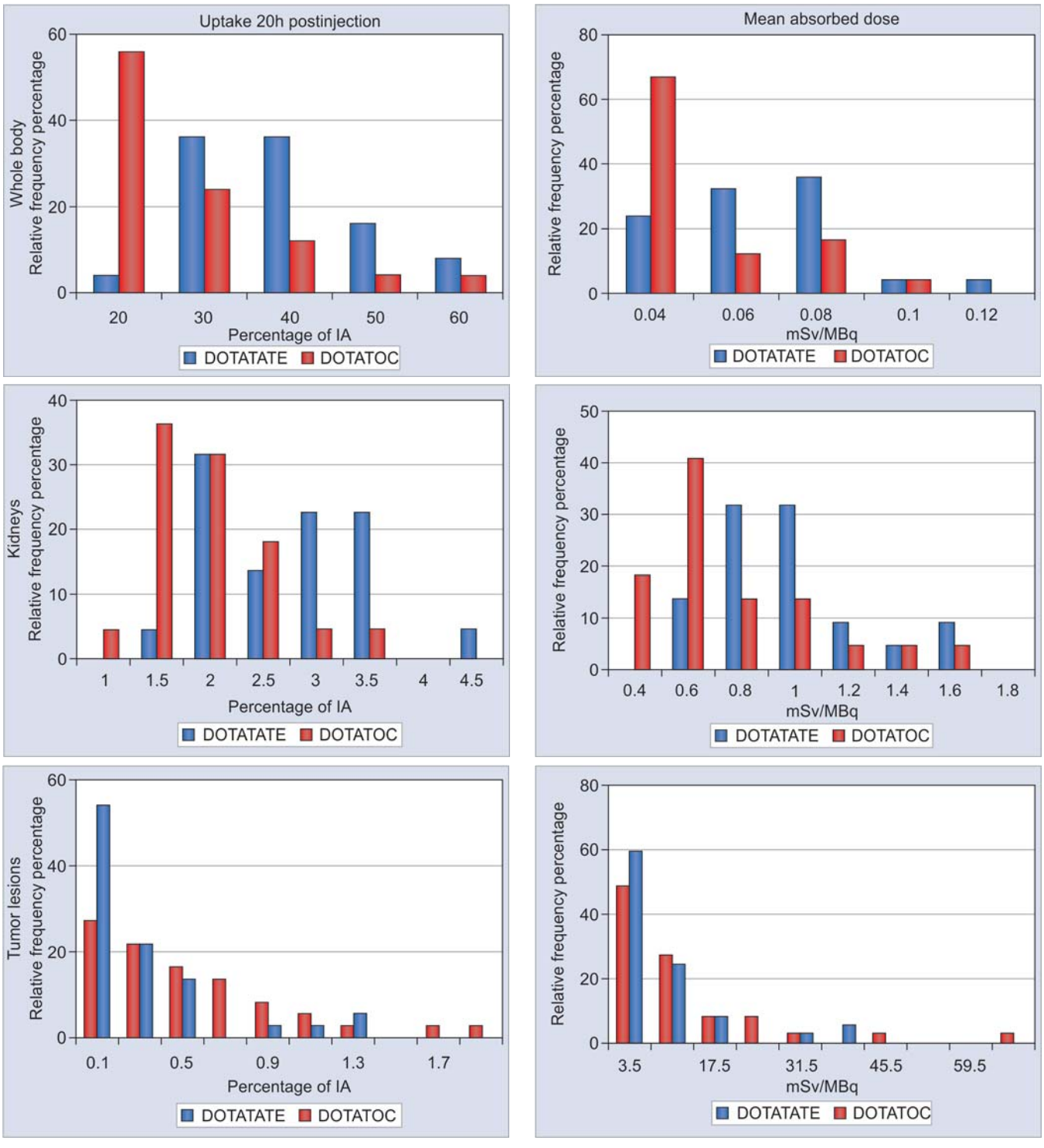

Graph 1: Comparison of ^{177}Lu DOTATATE and ^{177}Lu DOTATOC for uptake at 20 hours postinjection and mean absorbed dose in whole body, kidneys and tumor lesions in the same patient

cycle using ^{177}Lu-DOTATOC, were included in a study to compare kinetics and mean absorbed doses of the two peptides. The mean time between these therapy courses was 18 months. In case a patient underwent more than one cycle with each peptide, two consecutive cycles were chosen for dosimetric analyses. Graph 1 shows comparative dosimetric results for uptake at 20 hours postinjection and mean absorbed dose.

A higher whole-body uptake at 20 hours postinjection was found for DOTATATE as compared to DOTATOC in 24 out of the 25 patients (96%). The first effective half-life was longer for DOTATOC in 22 patients (88%), whereas for DOTATATE the second effective half-life was longer in 17/25 (68%) patients. In 22 patients (88%), whole-body dose was slightly but statistically significantly higher when using DOTATATE as compared to DOTATOC.

Renal dosimetric parameters (uptake, residence time and mean absorbed renal dose) were significantly higher for DOTATATE in 19 of 22 patients (86%). The effective half-life was found to be similar for both peptides.

A higher uptake of DOTATATE at 20 hours postinjection was observed in 85% of the analyzed tumor lesions and 50% had a longer effective half-life of DOTATATE. The mean absorbed dose to the lesions was higher for DOTATATE in 65% of the lesions. These differences were statistically significant for uptake and mean absorbed dose, but not significant concerning the effective half-life.

Serial Dosimetry

Graph 2 shows dosimetric results in 17 patients, which received three or four cycles of ^{177}Lu-DOTATATE or ^{177}Lu-DOTATOC. The administered activity was 3 to 8 GBq ^{177}Lu- DOTATATE or DOTATOC per cycle. 12/17 patients received 3 cycles of ^{177}Lu-DOTATATE, 3/17 patients were treated using three cycles of ^{177}Lu-DOTATOC and 2/17 patients underwent therapy using four cycles of ^{177}LU DOTATATE.

The mean absorbed renal doses showed a wide range. A low variation was found for the effective half-life, whereas the uptake and mean absorbed dose showed higher

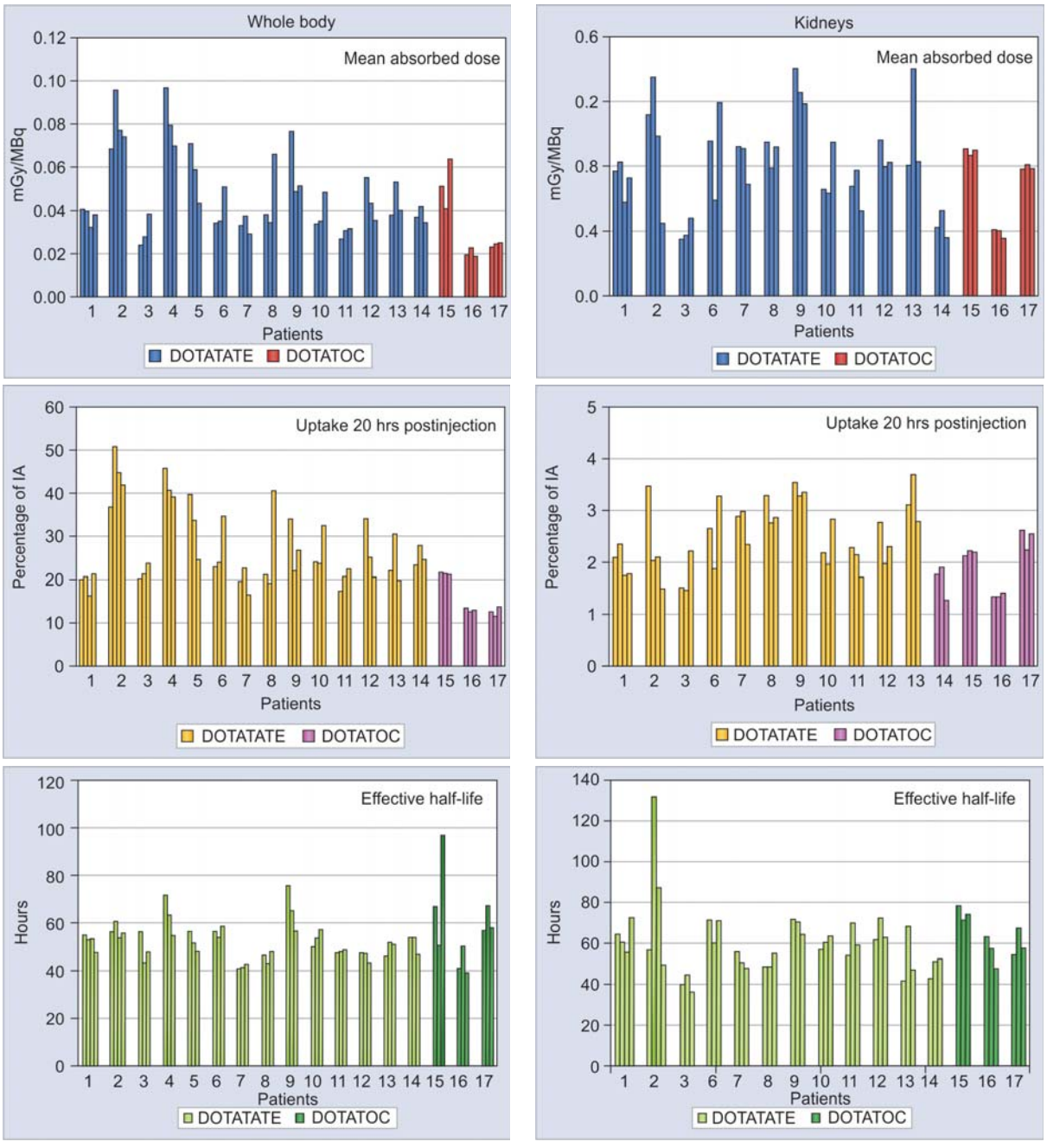

Graph 2: Serial dosimetry results for whole body and kidneys in 17 patients receiving 3 to 4 cycles of ^{177}Lu-DOTATATE and ^{177}Lu-DOTATOC. The mean absorbed dose, uptake at 20 hours postinjection and effective half-life are given in mGy/MBq, IA% and hours respectively

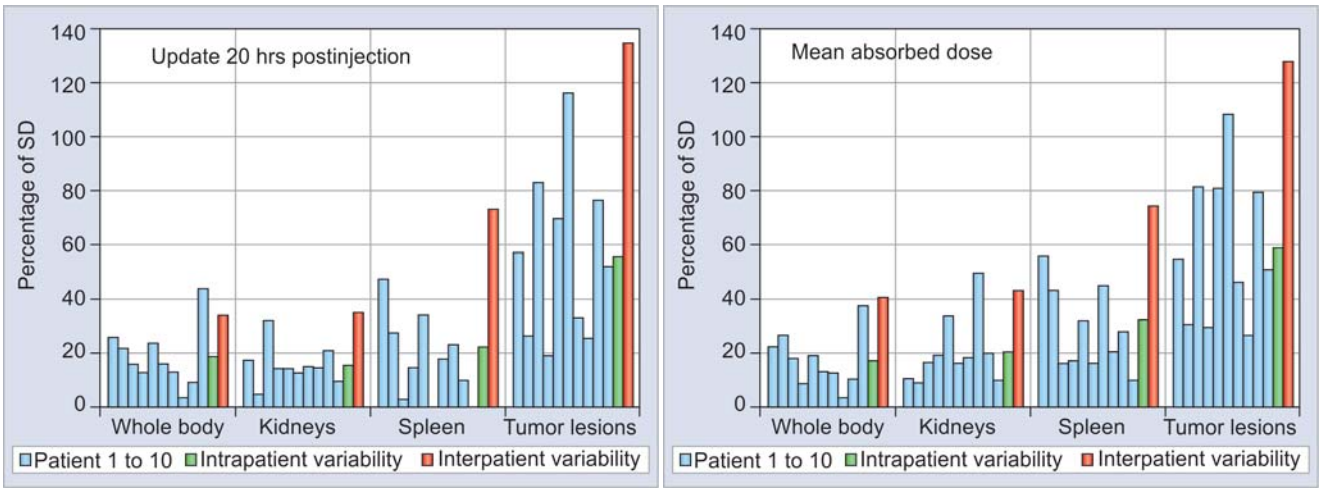

Graph 3: Intraindividual variability (10 patients) and interindividual variability (173 patients) for uptake at 20 hours postinjection and mean absorbed dose represented as percentage of SD (standard deviation)

differences between therapy cycles. Some of the dosimetric results of whole-body showed ascending or descending order in serial cycles, but for most of the dose parameters no systematic pattern was found in consecutive therapy courses.

A lower variation was found for ^{177}Lu-DOTATOC in the effective half-life, uptake at 20 hours postinjection and mean absorbed dose to whole-body and kidneys values as compared to ^{177}Lu-DOTATATE.

Variability

A high interpatient variability was found for all dosimetric results. This is not unexpected since it was a heterogeneous group of patients having varying receptor densities and tumor burden. In addition, the results showed a high intrapatient variability in the undergoing several cycles of therapy with different peptides.

Graph 3 shows both intra- and interindividual variability for uptake and mean absorbed dose: The variation is given in percent of the standard deviation (%SD = SD/mean value). The intraindividual variation was determined using dosimetric parameters from 10 patients which received three therapy cycles of ^{177}Lu-DOTATATE. Based on dosimetric analysis in 173 patients treated with ^{177}Lu-DOTATATE, the interindividual variation was determined. The lowest variation was seen for whole-body and kidneys, whereas tumor lesions showed the highest variability. The interpatient variability was higher than the intrapatient variability.

Graph 4 shows dosimetric results in one patient, who received six cycles of therapy using three different peptides. The highest whole-body uptake was observed during the first therapy when using DOTANOC, while the highest renal uptake was found at third therapy. For the liver lesions, maximum uptake was observed during the first two therapies. DOTATOC demonstrated the lowest whole-body uptake. Also noticeable were the differences in the initial renal uptake, similar effects being seen for liver lesions and the spleen. There was no systematic pattern of uptake or mean absorbed dose in consecutive therapies. Also in other patients who received more than one cycle of therapy using ^{177}Lu-DOTATATE, kinetics was variable and no specific order for consecutive therapies was found. Consequently, the dosimetric calculations in one cycle of PRRNT should not be used to predict doses during following cycles, even if the same peptide is used.

Although the variability may be attributed to the difference in biological behavior of the peptides, the fact that there might also have been an influence of previous radiopeptide therapies or other treatment modalities, must be taken into account. The possible effects of the previous treatments on the outcome of PRRNT (e.g. effect on the tumor radiosensitivity) are well known in literature.

Conclusion

BBDP in peptide receptor radionuclide therapy: From the studies concerning comparison of dosimetric results in PRRNT using ^{177}Lu-labeled peptides DOTATATE, DOTANOC and DOTATOC, the following conclusions could be drawn:

- The *in vitro* higher affinity of DOTANOC correlates with the *in vivo* higher uptake for whole-body and normal tissue, which results in a higher whole-body dose. Therefore, this peptide is not ideal for PRRNT.
- Concerning kidney uptake and mean absorbed dose to normal organs and whole-body, DOTATOC revealed the highest tumor-to-kidney ratio and is very appropriate for PRRNT.

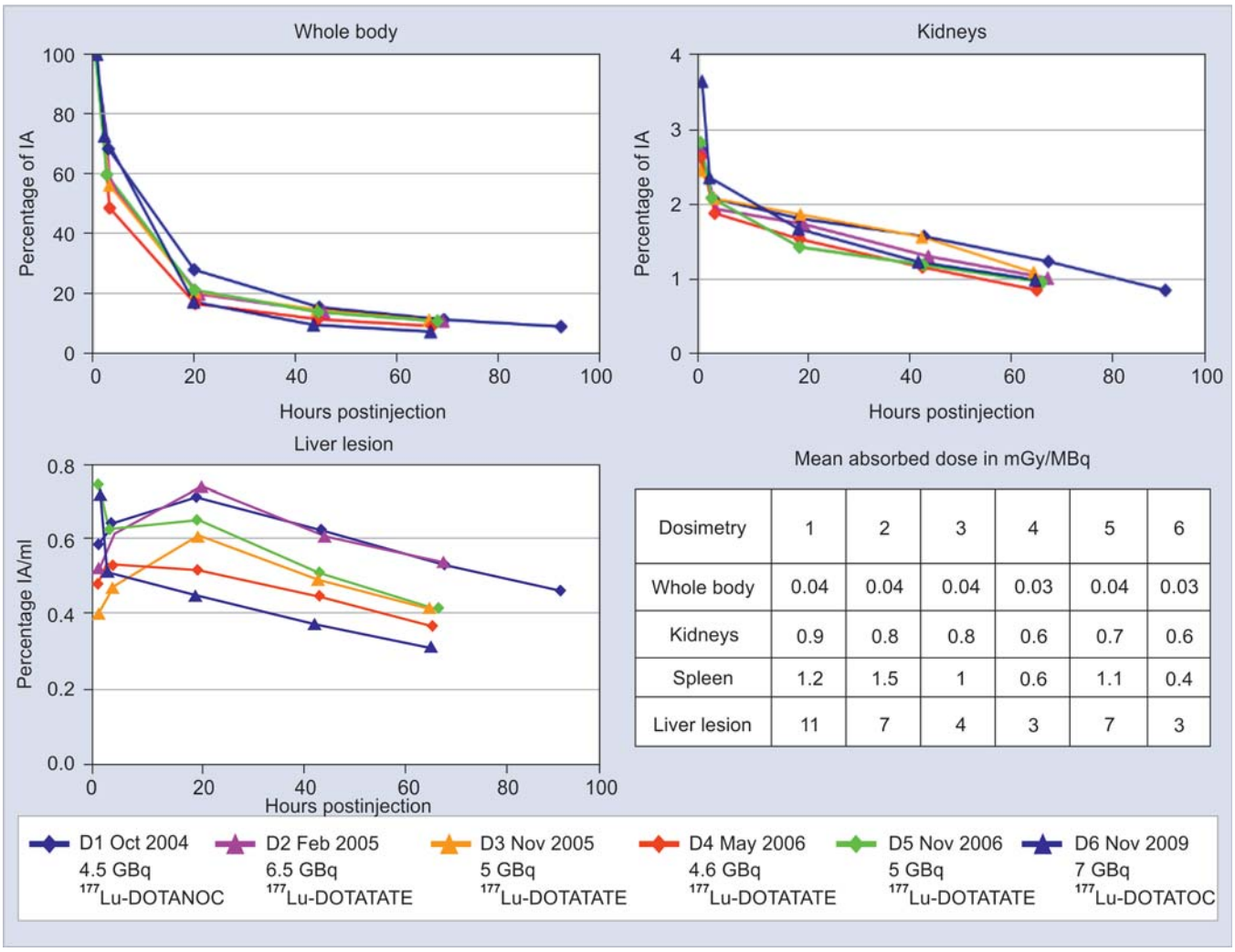

Dosimetry	1	2	3	4	5	6
Whole body	0.04	0.04	0.04	0.03	0.04	0.03
Kidneys	0.9	0.8	0.8	0.6	0.7	0.6
Spleen	1.2	1.5	1	0.6	1.1	0.4
Liver lesion	11	7	4	3	7	3

Graph 4: Dosimetric results in 6 cycles of PRRNT in one patient using three different peptides

- DOTATATE was shown to deliver the highest tumor dose (due to the longer residence time in the malignant lesions) and is also very suitable.

Additionally, the finding of large variability should be addressed in further studies. It is recommended that median values of absorbed doses among patients should not be the only criteria to plan PRRNT. The interindividual differences, particularly organ functionality, metabolism or receptor density in organs and tumor lesions, must be taken into account.

The studies demonstrate further, that the calculation of mean absorbed doses to critical organs and tumor lesions should be considered for estimation of possible toxicity from PRRNT. In conclusion, individual dosimetry in PRRNT is essential for optimal PRRNT.

More Possibilities for the use of the BBDP

In addition, the BBDP can be used to estimate dosimetric parameters of other radiopharmaceuticals used for internal radiotherapy.

^{177}Lu-BPAMD ((4-{[bis-(phosphonomethyl)) carbamoyl] methyl}-7, 10-bis (carboxymethyl)-1, 4, 7, 10-tetraazacyclo-dodec-1-yl acetic acid) is a promising new treatment option for skeletal metastases in prostate cancer. We used the BBDP to determine organ and tumor kinetics and to estimate the mean absorbed dose to normal organs and tumor lesions.

Graph 5 shows the time-activity graphs for the whole-body and the kidneys, and blood kinetics are shown in Graph 6. A fast clearance of ^{177}Lu-BPAMD from whole-body, normal organs as well as from blood was found. In contrary, skeletal lesions showed a very long retention / half-life of the radiopharmaceutical.

We concluded therefore, that ^{177}Lu-BPAMD has optimal characteristics for radionuclide therapy of osteoblastic bone metastases in prostate cancer.

CONCLUSION

We found a compromise between the calculation model and practical conditions by adapting the MIRD scheme to the

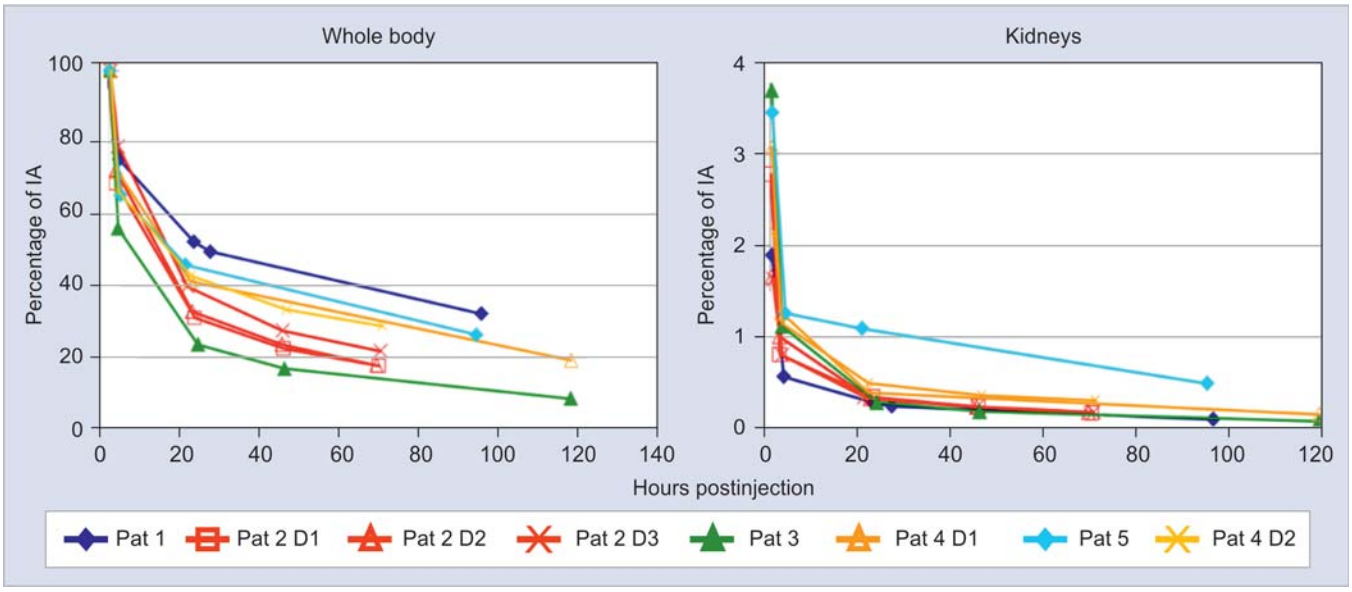

Graph 5: ^{177}Lu-BPAMD kinetics (P—patient; D—dosimetry) in five patients receiving 1 to 3 cycles of therapy

special conditions at our department. Although it is known that the quantification of the activity in different organs from planar data is hampered by inaccurate attenuation and scatter correction as well as because of background and organ overlay, the BBDP procedure is very practical approach. We showed that the dosimetric evaluation using the BBDP:

- Helps in identifying SSTA, which are preferable for PRRNT with Lu-labeled peptides.
- Helps to explain possible toxicity, e.g. renal, as the kidneys are dose limiting organs.
- Plays an important role in understanding therapy response and benefit.

The BBDP has ensured dose estimation in daily clinical routine with a reasonable effort and within acceptable time. In consequence, this approach allows each of our patients to undergo dosimetry after therapy using ^{177}Lu-labeled peptides.

Since, advanced methods for dose estimations based on 3D imaging using SPECT/CT and appropriate software are not routinely available, the BBDP remains an alternative solution for internal dose estimation.

Additionally, the BBDP can be used for any internal radiotherapy using a gamma-emitting radionuclide.

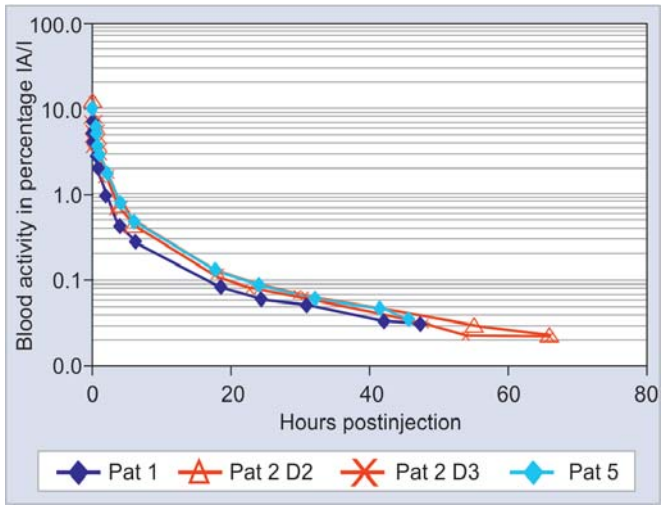

Graph 6: Blood kinetics of ^{177}Lu-BPAMD (P—patient; D—dosimetry)

REFERENCES

1. Cremonesi M, Ferrari M, Di Dia A, Botta F, De Cicco C, Bodei L, et al. Recent issues on dosimetry and radiobiology for peptide receptor radionuclide therapy. Q J Nucl Med Mol Imag 2011;55(2):155-67.
2. Lassmann M, Chiesa C, Flux G, Bardiès M. EANM Dosimetry Committee guidance document: Good practice of clinical dosimetry reporting. Eur J Nucl Med Mol Imag 2011;38: 192-200.
3. Sgouros G, Frey E, Wahl R, Bin H, Prideaux A, Hobbs R. 3-D imaging based, radiobiological dosimetry. Semin Nucl Med 2008;5:321-34.
4. Sandström M, Garske U, Granberg D, Sundin A, Lundqvist H. Individualized dosimetry in patients undergoing therapy with ^{177}Lu-DOTA-D-Phe1-Tyr3-octreotate. Eur J Nucl Med Mol Imaging 2010;37:212-25.
5. Siegel JA, Thomas SR, Stubbs JB. MIRD Pamphlet 16: Techniques for quantitative radiopharmaceutical biodistribution data acquisition and analysis for use in human radiation dose estimates. J Nucl Med 1999;40:37S-61S.
6. Sgouros G. Dosimetry of internal emitters. J Nucl Med 2005;46:18S-27S.
7. Stabin MG, Siegel JA. Physical models and dose factors for use in internal dose assessment. Health Phys 2003;85(3):294-310.

8. Wehrmann C, Senftleben S, Zachert C, Mueller D, Baum RP. Results of individual patient dosimetry in peptide receptor radionuclide therapy with ^{177}Lu DOTA-TATE and ^{177}Lu DOTANOC. Cancer Biother Radiopharm 2007;22(3):406-16.
9. Stabin MG, Sparks RP, Crowe E. OLINDA/EXM: The second-generation personal computer software for internal dose assessment in nuclear medicine. J Nucl Med 2005;46:1023-27.
10. Wessels BW, Bolch WE, Bouchet LG, et al. Bone marrow dosimetry using blood-based models for radiolabeled antibody therapy: A multi-institutional comparison. J Nucl Med 2004;45:1725-33.
11. Sgouros G. Bone marrow dosimetry for radioimmunotherapy: Theoretical considerations. J Nucl Med 1993;34:669.
12. Bardies M, Buvat I. Dosimetry in nuclear medicine therapy: What are the specifics in image quantification for dosimetry? Q J Nucl Med Mol Imag 2011;55(1):5-20.
13. Sandström M, Garske U, Granberg D, Sundin A, Lundqvist H. Individualized dosimetry in patients undergoing therapy with ^{177}Lu-DOTA-D-Phe1-Tyr3-octreotate. Eur J Nucl Med Mol Imag 2010;37:212-25.
14. Garkavij M, Nickel M, Sjögreen-Gleisner K, Ljungberg M, et al. ^{177}Lu-[DOTA0,Tyr3] Octreotate therapy in patients with disseminated neuroendocrine tumors: Analysis of dosimetry with impact on future therapeutic strategy. Cancer 2010;116(4 Suppl):1084-92.

ABOUT THE AUTHORS

Christiane Schuchardt

Medical Physicists, THERANOSTICS Center for Molecular Radiotherapy and Molecular Imaging, ENETS Center of Excellence, Zentralklinik Bad Berka, Germany

Harshad Kulkarni

Resident Physician, THERANOSTICS Center for Molecular Radiotherapy and Molecular Imaging, ENETS Center of Excellence Zentralklinik Bad Berka, Germany

Carolin Zachert

Senior Physician, THERANOSTICS Center for Molecular Radiotherapy and Molecular Imaging, ENETS Center of Excellence Zentralklinik Bad Berka, Germany

Richard P Baum (Corresponding Author)

Chairman and Clinical Director, THERANOSTICS Center for Molecular Radiotherapy and Molecular Imaging, ENETS Center of Excellence Zentralklinik Bad Berka, 99437, Bad Berka, Germany, Phone: +49-364 585-2200, Fax: +49-364-585-3515, e-mail: richard.baum@zentralklinik.de, www.zentralklinik-bad-berka.de

10.5005/jp-journals-10028-1059
COMMENTARY

Ga-68: A Versatile PET Imaging Radionuclide

Jaya Shukla, BR Mittal

ABSTRACT

Gallium-68, a positron emitter, is available via ^{68}Ge/^{68}Ga generators. The simple chemistry and easy availability has increased its application from the clinical diagnosis to personalized therapy and has lot more potential in future.

Keywords: ^{68}Ge/^{68}Ga generator, Cyclotron, Bifunctional chelators, Nanoparticles.

How to cite this article: Shukla J, Mittal BR. Ga-68: A Versatile PET Imaging Radionuclide. J Postgrad Med Edu Res 2013;47(1):74-76.

Source of support: Nil

Conflict of interest: None declared

INTRODUCTION

The availability of ^{68}Ga as a positron emission tomography (PET) radionuclide for imaging dates back to early 60's at a time when neither PET nor fluorine-18 (F-18) was established. With the emergence of cyclotron and automated chemistry modules, F-18 radiopharmaceuticals established their empire in nuclear medicine. The resurgence of ^{68}Ge/^{68}Ga generator was due to the consistent efforts by radiochemists from Czechoslovakia and Russia in 20th century.[1,2] The modern ^{68}Ge/^{68}Ga generators have proved to be a milestone for noninvasive state-of-art PET/CT imaging. After that there was no looking back for Ga-68 imaging.

The advantages of ^{68}Ga over other PET-based radionuclides are its availability from an in-house generator independent of an onsite cyclotron. The half-life of Ga-68 is 68 minutes. Eighty-nine percent of Ga-68 decays by emitting positron of 1.92 MeV and the rest 11% by electron capture. The parent ^{68}Ge is produced in accelerator by (p, 2n) reaction on Ga_2O_3 target. ^{68}Ge decays with a half-life of 270.8 days by electron capture which enable long shelf life to generator (>6 months) and reduces the unit-dose cost. Due to short half life, Ga-68 can be eluted 2 to 3 times a day (after 3-5 hours) as per the requirement/patients number.

^{68}Ge/^{68}Ga GENERATOR SYSTEM

In ^{68}Ge/^{68}Ga generator system, ^{68}Ge is strongly adsorbed on different solid supports such as, metal oxides (Al_2O_3, TiO_2 or SnO_2), organic (pyrogallol-formaldehyde resins) and inorganic supports (silica based).[3-6] The Ga-68 from currently available ^{68}Ge/^{68}Ga generators is eluted with dilute hydrochloric acid as a cationic $^{68}Ga^{3+}$. Initially the long processing was required to remove metallic impurities of solid support and Ge-68 breakthrough from Ga-68 elute. With the development of nonmetallic silica-based column, the processing step for the elution of Ga-68 was eliminated. Silica has high binding affinity for Ge which reduces the Ge-68 breakthrough to negligible level.

APPLICATION OF $^{68}Ga^{3+}$

Gallium acts as an iron analog and binds to transferrin and lactoferrin. The complex diffuses through loose endothelial junctions of capillaries at the sites of inflammation and enters the extracellular fluid. Leukocytes also migrate to sites of inflammation, degranulate and release large quantities of lactoferrin. Ga attaches to siderophores of bacteria and therefore can be used in leukopenic patients with bacterial infection and also in detecting sterile abscesses that provoke a leukocyte response.[7] In earlier times, Ga-67 citrate was very popular for infection imaging by exploiting above properties of Ga.[8] Due to low energy, long imaging time (half life: 78 hours) and poor image quality, the impact of Ga-67 imaging faded away. The resurgence of Ga-68, a PET radionuclide has revived the importance of ^{68}Ga as natural *in vivo* infection/inflammation imaging agent.[9,10] Now, the infection imaging is done using ^{68}Ga-citrate and $^{68}GaCl_3$.

$^{68}Ga^{3+}$ CHEMISTRY

^{68}Ga-complexes has simple aqueous coordinate chemistry based on Me(III).[11] Gallium, in aqueous solution, occurs solely in +3 oxidation state and is classified as a hard acid metal. Gallium can bond to highly ionic hard base ligand donors, such as carboxylic acids, amino nitrogens, hydroxamates, thiols and phenolates. The Ga chemistry is highly influenced by pH change. The optimum pH (3-5) is required for its aqueous chemistry. The pH below optimum inhibits the reaction and at pH above optimum range, i.e. >5, it tends to hydrolyze and leads to the precipitation as $Ga(OH)_3$.

Ga-68-LABELED MOLECULES

Several suitable bifunctional chelators have been developed, and coupled with biomolecules for Ga-68 labeling. DOTA, NOGADA and NOTA are commonly used bifunctional chelators. Many peptides/biomolecules like receptor

peptides and antibodies etc have now been successfully modified by these chelating agents without compromising their functional properties which further widened the role of Ga-68 PET/CT imaging. These peptides/biomolecules show very fast target localization and fast blood clearance thus, making the short half-life ideal for clinical studies. In the last decade ^{68}Ga-DOTA-octreotides replaced ^{99m}Tc/^{111}In-DTPA-octroescan used for neuroendocrine tumor (NET) imaging. ^{68}Ga-DOTA-octreotides proved to be a promising radiopharmaceutical for diagnosis, treatment planning, therapy response evaluation and disease recurrence of NET.[12] Several peptides like somatostatin for imaging NET, integrin peptide for imaging neoangiogenesis, etc. are now available as cold kits.

Ga-68 labeling has also been explored with other peptide receptors, like cholecystokinin/gastrin and GLP-1 analogs for NETs, bombesin and neuropeptide-Y analogs for prostate or breast cancers.[13-15] Arg-Gly-Asp (RGD) a cyclic tripeptide is used to image neoangiogenic/angiogenic vessels and mediated cell adhesion molecule by targeting overexpressed $\alpha_v\beta_3$ integrin. Inflammatory bowel disease, inflamed synovial tissue of rheumatoid arthritis and inflammatory atherosclerotic plaques can also be visualized by ^{68}Ga-RGD peptide.[16] Vascular adhesion protein-I (VAP 1) is an inflammation inducible endothelial cell molecule. It also contributes to extravasation cascade and controls trafficking of leukocyte at the site of inflammation. VAP-1 is expressed on the endothelial surface of intestinal blood vessels in inflammatory diseases, in skin inflammation (psoriasis), synovial blood vessels of inflamed joints (rheumatic arthritis) and cardiovascular diseases. However, VAP-1 is absent from the endothelial surface of normal tissues. Ga-68-labeled peptide against VAP-1 have been used for *in vivo* imaging of VAP-1 knockout.[17]

FUTURE

In the modern era of 'personalized medicine', Ga-68 has a promising role. The targets can be defined with the help of diagnostic Ga-68 PET/CT using appropriate ligands (peptides/biomolecules) for detection of disease, pretherapeutic measurement of organ and tumor doses. The therapeutic analog of imaging radionuclide (Lu-177/Y-90) can be selected for therapy using the same peptide. Nanomedicine in future has a great potential for early detection, accurate diagnosis and personalized treatment of various diseases, particularly cancer. Nanomedicine can offer unprecedented interactions with biomolecules, on the surface as well as inside the cells which may revolutionize disease diagnosis and treatment. Molecular imaging can measure the expression of molecular markers at different stages of diseases and provide relevant and reliable information in an intact system. The information may speed up the drug development process and help in individualized treatment monitoring and dose optimization. Ga-68 is an ideal radionuclide for labeling various nanoparticles like single-walled carbon nanotubes (SWNTs), quantum dots (QD), polymeric and metallic nanoparticles, etc. for evaluation of their biodistribution, pharmacokinetic properties and tumor targeting efficacy.[18-20] The information may be utilized for early diagnosis, selecting better treatment options and predicting the disease prognosis.

With each passing day, the reign of Ga-68 in research and clinical application is increasingly being established. It has a lot in store for future. The easy availability and simple chemistry based on sophisticated chelating agents for Ga-68 will make it parallel to kit-based Tc-99m chemistry as predicted by Deutsch.[21]

REFERENCES

1. Kopecký P, Mudrová B, Svoboda K. The study of conditions for the preparation and utilization of ^{68}Ge-^{68}Ga generator. Int J Appl Radiat Isot 1973;24:73-80.
2. Schuhmacher J, Maier-Borst W. ^{68}Ge-^{68}Ga generator for the production of ^{68}Ga in an ionic form. Int J Appl Radiat Isot 1974;25:263-68.
3. Mirzadeh S, Lambrecht R. Radiochemistry of germanium. J Radioanal Nucl Chem 1996;202:7-102.
4. Meyer GJ, Maecke H, Schuhmacher J, Knapp WH, Hofmann M. ^{68}Ga-labelled DOTA-derivatised peptide ligands. Eur J Nucl Med Mol Imag 2004;31:1097-104.
5. Velikyan I, Beyer GJ, Langstrom B. Microwave-supported preparation of ^{68}Ga bioconjugates with high specific radioactivity. Bioconjug Chem 2004;15:554-60.
6. Schuhmacher J, Maier-Borst W. A new ^{68}Ge/^{68}Ga radioisotope generator system for production of ^{68}Ga in dilute HCl. Int J Appl Radiat Isot 1981;32:31-36.
7. El-Maghraby TA. Nuclear medicine methods for evaluation of skeletal infection among other diagnostic modalities. Q J Nucl Med Mol Imaging 2006;50:167-92.
8. Palestro CJ. The current role of gallium imaging in infection. Semin Nucl Med 1994;24:128-41.
9. Mäkinen TJ, Lankinen P, Pöyhönen T, Jalava J, Aro HT, Roivainen A. Comparison of ^{18}F-FDG and ^{68}Ga PET imaging in the assessment of experimental osteomyelitis due to Staphylococcus aureus. Eur J Nucl Med Mol Imaging 2005;32:1259-68.
10. Silvola J, Laitinen I, Sipilä H, Laine VJO, Leppänen P, Ylä-Herttuala S, et al. Uptake of ^{68}gallium in atherosclerotic plaques in LDLR/ApoB100/100 mice. EJNMMI Res 2011;1:14.
11. Green MA, Welch MJ. Gallium radiopharmaceutical chemistry. Int J Rad Appl Instrum B 1989;16:435-48.
12. Naji M, AL-Nahhas A. ^{68}Ga-labelled peptides in the management of neuroectodermal tumours. Eur J Nucl Med Mol Imaging 2012;39(Suppl 1):S61-67.
13. Von Guggen Berg E, Rangger C, Sosabowski J, Laverman P, Reubi JC, Virgolini IJ, et al. Preclinical evaluation of radiolabeled DOTA-derivatized cyclic minigastrin analogs for

targeting cholecystokinin receptor expressing malignancies. Mol Imaging Biol 2012 Jun;14(3):366-75.
14. Brom M, Oyen WJG, Joosten L, Gotthardt M, Boerman OC. Ga-labelled exendin-3, a new agent for the detection of insulinomas with PET. Eur J Nucl Med Mol Imaging 2010; 37:1345-55.
15. Schuhmacher J, Zhang H, Doll J, Mäcke HR, Matys R, Hauser H, et al. GRP receptor-targeted PET of a rat pancreas carcinoma xenograft in nude mice with a 68Ga-labeled bombesin (6-14) analog. J Nucl Med 2005;46:691-99.
16. Knetsch PA, Petrik M, Griessinger CM, Rangger C, Fani M, Kesenheimer C, et al. [68Ga]NODAGA-RGD for imaging $\alpha_v\beta_3$ integrin expression. Eur J Nucl Med Mol Imaging 2011;38: 1303-12.
17. Autio A, Ujula T, Luoto P, Salomäki S, Jalkanen S, Roivainen A. PET imaging of inflammation and adenocarcinoma xenografts using vascular adhesion protein 1 targeting peptide (68)Ga-DOTAVAP-P1: Comparison with (18)F-FDG. Eur J Nucl Med Mol Imag 2010;37:1918-25.
18. Liu Z, Cai W, He L, Nakayama N, Chen K, Sun X, et al. In vivo biodistribution and highly efficient tumor targeting of carbon nanotubes in mice. Nat Nanotechnol 2007;2:47.
19. Cai W, Chen K, Li ZB, Gambhir SS, Chen X. Dual-function probe for PET and near-infrared fluorescence imaging of tumor vasculature. J Nucl Med 2007;48:1862-70.
20. Lee HY, Li Z, Chen K, Hsu AR, Xu C, Xie J, et al. PET/MRI dual-modality tumor imaging using arginine-glycine-aspartic (RGD)–conjugated radiolabeled iron oxide nanoparticles. J Nucl Med 2008;49:1371-79.
21. Deutsch E. Clinical PET: Its time has come? J Nucl Med 1993; 34:1132-33.

ABOUT THE AUTHORS

Jaya Shukla (Corresponding Author)

Assistant Professor, Department of Nuclear Medicine, Postgraduate Institute of Medical Education and Research, Chandigarh, India
e-mail: shuklajaya@gmail.com

BR Mittal

Professor and Head, Department of Nuclear Medicine, Postgraduate Institute of Medical Education and Research, Chandigarh, India